

**Removal of Polar VOCs at Low Concentration Using a Sacrificial Carbon Bed**

by

Nusrat Fatema Nayan

A thesis submitted in partial fulfillment of the requirements for the degree of

Master of Science

in

Environmental Engineering

Department of Civil and Environmental Engineering  
University of Alberta

© Nusrat Fatema Nayan, 2020

## Abstract

Volatile organic compounds' (VOCs) emissions from automotive painting operations consist of a mixture of polar and nonpolar compounds. Adsorption is a widely used method for capturing VOCs from industrial gas streams. Typically, most of the non-polar pollutants are captured using adsorption onto activated carbon. Polar VOCs can be challenging to control, particularly at very low concentrations, due to the hydrophobic nature of activated carbon. Moreover, the driving force at low concentration is not high enough to readily overcome mass transfer resistances during the adsorption. Since adsorption is a selective capture process, it is of great interest to find the most suitable adsorbent with high capacity and affinity for the target polar pollutants, especially when dealing with VOCs at low concentrations.

In the present study, a sacrificial fixed bed containing carbon adsorbents is utilized to treat a VOC-laden air stream. Adsorption of several polar VOCs (ethanol, acetone, 2-propanol, isobutanol, and 1-butanol) on different carbon materials with distinct properties was investigated. Eleven activated carbons from three major types namely beaded activated carbon (BAC), granulated activated carbon (GAC) and activated carbon clothes (ACFCs) were tested in this project. In order to acquire information regarding the key properties of the adsorbents, nitrogen adsorption isotherms, X-ray photoelectron spectroscopy,  $\text{pH}_{\text{pzc}}$  and Boehm titration analyses were performed. BET surface area and micropore volume for wood based crushed GACs (OVC and VC48C) and ACFC 15 were close to virgin BAC and higher than coal-based ones (BPL and VCRSD) and ACFC 10. Pelleted GACs showed highest BET surface area, lowest micropore volume and considerable amount of mesopore volume. Based on XPS analysis, oxygen content for BACs, crushed GACs and pelleted GACs was more than 5% up to 8%, but less than 4% for

activated carbon fiber clothes. Findings from Boehm titration analysis were consistent with  $\text{pH}_{\text{pzc}}$  values.

Adsorption capacity of activated carbons challenged with polar compounds such as ethanol, acetone and 2-propanol were not high enough (maximum 6% for 2-propanol with ACFC-10) but less polar compounds such as iso-butanol and n-butanol showed up to 26% and 33% capacity respectively. In general, adsorption capacity of carbon samples did not follow any specific trend which could be accurately described by their chemical or physical properties. Adsorption capacity of activated carbons challenged with polar compounds better correlated with micropore volume while total acidity contributed highest to the less or non-polar compounds.

Based on the experimental data, several performance indicators including adsorption capacity, 5 % breakthrough time, throughput value and length of unused bed were determined. Considering cost, adsorption capacity and ease of handling pelleted carbon samples were recommended for the design of the sacrificial bed.

## ***Dedication***

*First, I am very much grateful to almighty for all the blessings and opportunities in life.*

*I dedicate this thesis to my beloved and joyful family. A special gratitude to my loving parents, Fatema and Nawsher. This success would not be possible without their endless love, tremendous support and encouragement.*

*I would also like to dedicate this work to my lovely husband Tanim and my adorable daughter Anoosha for providing me with constant and endless motivation, inspiration and courage throughout my life.*

*I also want to remember the general people of my country Bangladesh, who always manage to survive wonderfully, despite all kinds of turmoil.*

## **Acknowledgement**

I am completely indebted to my supervisor Dr. Zaher Hashisho, Professor, Department of Civil and Environmental Engineering, University of Alberta, for his outstanding supervision in this thesis project. As a supervisor, Dr. Hashisho helped me tremendously in carrying out the project through his kind and valuable suggestion, guidance and inspiration. I am also grateful to him for his patience, time to time co-operation and constant constructive feedback.

The laboratory work reported in this thesis paper has been carried out at the Air Quality Characterization Lab of Civil and Environmental Engineering Department in University of Alberta under the financial support from Ford Motor Company and NSERC. I am very much grateful to them. I would also like to express my gratitude to my colleagues in the lab, especially to Dr. Alireza Haghghat Mamaghani and Imranul Laskar for their demonstration, suggestions and assistance in my experiments and manuscript review. And last but not the least I would also like to thank the technicians Chen Liang and David Zhao who helped me a lot during the experiment.

## Table of Contents

Abstract.....	ii
<i>Dedication</i> .....	iv
Acknowledgement .....	v
<b>Chapter 1. Introduction</b> .....	<b>1</b>
1.2.1 VOCs emission from automotive painting.....	5
1.4 VOC abatement techniques .....	7
1.5 Problem statement and significance .....	11
1.6 Objective of thesis .....	12
1.7 Thesis outline.....	12
<b>Chapter 2. Literature Review</b> .....	<b>13</b>
2.1 Adsorption overview .....	14
2.2 Isotherms .....	15
2.3 Adsorbents and their characterization .....	18
2.4 Carbon based adsorbents .....	19
2.5 Factors affecting adsorption .....	23
2.5.1 Influential properties of adsorbent .....	24
2.5.2 Influential properties of adsorbate.....	27
2.5.3 Influential operating conditions during gaseous adsorption.....	30
2.6 Adsorbent selection criteria .....	33
2.7 Adsorber types.....	33
2.8 Design of a sacrificial fixed bed .....	34
2.8.1 Estimating carbon requirement .....	34
<b>Chapter 3. Materials &amp; Methods</b> .....	<b>38</b>

3.1 Adsorbents .....	39
3.2 Adsorbates .....	42
3.3 Characterization tests.....	44
3.3.1 Micropore surface analysis.....	44
3.3.2 XPS analysis.....	44
3.3.3 Boehm titration.....	45
3.3.4 pH at point zero charge ( $\text{pH}_{\text{pzc}}$ ) determination .....	46
3.4 Experimental procedure.....	47
3.4.1 Adsorption test experiments.....	47
3.3.2 Adsorption-regeneration experiments .....	50
3.3.3 Adsorption isotherms .....	50
3.5 Mass balance calculation .....	51
3.6 Design of sacrificial bed .....	52
3.6.1 LUB method.....	52
3.6.2 Thomas model.....	54
3.6.3 Wheeler-Jonas model.....	56
<b>Chapter 4. Result Analysis and Discussion .....</b>	<b>58</b>
4 Adsorbents characterization.....	59
4.1 $\text{N}_2$ adsorption analysis.....	59
4.2 XPS analysis.....	62
4.3 Boehm titration analysis.....	74
4.4 pH at point zero charge determination .....	76
4.5 Adsorption breakthrough study.....	78
4.6 Adsorption isotherms .....	99
4.7 Cyclic adsorption-desorption .....	100

<b>Chapter 5. Conclusion &amp; Recommendation</b> .....	104
5.1 Conclusion.....	105
5.2 Recommendations .....	106
<b>References</b> .....	108
<b><i>Appendices</i></b> .....	124
<i>Appendix A</i> .....	125
<i>Appendix B</i> .....	126
<i>Appendix C</i> .....	127
<i>Appendix D</i> .....	128
<i>Appendix E</i> .....	129
<i>Appendix F</i> .....	130
<i>Appendix G</i> .....	131
<i>Appendix H</i> .....	132
<i>Appendix I</i> .....	133
<i>Appendix J</i> .....	140



## List of Tables

<b>Table 1.</b> Classification of organic pollutants according to WHO. <sup>[1]</sup> .....	3
<b>Table 2.</b> Merits and demerits of different VOC abatement techniques*. <sup>[7,24]</sup> .....	10
<b>Table 5.</b> Physical and chemical properties of target adsorbates. ....	43
<b>Table 6.</b> Textural properties of adsorbent samples.....	60
<b>Table 7.</b> Elemental composition of adsorbent samples by XPS analysis. ....	62
<b>Table 8.</b> Comparison of functional groups' concentrations from C1s for different carbon samples. ....	72
<b>Table 9.</b> Comparison of functional groups' concentrations based on O1s deconvolution. ....	73
<b>Table 10.</b> pH <sub>pzc</sub> , overall oxygen content (%), degree of oxidation (C <sub>ox</sub> /C <sub>gr</sub> , %), and total acidity for carbon samples.....	76
<b>Table 11.</b> Adsorbents textural properties and adsorption capacity for iso-butanol and n-butanol. ....	88
<b>Table 12.</b> Adsorbent's chemical properties and adsorption capacity of ethanol, acetone and 2-propanol. ....	90
<b>Table 13.</b> Adsorption capacity in weight % (with standard deviation) based on breakthrough curves for various ACs.....	93
<b>Table 14.</b> Summary of performances parameters calculated based on single-VOC breakthrough curves..	93
<b>Table 15.</b> Full-scale sacrificial bed designed with WV-A 1100 for 2-propanol adsorption.....	98
<b>Table 16.</b> Summary of results for adsorption of 10 ppmv Ethanol on different adsorbents (IB: Immediate Breakthrough) .....	125
<b>Table 17.</b> Summary of results for adsorption of 10 ppmv Acetone on different adsorbents (IB: Immediate Breakthrough) .....	126
<b>Table 18.</b> Summary of results for adsorption of 10 ppmv 2-propanol on different adsorbents (IB: Immediate Breakthrough) .....	127
<b>Table 19.</b> Summary of results for adsorption of 10 ppmv iso-butanol on different adsorbents (IB: Immediate Breakthrough) .....	128

<b>Table 20.</b> Summary of results for adsorption of 10 ppmv n-butanol on different adsorbents (IB: Immediate Breakthrough) .....	129
<b>Table 21.</b> Results of 5 cycle Adsorption Desorption for WV-A 1100 With 2- propanol.....	131
<b>Table 22.</b> Summary of results for adsorption isotherms of 2-propanol on WV-A 1100 at 20 °C. ....	132

## List of Figures

<b>Figure 1.</b> Major contributors to national volatile organic compound trends in Canada. <sup>[14]</sup> .....	4
<b>Figure 2.</b> Painting operation and VOCs emission from spray paint booths (adapted from Kim, 2011). <sup>[12]</sup> .	5
<b>Figure 3.</b> Classification of VOCs emission from spray paint booths (adapted from Kim, 2011). <sup>[12]</sup> .....	6
<b>Figure 4.</b> Classification of VOCs' emission abatement techniques (adapeted from Khan and Ghoshal, 2000 and Prammar and Rao, 2009). <sup>[7,24]</sup> .....	8
<b>Figure 5.</b> General practice for VOCs' emission abatement from spray paint booths (adapted from Kim, 2011). <sup>[12]</sup> .....	11
<b>Figure 6.</b> Five different types of adsorption isotherms (adapted from Brunauer et el, 1940). <sup>[38,39]</sup> .....	16
<b>Figure 7.</b> Details of type II isotherm (adapted from Bansal and Goyal, 2005). <sup>[27]</sup> .....	17
<b>Figure 8.</b> Favorable and unfavorable adsorption isotherms (adapted from Alan Gabelman, 2017). <sup>[40]</sup> .....	18
<b>Figure 9.</b> Different types of activated carbons- <b>a.</b> PAC, <sup>[49]</sup> <b>b.</b> non-pelleted GAC, <sup>[50]</sup> <b>c.</b> pelleted GAC, <sup>[51]</sup> <b>d.</b> BAC, <sup>[52]</sup> <b>e.</b> ACFC, <sup>[53]</sup> <b>f.</b> ACF. <sup>[54]</sup> .....	21
<b>Figure 10.</b> Range of decomposition temperatures by TPD for carbon surface functional groups. <sup>[42]</sup> .....	26
<b>Figure 11.</b> Carbon surface functional groups with basicity. <sup>[73]</sup> .....	27
<b>Figure 12.</b> Preferential adsorption of ethylbenzene and p-xylene as compared to o-xylene and m-xylene. <sup>[18]</sup> .....	28
<b>Figure 13.</b> Typical breakthrough profile of adsorbents. <sup>[90]</sup> .....	35
<b>Figure 14.</b> Boehm titration procedure (adapted from Goertzen et el.). <sup>[117,118,119]</sup> .....	46
<b>Figure 15.</b> Flow diagram for adsorption-regeneration test.....	48
<b>Figure 16.</b> Inside view of adsorption regeneration tube.....	48
<b>Figure 17.</b> Typical breakthrough curve. <sup>[90,95]</sup> .....	52
<b>Figure 18.</b> Pore size distribution of virgin carbon samples. <b>a.</b> Virgin and Spent BAC, <b>b.</b> ACFCs, <b>c.</b> Crushed GACs (wood-based), <b>d.</b> Crushed GACs (coal-based), <b>e.</b> Pelleted GACs.....	61
<b>Figure 19.</b> Full range survey spectrum for WV-A 1100. ....	63

<b>Figure 20.</b> Survey scan deconvolution for <b>a.</b> virgin BAC (C1s and O1s respectively) and <b>b.</b> spent BAC (C1s and O1s respectively). .....	65
<b>Figure 21.</b> Survey scan deconvolution for <b>a.</b> ACFC 10, <b>b.</b> ACFC 15 and <b>c.</b> ACFC 20. ....	662
<b>Figure 22.</b> Survey scan deconvolution for wood-based non-pelleted GACs, <b>a.</b> OVC (C1s and O1s respectively) and <b>b.</b> VC48C (C1s and O1s respectively). ....	67
<b>Figure 23.</b> Survey scan deconvolution for coal-based non-pelleted GACs, <b>a.</b> BPL (C1s and O1s respectively) and <b>b.</b> VCRSD (C1s and O1s respectively). ....	68
<b>Figure 24.</b> Survey scan deconvolution for wood-based pelleted GACs, <b>a.</b> WV-A 1100 (C1s and O1s respectively) and <b>b.</b> WV-A 1500 (C1s and O1s respectively). ....	69
<b>Figure 25.</b> Contribution of SOFG to total acidity derived from Boehm titration. ....	75
<b>Figure 26.</b> Relative amount of acidity originated from SOFGs. ....	75
<b>Figure 27.</b> Single-component adsorption breakthrough profiles of 10 ppmv 2-propanol, acetone, ethanol, iso-butanol and n-butanol on 2 g virgin BAC at 22 °C. ....	79
<b>Figure 28.</b> Single-component adsorption breakthrough profiles of 10 ppmv 2-propanol, acetone, ethanol, iso-butanol and n-butanol on 4 g spent BAC at 22 °C. ....	79
<b>Figure 29.</b> Single-component adsorption breakthrough profiles of 10 ppmv 2-propanol, acetone, ethanol, iso-butanol and n-butanol on 0.5 g ACFC 10 at 22 °C. ....	82
<b>Figure 30.</b> Single-component adsorption breakthrough profiles of 10 ppmv 2-propanol, acetone, ethanol, iso-butanol and n-butanol on 0.5 g ACFC 15 at 22 °C. ....	82
<b>Figure 31.</b> Single-component adsorption breakthrough profiles of 10 ppmv 2-propanol, acetone, ethanol, iso-butanol and n-butanol on 0.5 g ACFC 20 at 22 °C. ....	83
<b>Figure 32.</b> Single-component adsorption breakthrough profiles of 10 ppmv 2-propanol, acetone, ethanol, iso-butanol and n-butanol on 2 g OVC at 22 °C. ....	84
<b>Figure 33.</b> Single-component adsorption breakthrough profiles of 10 ppmv 2-propanol, acetone, ethanol, iso-butanol and n-butanol on 2 g VC48C at 22 °C. ....	84

<b>Figure 34.</b> Single-component adsorption breakthrough profiles of 10 ppmv 2-propanol, acetone, ethanol, iso-butanol and n-butanol on 2 g BPL at 22 °C. ....	85
<b>Figure 35.</b> Single-component adsorption breakthrough profiles of 10 ppmv 2-propanol, acetone, ethanol, iso-butanol and n-butanol on 2 g VCRSD at 22 °C. ....	85
<b>Figure 36.</b> Single-component adsorption breakthrough profiles of 10 ppmv 2-propanol, acetone, ethanol, iso-butanol and n-butanol on 2 g WV-A 1100 at 22 °C. ....	86
<b>Figure 37.</b> Single-component adsorption breakthrough profiles of 10 ppmv 2-propanol, acetone, ethanol, iso-butanol and n-butanol on 2 g WV-A 1500 at 22 °C. ....	86
<b>Figure 38.</b> Correlations to micropore volume of the carbon samples with adsorption capacity of Iso-butanol and n-butanol. ....	86
<b>Figure 39.</b> Correlations to total acidity (mmol/g AC) of the carbon samples with adsorption capacity of 2-propanol, acetone and ethanol. ....	92
<b>Figure 40.</b> Adsorption Isotherms of 2-propanol on WV-A 1100 at 22 °C. ....	99
<b>Figure 41. a.</b> Adsorption breakthrough profiles of 2-propanol on 2 g WV-A 1100 at 22 °C and <b>b.</b> Adsorption capacity for 2-propanol on 2 g WV-A 1100 at 22 °C. ....	100
<b>Figure 42. a.</b> Desorption concentration and temperature profiles of 2-propanol on 2 g WV-A 1100 and <b>b.</b> Desorption efficiency for 2-propanol on 2 g WV-A 1100 at 288 °C. ....	101
<b>Figure 43.</b> Micropore size distribution of virgin and spent WV-A 1100. ....	103
<b>Figure 44.</b> Mesopore size distribution of virgin and spent WV-A 1100. ....	103
<b>Figure 45.</b> Adsorption Breakthrough profiles of 2-propanol on as received 3 g BPL (4×10) at 22 °C. ...	130

## List of Acronyms

AC	Activated Carbon
ACFC	Activated Carbon Fiber Cloth
ACC	Activated Carbon Cloth
BAC	Beaded Activated Carbon
BDST	Bed Depth Service Time
BET	Brunauer-Emmett-Teller
BT	Breakthrough Time
BWC	Butane working capacity
CEPA	Canadian Environmental Protection Act
CPS	Counts Per Second
DAC	Data Acquisition and Control
DDT	Dichloro-diphenyl-trichloroethane
DFT	Density Functional Theory
EPA	Environmental Protection Agency
FID	Flame Ionization Detector
FTIR	Fourier Transform Infrared Spectroscopy
NMR	Nuclear magnetic resonance
NG	Natural Gas
GAC	Granular Activated Carbon
GWC	Gasoline working capacity
IUPAC	International Union of Pure and Applied Chemistry
IB	Initial Breakthrough
LUB	Length of Unused Bed
LPG	Liquefied petroleum gas
MW	Molecular weight

PAC	Powdered Activated Carbon
PBBs	Polybrominated biphenyls
PCBs	polychlorinated biphenyls
ppbv	Parts per billion (volume fractions)
ppmv	Parts per million (volume fractions)
PSD	Pore Size Distribution
pH <sub>pzc</sub>	pH at Point Zero Charge
QSDFE	Quenched Solid Density Functional Theory
RFR	Reverse Flow Reactor
RH	Relative Humidity
SCCM	Standard cubic centimeters per minute
SFG	Surface Functional Groups
SOFG	Surface Oxygen Functional Groups
SLPM	Standard Liter per Minute
SVOCs	Semi-volatile organic compounds
TGA	Thermogravimetric analysis
TH	Total heel
TPD	Temperature Programmed Desorption
TPR	Throughput Ratio
UV	Ultraviolet
VOCs	Volatile Organic Compounds
VVOCs	Very volatile organic compounds
WHO	World Health Organization
Wt	Weight
XANES	X-ray absorption near edge structure
XPS	X-ray Photoelectron Spectroscopy

### List of Symbols

A	Cross sectional area ( $m^2$ )
$C_b$	gas concentration in the bulk phase ( $mg/m^3$ air)
$C_{in}$	Inlet concentration (ppmv)
$C_{out}$	Effluent concentration (ppmv)
$C^*$	gas phase concentration adjacent to the surface of the adsorbent in equilibrium with the adsorbed phase concentration ( $mg/m^3$ air)
$\check{D}$	Depth of column (m)
D	Diameter of the column (m)
$G_s$	Superficial flow rate of gas ( $kgm^{-2}min^{-1}$ )
$h_m$	convective mass transfer coefficient
$K_{th}$	Thomas rate constant ( $kg^{-1}m^3s^{-1}$ )
$K_v$	Adsorption rate coefficient ( $min^{-1}$ )
L	Length of Colum (m)
$\check{N}$	adsorption capacity of carbon
$N_A$	mass flux ( $mg/m^2s$ )
Q	Superficial flow rate of gas ( $kgm^{-2}min^{-1}$ )
$t_b$	5% breakthrough time (min)
v	Superficial gas velocity ( $ms^{-1}$ )
W	carbon bed weight (kg)
$W_e$	adsorption capacity of carbon (kg VOC/kg-carbon)
$W_{b5}$	Adsorption capacity at 5% (Kg VOC/ Kg adsorbent)
$W_{t100}$	adsorbent's capacity from lab scale (Kg VOC/ Kg adsorbent)
$\rho_b$	Bulk density ( $kg/m^3$ )
$\tau$	Empty bed contact time (sec)



## **Chapter 1. Introduction**

## 1.1 Definition of VOCs

There are a multitude of definitions for Volatile Organic Compounds (VOCs) among different regulatory bodies depending on their health and environmental aspects. According to the United States Environmental Protection Agency (EPA)<sup>[1]</sup> VOCs can be defined as –"any compound of carbon, excluding carbon monoxide, carbon dioxide, carbonic acid, metallic carbides or carbonates, and ammonium carbonate, which participates in atmospheric photochemical reactions, except those designated by EPA as having negligible photochemical reactivity (such as methane and ethane)." Similarly, Environment and Climate Change Canada describes VOCs as “organic compounds containing one or more carbon atoms that evaporate readily to the atmosphere, and do not include photo chemically non-reactive compounds such as methane, ethane and the chlorofluorocarbons.”<sup>[2]</sup>

Though thousands of compounds meet this definition, it emphasizes mainly on the 50 to 150 most plentiful compounds containing two to twelve carbon atoms.<sup>[2,3]</sup> Sometimes VOCs are classified based on their boiling points - “organic compounds having an initial boiling point less than or equal to 250 °C measured at a standard atmospheric pressure of 101.3 kPa.”<sup>[1]</sup> The World Health Organization (WHO) also describes VOCs based on boiling point and categorizes indoor organic pollutants as<sup>[1]</sup>:

- Very volatile organic compounds (VVOCs)
- Volatile organic compounds (VOCs)
- Semi-volatile organic compounds (SVOCs)

Details of above mentioned classification is explained in Table 1.

**Table 1.** Classification of organic pollutants according to WHO.<sup>[1]</sup>

<b>Description</b>	<b>Abbreviation</b>	<b>Boiling Point Range (°C)</b>	<b>Example Compounds</b>
Very volatile (gaseous) organic compounds	VVOC	<0 to 50-100	Propane, butane, methyl chloride
Volatile organic compounds	VOC	50-100 to 240-260	Formaldehyde, d-Limonene, toluene, acetone, ethanol (ethyl alcohol) 2-propanol (isopropyl alcohol), hexanol
Semi volatile organic compounds	SVOC	240-260 to 380-400	Pesticides (DDT, chlordane, plasticizers (phthalates), fire retardants (PCBs, PBB)

## 1.2 Sources of VOCs

VOCs are omnipresent in ambient air and the emission sources can be divided into two major groups - natural sources and anthropogenic sources (human-made). Natural sources include woods, crops, wetlands, forests oceans, and volcanic eruptions.<sup>[4]</sup> Oil and natural gas production, petroleum refining, paint production, pulp and paper industry, automotive industry, vehicular emissions, chemical process facilities are examples of main anthropogenic or man-made sources of VOCs' emission.<sup>[5]</sup> Chemical cleaners, varnishes, solvents, solvent thinners, degreasers, lubricants, liquid fuels, printing, adhesives, coating and pharmaceutical industries also generate large amounts of VOCs.<sup>[6,7,8,9,10,11,12,13]</sup>

From 1990 to 2017, overall VOCs' emission in Canada dropped by 40 % (1.2 Mt). (Figure 1). About 1.8 Mt VOCs were released in 2017 in Canada. Oil and gas industries were the largest contributors (37 % of total) while paints and solvents are the second largest (18 % of total) in this respect.<sup>[14]</sup>

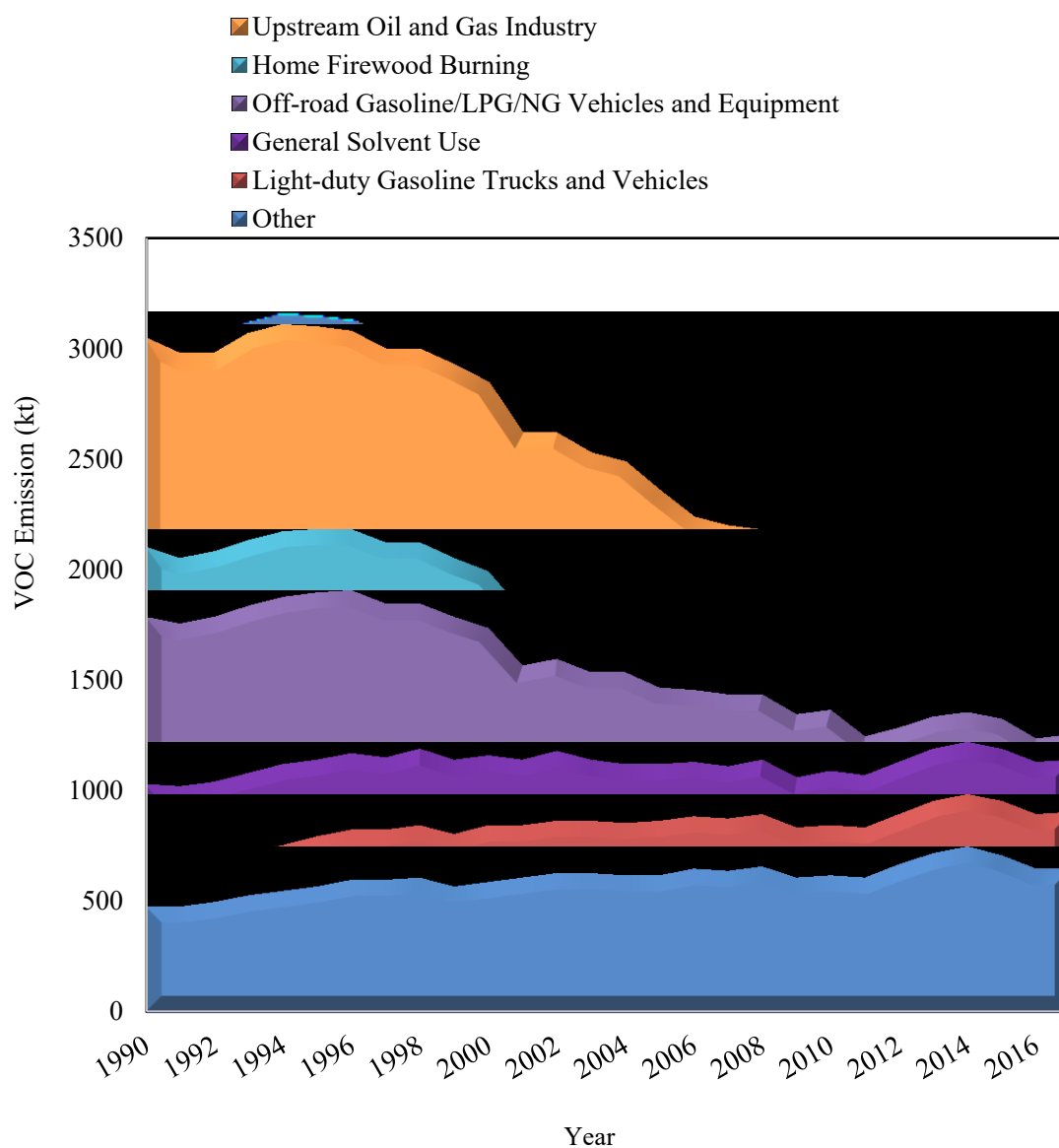


**Figure 1.** Major contributors to national volatile organic compound trends in Canada.<sup>[14]</sup>

### 1.2.1 VOCs emission from automotive painting

Painting operations of various metals and plastics parts are a major source of VOCs' emission in automotive industries. Consequently, many researches have been dedicated to investigating various VOC abatement strategies.<sup>[12,15,16]</sup> These painting operations are accountable for almost 80 % of the total emitted VOCs from automotive industries.<sup>[16]</sup> Normally these paints contain organic polymers and solvents. Figure 2 depicted the VOCs' generating steps during entire painting operation.

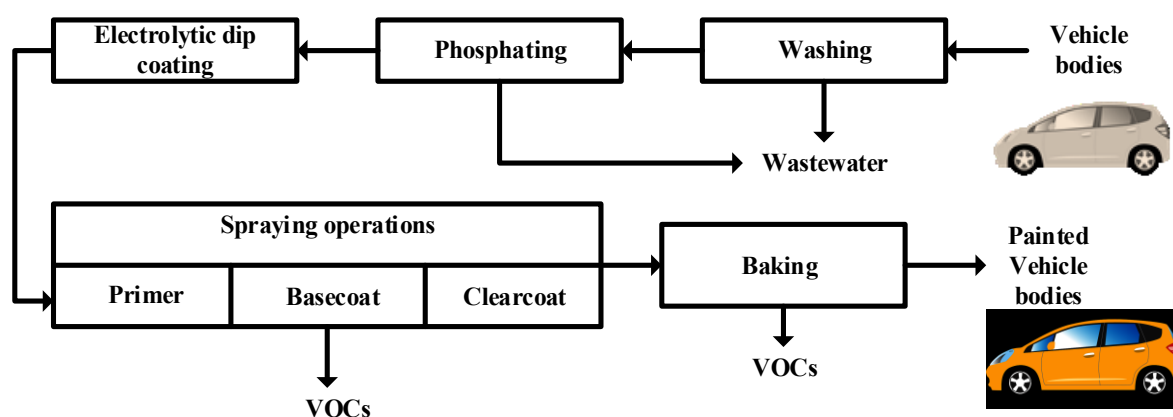


**Figure 2.** Painting operation and VOCs emission from spray paint booths (adapted from Kim, 2011).<sup>[12]</sup>

Solvents in the paints contain aromatic and/or aliphatic hydrocarbons, esters, ketones, alcohols, and glycol ethers. Broadly, they can be categorized as hydrophobic and hydrophilic VOCs based on the relative magnitude of Henry's law constant of the solvent.<sup>[12]</sup> Henry's law constant also referred as air–water partition coefficient) which is the ratio of a compound's partial pressure in gas phase to the concentration of the compound in water at a certain temperature.<sup>[17]</sup> The detail classification of VOCs is presented in Figure 3.<sup>[12,16]</sup>

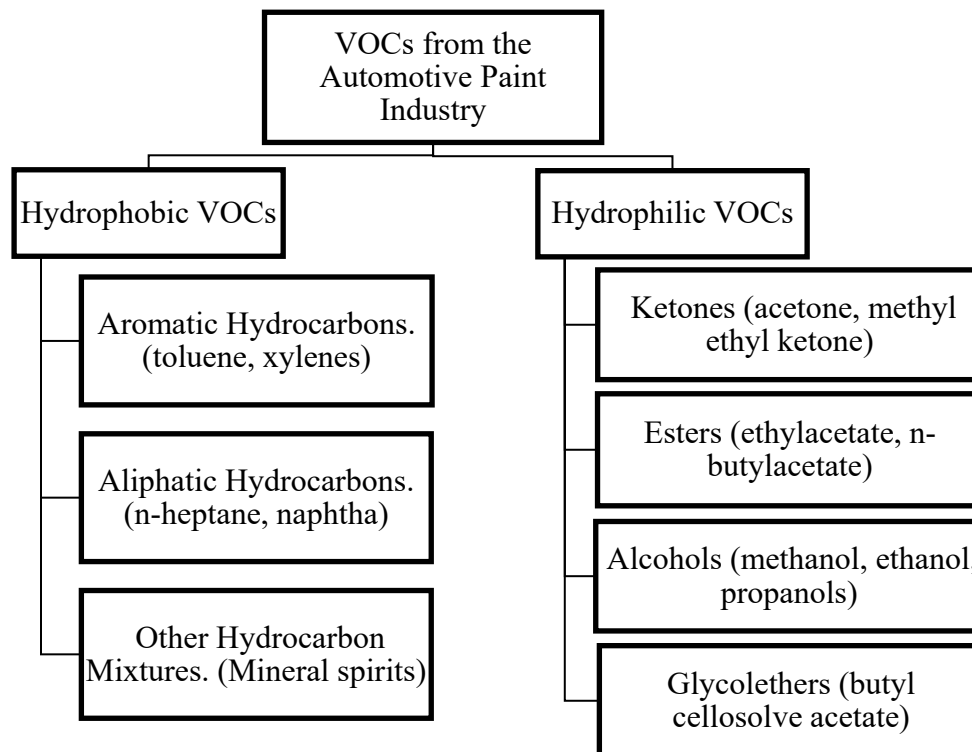


**Figure 3.** Classification of VOCs emission from spray paint booths (adapted from Kim, 2011).<sup>[12]</sup>

### 1.3 Health and environmental impacts

In presence of sunlight VOCs undergo photochemical oxidation in combination with NO<sub>x</sub>, to produce ground-level ozone and eventually photochemical smog.<sup>[1,2,12]</sup> Photochemical smog adversely affects human and animal lives as well as plants' growth.<sup>[7,16]</sup> VOC exposure is responsible for headaches, eye, nose and throat irritations, shortness of breath and chest tightness, nausea, dizziness, and memory loss at low concentration for short time exposure.<sup>[18]</sup> In addition, damages to liver, central nervous system and lungs can occur at high concentration for short time exposure or even at very low concentration for chronic exposure.<sup>[18,19,20,21]</sup> Some VOCs are considered carcinogen and mutagen even at very low concentration.<sup>[21]</sup> Exposure to some VOCs

can lead to unconsciousness or even death (like benzene) if the consumption exceeds a certain level.<sup>[18]</sup> Ground level ozone is very harmful to forestlands and crops since it reduces growth and survivability of tree seedlings, and increase the plant susceptibility to disease, pests and other environmental stressors.<sup>[2]</sup> Besides being harmful to human and plants, VOCs (specially halogenated VOCs) are broadly responsible for stratospheric ozone depletion.<sup>[18]</sup> Due to their health and environmental effects, governments and intergovernmental organizations of many countries around the world have set regulations to reduce the emission of and exposure to VOCs.<sup>[7]</sup> For instance, Goteborg Protocol states that European Union members should reduce their VOC emission by half by 2020 with respect to their total emission in 2000.<sup>[22]</sup>

#### **1.4 VOC abatement techniques**

The best suited technology to control VOCs emission is determined by assessing several criteria including pollutant type and sources, presence of specific non-VOC compounds, concentration, flow rate, reusability of removed VOCs, efficiency of removal, regulatory aspects, process safety, location, cost, specific control requirement, secondary waste generation, maintenance frequency and overall feasibility of the operation.<sup>[7,23,24,25]</sup> A hierarchic diagram is presented here to illustrate the classification of VOC removal technologies (Figure 4).

Process and equipment modification techniques are applied by substitution of new raw materials, change in process operating condition, installation of monitoring and repair programs and machinery modification to reduce VOC emission.<sup>[7,24]</sup> Additional control methods are categorized into destruction or recovery of VOCs. Besides the promising and cost-effective bio-filtration process, destruction method also includes different oxidation techniques. Destruction methods are generally applied when VOC recovery is not technically or economically feasible.<sup>[24]</sup>

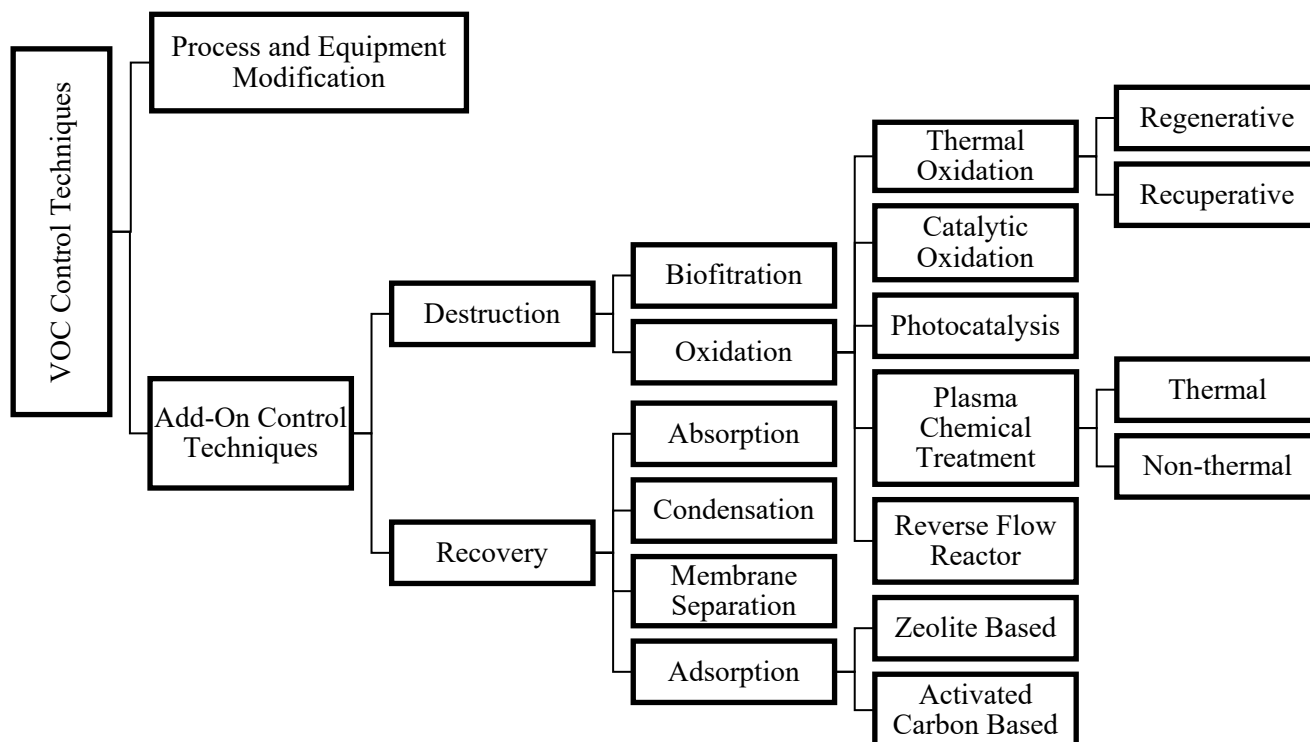


**Figure 4.** Classification of VOCs' emission abatement techniques (adapeted from Khan and Ghoshal, 2000 and Pramar and Rao, 2009).<sup>[7,24]</sup>

Bio-filtration is a continuous method to oxidize VOCs into CO<sub>2</sub> and H<sub>2</sub>O by utilizing a filter bed of biologically active compost, wood, peat or soil over a perforated pipe system. Thermal oxidation or fume incinerators are of two types- regenerative and recuperative, both utilize thermal energy recovery system by heating the incoming gas stream before entering the combustion zone with combustion exhaust stream. The operating temperature depends on type and concentration of VOCs and the desired removal efficiency.<sup>[7]</sup> Catalytic oxidation system requires less combustion energy and operates at lower temperatures due to the use of catalyst.<sup>[7]</sup> A reverse flow reactor (RFR) operates under constant transient condition due to periodic reverse of feed flow in adiabatic



packed bed reactor.<sup>[7]</sup> Plasma chemical treatments are of two types: thermal and non-thermal. During the plasma treatment, free electrons with high energy are generated to produce radicals, which then decompose VOCs.<sup>[24]</sup> Photocatalysis refers to utilization of appropriate light energy by heterogeneous (semiconductor material) or homogeneous catalysts to generate primary oxidants such as hydroxyl and oxygen radicals to degrade VOCs.<sup>[24]</sup> In recovery method, absorption is done by contacting VOCs in the gaseous stream with a liquid solvent to purify the contaminated air.<sup>[7]</sup> High concentration VOC streams (above 5000 ppmv) with boiling points above 100 °F can be effectively separated by condensation. Condensation's basic principle is oversaturation through chilling and/or pressurizing below the stream dew point.<sup>[7,24]</sup> Membrane separation is used by gas permeation and reverse osmosis to recover VOCs by applying pressure difference.<sup>[7,24]</sup> Adsorption is an efficient and cost-effective technology which will be discussed in length in Chapter 2.

Apart from these, there are some other novel and promising technologies like spark-generated carbon aerosol particle treatment, negative air ions treatment, treatment by novel mesoporous chromium oxide, treatment by mesoporous silica fiber matrix, electron beam treatment, etc. which are yet to be explored and commercialized. But merely a single technology is seldom used to remove VOCs completely, rather an integrated removal process is used along with treatment facilities for secondary waste generated.<sup>[7,24]</sup> Table 2 lists the key advantages and disadvantages of the most common VOC control methods.

Table 2. Merits and demerits of different VOC abatement techniques\*. [7,24]

Technology		Merits	Shortcomings		
<b>Process &amp; Equipment Modification</b>		<ul style="list-style-type: none"> <li>Most effective and efficient method.</li> </ul>	<ul style="list-style-type: none"> <li>It is not always feasible.</li> </ul>		
<b>Add-On Control Techniques</b>	<b>Destruction</b>	<b>Bio-filtration</b>	<ul style="list-style-type: none"> <li>Less initial investment &amp; operating cost,</li> <li>Nonhazardous and less secondary waste,</li> <li>Green technology,</li> <li>Operates at low concentration,</li> <li>60–95 % efficiency.</li> </ul>	<ul style="list-style-type: none"> <li>Slow and selective process,</li> <li>Required mixed culture &amp; proper moisture control,</li> <li>No recovery of VOCs &amp; solvents,</li> <li>Not effective for halogenated compounds.</li> </ul>	
		<b>Oxidation</b>	<b>Thermal Oxidation</b>	<ul style="list-style-type: none"> <li>95–99 % VOC removal efficiency,</li> <li>Prospect for energy recovery,</li> <li>Can handle high VOC concentration.</li> </ul>	<ul style="list-style-type: none"> <li>Secondary waste treatment required,</li> <li>Corrosion resistant materials required.</li> </ul>
			<b>Catalytic Oxidation</b>	<ul style="list-style-type: none"> <li>Handle low VOC concentration,</li> <li>Operates at low temperature,</li> <li>Attain 90–98 % efficiency,</li> <li>Energy recovery up to 70 %.</li> </ul>	<ul style="list-style-type: none"> <li>Possibilities of catalyst poisoning And high costs of replacement,</li> <li>Large units are not popular,</li> <li>May produce secondary wastes.</li> </ul>
			<b>Photo - catalysis</b>	<ul style="list-style-type: none"> <li>Low UV light energy requirement,</li> <li>Extremely high decomposition rates,</li> <li>Entire system can be easily monitored,</li> <li>Promising for indoor air purification.</li> </ul>	<ul style="list-style-type: none"> <li>Deactivation of the catalyst by reaction intermediates and reaction products,</li> <li>Effect of moisture is not clear yet.</li> </ul>
			<b>Reverse Flow Reactor</b>	<ul style="list-style-type: none"> <li>Auto thermal process,</li> <li>Handle fluctuations in inlet conditions,</li> <li>Low operating cost.</li> </ul>	<ul style="list-style-type: none"> <li>Required minimum adiabatic temperature rise,</li> <li>Higher initial investment and maintenance costs.</li> </ul>
			<b>Plasma Chemical Treatment</b>	<ul style="list-style-type: none"> <li>Handle high or low VOC concentration,</li> <li>No fuel requirement, low operating cost,</li> <li>Can operate at ambient temperature,</li> <li>Low capital costs.</li> </ul>	<ul style="list-style-type: none"> <li>Incomplete destruction of the contaminants,</li> <li>Scale up problems,</li> <li>No Solvent recovery.</li> </ul>
	<b>Recovery</b>	<b>Adsorption</b>	<b>Zeolite Based</b>	<ul style="list-style-type: none"> <li>Thermally stable and non-flammable,</li> <li>Hydrophobic &amp; Selective adsorption.</li> </ul>	<ul style="list-style-type: none"> <li>Highly expensive,</li> <li>Restriction in availability.</li> </ul>
			<b>Activated Carbon Based</b>	<ul style="list-style-type: none"> <li>Recovery of VOCs is possible,</li> <li>Less installation &amp; operating cost,</li> <li>Flexible operation &amp; high capacity,</li> <li>Suitable for wide range of VOCs,</li> <li>Can handle low-concentration situations,</li> <li>Carbon source is relatively cheap.</li> </ul>	<ul style="list-style-type: none"> <li>Flammable; fire hazard,</li> <li>Require humidity control,</li> <li>High boiling point solvent, regeneration is difficult,</li> <li>Polymerization or oxidation of some solvents.</li> </ul>
		<b>Absorption</b>	<ul style="list-style-type: none"> <li>Removal efficiency up to 90 to 98 %,</li> <li>Good for a high humidity (50 % RH).</li> </ul>	<ul style="list-style-type: none"> <li>Not suitable for cyclic operation,</li> <li>Complexity during startup.</li> </ul>	
		<b>Condensation</b>	<ul style="list-style-type: none"> <li>Efficient for high boiling point VOCs,</li> <li>High concentrations above 5000 ppm,</li> <li>Attain 70–85 % efficiency,</li> <li>Best suited for mono-solvent systems.</li> </ul>	<ul style="list-style-type: none"> <li>Extensive cooling or pressurization for VVOCs,</li> <li>Explosion hazard associated with higher concentration,</li> <li>Potential for fouling.</li> </ul>	
		<b>Membrane Separation</b>	<ul style="list-style-type: none"> <li>Better VOC recovery,</li> <li>Less by-product generation,</li> <li>Can handle high concentration VOCs,</li> <li>Can operate in different flow pattern.</li> </ul>	<ul style="list-style-type: none"> <li>High capital and operating costs,</li> <li>Slow process,</li> <li>Membrane fouling,</li> <li>Environmental hazard for Membrane disposal.</li> </ul>	

\* (adapted from Khan and Ghoshal, 2000 and Pramar and Rao, 2009)

### 1.5 Problem statement and significance

A typical spray paint booth is depicted in Figure 5. It includes a spraying section and a water scrubber system which captures the overspray paint materials. Air coming out from the scrubber is passed through a separator (filter/wet electrostatic precipitator) to remove the particulates. Removal of VOCs from this exhaust air should meet the minimum requirement according to environmental regulations and is commonly done by adsorption. If VOCs concentration is high, exhaust air from the adsorber is sent to an additional thermal oxidiser before release to the atmosphere.<sup>[12]</sup> The entire adsorption process is composed of two units<sup>[12]</sup>:

- A fixed or fluidised bed adsorber with continuous regeneration
- A sacrificial activated carbon adsorber without any regeneration

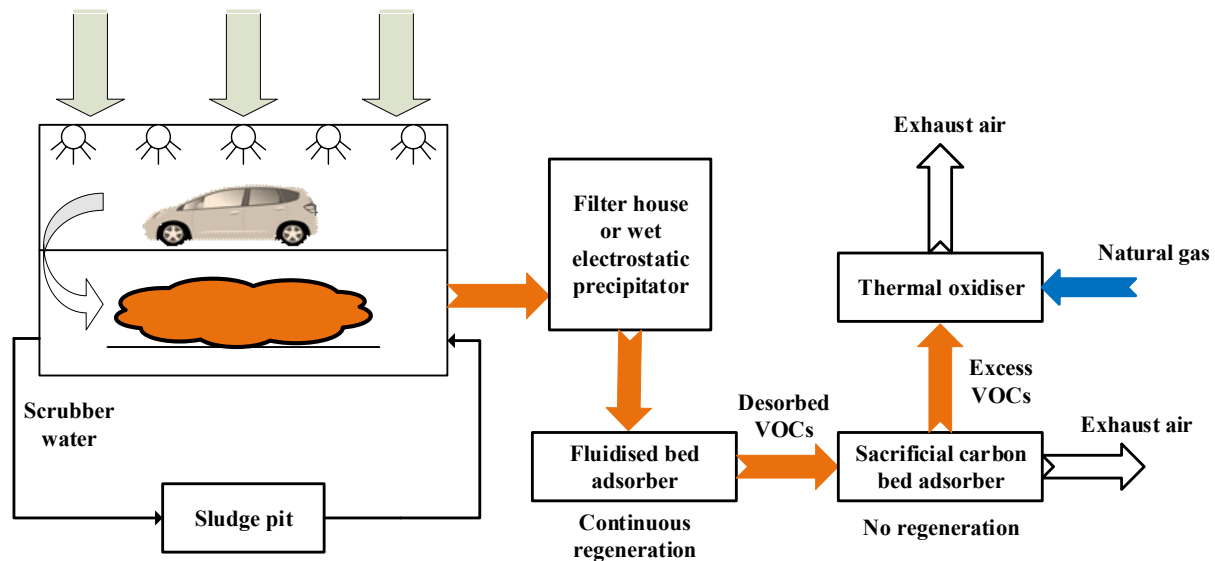


**Figure 5.** General practice for VOCs' emission abatement from spray paint booths (adapted from Kim, 2011).<sup>[12]</sup>

## 1.6 Objective of thesis

The main objectives of this research work are:

- i. To investigate the performance of different commercial carbon-based adsorbents for the removal of polar VOCs at low concentration.
- ii. To analyze adsorbents' physical or textural and surface chemical properties which are deemed to play important roles in capturing polar VOCs.
- iii. To design a full-scale sacrificial bed.

## 1.7 Thesis outline

The thesis consists of five chapters that are essential for the fulfillment of the overall goal of this research. Chapter 1 outlines the background and goal of the present work. Chapter 2 includes literature review on adsorption process, adsorption of VOCs on different carbon-based adsorbents and parameters affecting adsorption performance. The materials, experimental methodology, and characterization methods are described in Chapter 3. The results of characterization tests and activated carbons adsorption performance along with the sacrificial bed design parameters are discussed in Chapter 4. Finally, Chapter 5 summarizes the conclusions derived from this project and put forward several recommendations for future works in this field.

## **Chapter 2. Literature Review**

## 2.1 Adsorption overview

According to IUPAC, adsorption is defined as "increase in the concentration of a substance at the interface of a condensed and a liquid or gaseous layer owing to the operation of surface forces."<sup>[26]</sup> Particles inside a solid are held together by a force field originated from ions, atoms or molecules. This force field extends beyond the inside matrix to the surface in an unbalanced way making the solid attract any molecules (gas/liquid or dissolved solid<sup>[26]</sup>) close to its surface. Molecules get trapped into those surface energy sites either physically or by creating chemical bond, shaping a concentration gradient with their bulk phase. Technically, this mass transfer phenomenon is known as adsorption.<sup>[27]</sup> The solid substance is termed as adsorbent while the counterpart is named adsorbate.<sup>[28]</sup> Normally, adsorption is an exothermic process from thermodynamic point of view due to the reduction in the free energy and entropy of the system.<sup>[27]</sup> Heat of adsorption depends on types of adsorbate-adsorbent couple and other physiochemical factors like temperature, pressure, surface functional groups, and so on.<sup>[29]</sup> Adsorption process is spontaneous, efficient, cost effective, and environmentally-friendly; therefore, it has been acknowledged as a viable technique to meet environmental regulations for effluent control.<sup>[27,30,31]</sup>

A porous solid media is the heart of adsorption process and comprises micropores (5 – 20 Å), mesopores (20 – 500 Å), and macropores (> 500 Å).<sup>[32,33]</sup> Micropores and mesopores are the sites to capture the adsorbate molecules depending on relative pressure or concentration while macropores and mesopores serves as diffusion path for them. Three diverse mechanisms play during adsorption based separation process: steric, kinetic and equilibrium. Steric separation mechanism refers to similar sized pores usually micropores, which can screen out larger molecules. Kinetic separation mechanism concerns the difference in diffusion rates of various compounds

which leads to competitive adsorption phenomena. Equilibrium-based separation offers different adsorption capacity for different species where strong adsorbing molecules get the advantage.<sup>[33]</sup>

Adsorption can be categorized by numerous ways. Based on the force field mentioned above, it is of two types: physisorption and chemisorption. The main force in case of physisorption is London type Van der Waals force, which is a weak electrostatic force between the adsorbent and adsorbate.<sup>[27,31,34]</sup> In contrast, chemisorption takes place through chemical reaction by sharing electrons between the adsorbent and adsorbate(s), resulting in a strong chemical bond (usually of covalent type).<sup>[35]</sup> Adsorption can be reversible or irreversible depending on several factors. Usually, physisorption is easily reversible.<sup>[27]</sup> There are ample differences between physisorption and chemisorption, but the most important one is related to their heat of adsorption. In the case of physisorption, the heat of adsorption is about 10-20 kJ/mole while its approximately 400 times higher in chemisorption.<sup>[27]</sup> Physisorption is not so specific; it can imprison all kinds of molecules and deals with multilayer adsorption, but chemisorption is completely specific to certain adsorbate-adsorbent monolayer adsorption process.<sup>[27]</sup>

## 2.2 Isotherms

At equilibrium and at a specific temperature adsorption can be depicted by equations called isotherms, to quantify the extent of fluid with specific concentration attached to the surface.<sup>[36]</sup> Adsorption isotherm is a relation between fluid phase concentration to the adsorbed/solid phase concentration. Adsorbent's specific surface area, pore volume and pore size distribution, microporosity, heat of adsorption and the relative adsorbing capability for diverse adsorbates can be estimated by isotherms.<sup>[27,37]</sup> Langmuir, Freundlich, Dubinin-Radushkevich and Brunauer-Emmett-Teller (BET) isotherm models are most widely used among numerous isotherms which are proposed to fit the classification shown in Figure 6, given by IUPAC.<sup>[38]</sup> The reason for this

classification is that no single adsorption isotherm can fully explain all adsorption data. However, at low concentration (approaching to zero) all the isotherms resemble Henry's law, revealing a linear relationship between amount adsorbed and the pressure of adsorbate.<sup>[27,38]</sup>

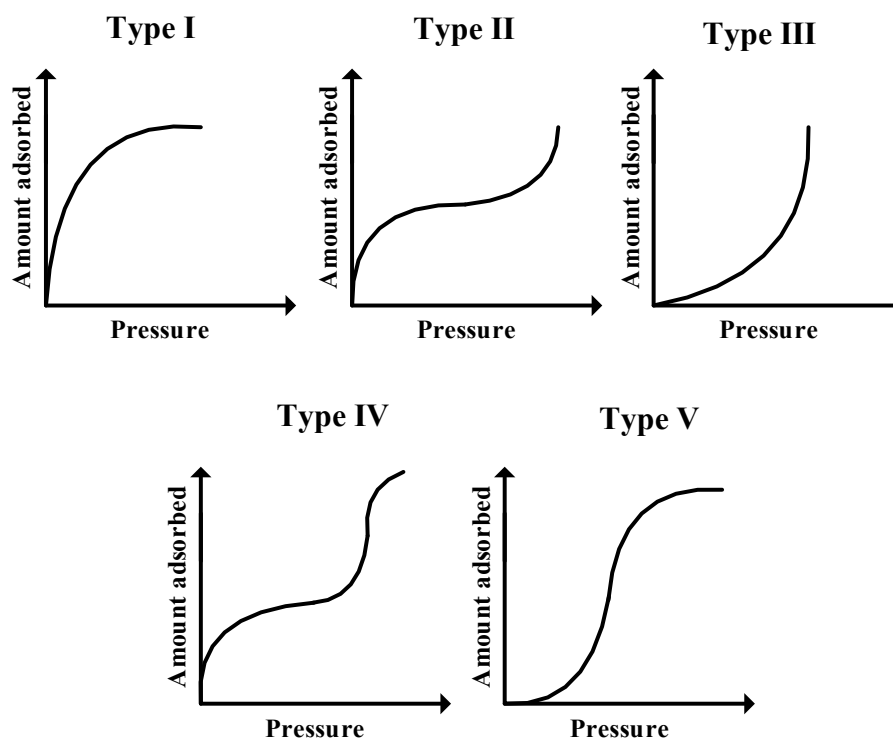


**Figure 6.** Five different types of adsorption isotherms (adapted from Brunauer et al, 1940).<sup>[39]</sup>

Usually chemisorption and physisorption by an adsorbent with extremely high microporous surface (activated carbon or carbon molecular sieves) reveals type I isotherm. Type I mostly deals with monolayer adsorption, so it often can be correlated by Langmuir isotherm model. In fine micropores, force field from neighbouring atoms or molecules tend to overlap, increasing high interaction with adsorbate even at low concentration. At higher concentration or relative pressure, it reaches a plateau, indicating the pores are already filled up.<sup>[27,38]</sup> At point B in Figure 7, it is assumed that monolayer adsorption ends and this serves as a basis for the determination of textural properties of pores.<sup>[27]</sup>



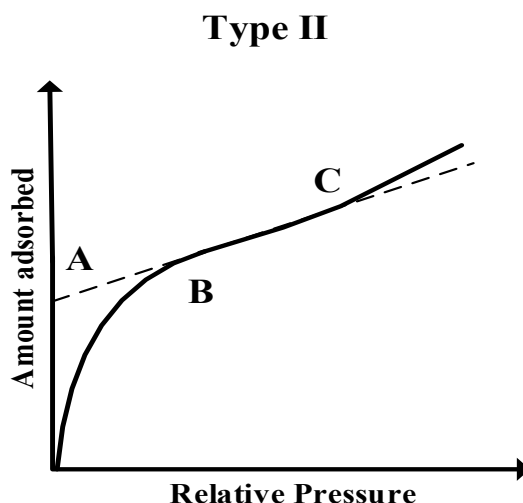


**Figure 7.** Details of type II isotherm (adapted from Bansal and Goyal, 2005).<sup>[27]</sup>

Type III and V isotherms come with convex shape against the pressure or concentration axis. Types III and V belong to non-porous materials and mesoporous structures with micropores, respectively. Owing to these facts, type III convexity continues to grow while type V reaches to a plateau at high pressure. These features are due to the cooperative adsorption where already-adsorbed molecules take part in further adsorption. In other words, adsorbate-adsorbate interaction dominates adsorbent-adsorbate interaction here. Adsorption of water molecules on activated carbons, graphitized carbon blacks and few dehydrated oxide catalysts are some examples of type V isotherm.<sup>[27,38]</sup>

Type IV isotherms are representatives of mesoporous adsorbents. Type IV, to some extent, has resemblance with type II at low relative pressures. It has a linear mid section indicating the filling accomplished through capillary condensation of larger pores. At higher concentration, it reaches saturation and it possesses a hysteresis loop due to the difference in the curvature of the meniscus on adsorption and desorption profiles.<sup>[27,38]</sup>

Isotherms described above can be categorized into two general types – favourable and unfavourable isotherms depending on convex or concave shapes (presented in Figure 8). A convex shape isotherm is favourable at low concentration of adsorbate or low partial pressure where a considerable amount of adsorption occurs before reaching to plateau. In contrary, isotherms with concave shape requires higher partial pressure or higher concentration to attain an economical amount of adsorption. Isotherms which are more favorable for adsorption indicate more unfavorable desorption as well as irreversibility.<sup>[40]</sup>

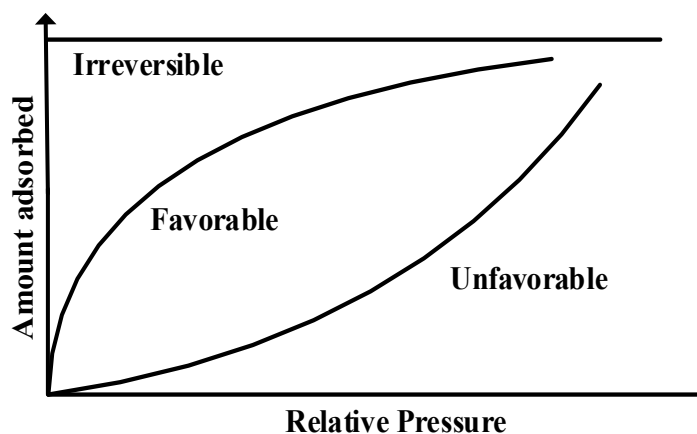


**Figure 8.** Favorable and unfavorable adsorption isotherms (adapted from Alan Gabelman, 2017).<sup>[40]</sup>

### 2.3 Adsorbents and their characterization

Porous solids can act as adsorbent and their adsorption capability depends on several properties which can be classified into two main categories: physical and chemical. Mostly their performance is determined by surface physical properties than chemical ones.<sup>[27,31,35,41]</sup>

Total pore volume can be determined by helium and mercury displacement methods. In addition, pore size distribution (PSD) can be measured by several methods such as - mercury

porosimetry, N<sub>2</sub> adsorption-desorption and/or molecular sieving depending on the ranges of the pore sizes.<sup>[35]</sup>

Chemical properties include elemental composition, surface functional groups, surface oxygen functional groups, surface acidity and basicity, pH at point zero charge (pH<sub>pzc</sub>), and isoelectric point. These can be analysed through a multitude of techniques like X-ray photoelectron spectroscopy (XPS), nuclear magnetic resonance (NMR), Fourier transform infrared spectroscopy (FTIR), temperature-programmed desorption (TPD), X-ray absorption near edge structure (XANES), thermogravimetric analysis (TGA), acid-base neutralization (e.g. Boehm titration and potentiometric titration) and etc.<sup>[42]</sup> The procedures used to characterize samples during this project are explained in Chapter 3.

Adsorbents can be prepared from wealth of sources and through numerous preparation routes. Microporous materials have the capability for gas purification and are generally classified into carbon based and non-carbon based. Among non-carbon based materials calcinated clays, iron oxide, calcinated bauxites, activated alumina, silica gel, silica alumina impregnates, zeolites, and polymeric adsorbents have been commercially used for years.<sup>[31,35,43]</sup> Metal frameworks, mesoporous silicas, synthetic zeolite, clay type natural porous minerals (like bentonite and diatomite) all are under investigation for their future commercialisation.<sup>[43,44]</sup> Carbon based adsorbents and especially activated carbons are the most widely investigated and applied adsorbents and are discussed in length in the next section.

## **2.4 Carbon based adsorbents**

Active carbons comprise a wide range of carbonaceous materials exhibiting high porosity and high intraparticle surface area.<sup>[27]</sup> They are prepared from variety of carbon containing

precursors like coal (anthracite, bituminous and brown coal), chars (bone or coals), lignite, wood, coconut shell, petroleum pitch and also from synthetic polymers by combustion, partial combustion or thermal decomposition.<sup>[27,38]</sup> Novel carbon materials are also emerging like nanofibers, nanotubes, graphene, nano diamonds, fullerene, etc.<sup>[13,45,46,47]</sup>

Usually elemental analysis provides the composition of activated carbons. They are mostly made of 85 – 95 % carbon, 6 – 7 % oxygen (may rise to 20 %), 0.5 % hydrogen, 0.5 % nitrogen, 1 % sulphur, and the rest is inorganic metallic content termed as ash.<sup>[35]</sup> Most carbons have some kind of oxygen surface functional groups along with ash both arising from source material or activation process.<sup>[35]</sup> Ash is mainly silica, alumina, iron alkaline, and alkaline earth metals, and its quantity may vary from 1 to 12 %.<sup>[31]</sup> Ash can affect adsorption performance of activated carbons through inducing hydrophilicity, modifying pore size distribution (PSD) by implanting larger pores, and to some degree enhance irreversibility through oxidative coupling.<sup>[31,48]</sup>

Commercial production of activated carbon encompasses raw material or base preparation, pelletization, pyrolysis, carbonization and activation stages. After basic treatment and pelletizing, base materials undergo high temperature pyrolysis at 1000 °C (or slightly below) to remove all the volatile contents. Carbonization is accomplished at around 800 °C to generate a microcrystalline structure. Finally, activation is done at 950 -1000 °C under inert environment to produce the desired porous structure. Properties of the final product exclusively depend on source content, activation agent and process condition.<sup>[31,35]</sup> Phosphoric acid, zinc chloride, potassium sulfide, and potassium thiocyanate are common strong activators and oxidizing gases such as CO<sub>2</sub>, steam, and flue gas are considered mild activators.<sup>[27,31,35]</sup> ACs come in a wide range of shapes or morphologies like powdered, granular, pelleted, beaded, fibers, felt, and clothes (Figure 9).

**a.****b.****c.****d.****e.****f.**

**Figure 9.** Different types of activated carbons- **a.** PAC,<sup>[49]</sup> **b.** non-pelleted GAC,<sup>[50]</sup> **c.** pelleted GAC,<sup>[51]</sup> **d.** BAC,<sup>[52]</sup> **e.** ACFC,<sup>[53]</sup> **f.** ACF.<sup>[54]</sup>

**Powdered Activated Carbons (PACs)**- powdered form of activated carbons are produced from wood-based materials like saw dust and rice husks. Their average particle size varies from 15 to 25  $\mu\text{m}$ , which is suitable for the use in liquid medium and facilitates subsequent separation and regeneration. Mostly they are used in food industries, brewery section and wastewater treatment plants. They are rarely regenerated due to the utilization of their surface charge, making it difficult to separate them from bulk.<sup>[31]</sup>

**Granular Activated Carbon (GACs)**- They might be either crushed or pelleted with some binders like coal tar pitch.<sup>[31]</sup> GACs are prepared from both wood and coal-based sources. They can be produced in many sizes depending on specific applications. For instance, small particle dimension is favorable for adsorption, but they complicate handling and other factors.<sup>[31]</sup> Nevertheless, for liquid medium 8  $\times$  20, 20  $\times$  40, and 8  $\times$  30 mesh sizes are applicable, and 4  $\times$  6, 4  $\times$  8 or 4  $\times$  10 sizes are more suitable for gas phase applications.<sup>[55,56]</sup> GACs are often used in solvent recovery, decontamination of air and gases, desulfurization of flue gas, gas-gas separation, sugar refinery and wastewater treatment.<sup>[31]</sup>

**Beaded Activated Carbons (BACs)** – Their high hardness and high attrition resistance provide higher structural integrity as compared to other coal or wood-based carbon materials.<sup>[57]</sup> Their high flowability resulting from spherical shape helps them to reach every corner of a complex vessel during industrial applications like fluidized bed reactors. They are commercially produced from pitch, usually free from metal impurities because of no use of binders. So, the final product is free of dust and ash content. <sup>[52,57]</sup>

**Activated Carbon Fiber Clothes (ACFCs)** – Activated carbon fibers or clothes or felts are promising materials for gas phase application and they are suitable for filtering applications.

They are prepared from organic fibers (including polyacrylonitrile, cellulose, phenolic resin, and pitch) by carbonization at 700-1000 °C followed by activation using steam/CO<sub>2</sub>. Their carbon content is high, they possess low amount of oxygen and hold no ash content.<sup>[58]</sup> Micropores are readily available at their surface, so adsorption rate is quite faster as compared to other carbon materials.<sup>[59]</sup> Furthermore, ACFs morphology (felt, fiber, mesh, or cloth) makes them favorable due to ease of handling.<sup>[18]</sup>

Apart from high porosity, there are some other general advantages related to activated carbon adsorbents<sup>[18,35]</sup>:

- It can perform separation and purification at a time in both gaseous and liquid medium without prior moisture elimination.<sup>[35]</sup>
- Different pore sizes and large reachable internal surface (different from pore surface<sup>[27]</sup>) can trap both polar and non-polar organic compounds.<sup>[35]</sup>
- The heat of adsorption is usually lower compare to other adsorbents; thus, regeneration is quite easier.<sup>[35]</sup>

The most important drawbacks of carbon materials are their flammability during high temperature applications and regeneration along with pore blockage, fouling, and generation of toxic compounds from adsorbates.<sup>[60,61,62]</sup>

## **2.5 Factors affecting adsorption**

Breakthrough curve, mass transfer zone, adsorption capacity and isotherms are quantitative indicators that are often used to gain insight into the adsorption process. Adsorption process is influenced by adsorbent and adsorbate properties and operating conditions, which will be discussed briefly in the following section.

### **2.5.1 Influential properties of adsorbent**

Specific surface area, pore size, pore size distribution, and surface functional groups play important roles in VOCs adsorption. Bulk density is also another important property which is very relevant for design purposes.<sup>[18]</sup>

#### **Specific surface area**

Larger surface area benefits the adsorption process and, consequently, numerous studies have been focused on the effect of surface area on adsorption capacity. Specific surface area can be modified either by opening the inaccessible pores or creating new pores through treating with acid, base heat, microwave, plasma, impregnation, etc.<sup>[18]</sup>

#### **Pore size**

Pore size distribution is a critical factor during adsorption since large molecules prefer mesopores, while small ones show more affinity towards micropores.<sup>[63]</sup> Among the micropores, narrower ones (5-8 Å) predominates the entire mass transfer for smaller molecules.<sup>[18,64]</sup> In some cases, macropores or mesopores mainly serve as transport channels to smaller pores and in such way contribute to the adsorption.<sup>[18]</sup> It has been proposed that mesopores can lead to faster adsorption rate due to higher intraparticle diffusion rate.<sup>[41]</sup> To investigate the influence of PSD, it is crucial to first rule out the impact of surface functional groups and surface area of the adsorbent(s).<sup>[18]</sup>

#### **Surface functional groups**

Nature of the source material, way of activation, modification through heating, and chemical and electrochemical treatments can introduce surface functional groups.<sup>[18,27,41,65,66,67]</sup> Functional groups are usually located at the edges and corners of atomic sheets or defect



positions.<sup>[27]</sup> Oxygen surface functional groups are of three types: acidic, basic and neutral. Oxygen groups can alter wettability, acidity, polarity, catalytic, electrical and chemical reactivity.<sup>[18,27]</sup> Four different acidic groups arise from oxidation phase:

- Carboxylic groups,
- Carbonyl groups,
- Lactone groups and
- Phenolic groups.

Cyclic ether groups are also available and carboxylic groups can merge with carbonyl and lactone groups in activated carbons.<sup>[31]</sup> Liquid phase oxidation introduces carboxylic groups, while gaseous oxidation leads to formation of hydroxyl or carbonyl groups in activated carbons.<sup>[18]</sup> To increase the acidic range as well as polarity of activated carbons (indicated by the reduction of  $\text{pH}_{\text{pzc}}$  from basic to acidic), ozone treatment is employed.<sup>[68,69]</sup> At elevated temperatures, these acidic groups decompose and make the carbon surface less favorable to hydrophilic compounds. The decomposition temperature of acidic groups is very specific and depends on their thermal stability. The differences in thermal stability of various acidic groups allows one to employ Temperature Programmed Desorption (TPD) method to quantify each group in activated carbon.<sup>[42]</sup> Figure 10 depicts the temperature range for different acidic groups using TPD method.

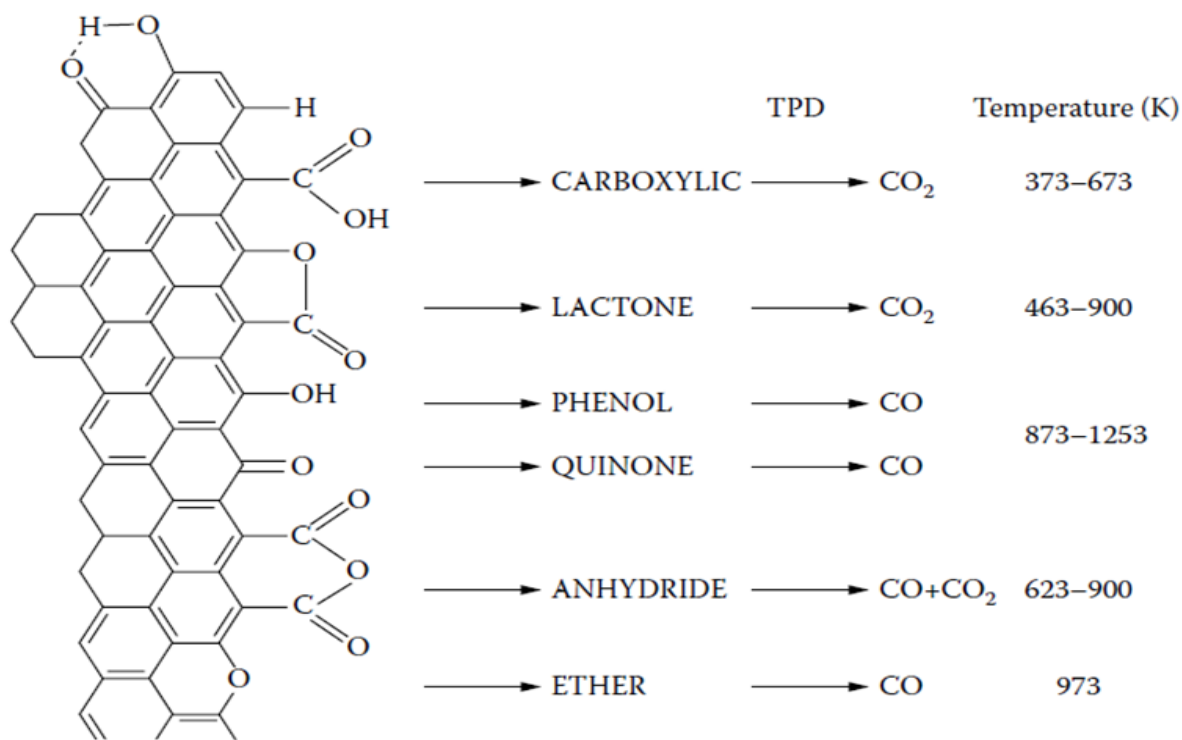


**Figure 10.** Range of decomposition temperatures by TPD for carbon surface functional groups.<sup>[42]</sup>

If carbon is treated with ammonium, nitric acid, and N-containing compounds at elevated temperatures, basicity is introduced due to the formation of imide structures from cyclic anhydrides and/or lactone groups.<sup>[27]</sup> Basic nature of activated carbon comes either from oxygen or nitrogen; however, several studies suggested that basicity in fact results from the pyrone structures.<sup>[42,70,71,72]</sup> Figure 11 depicts all the surface functional groups in activated carbons.

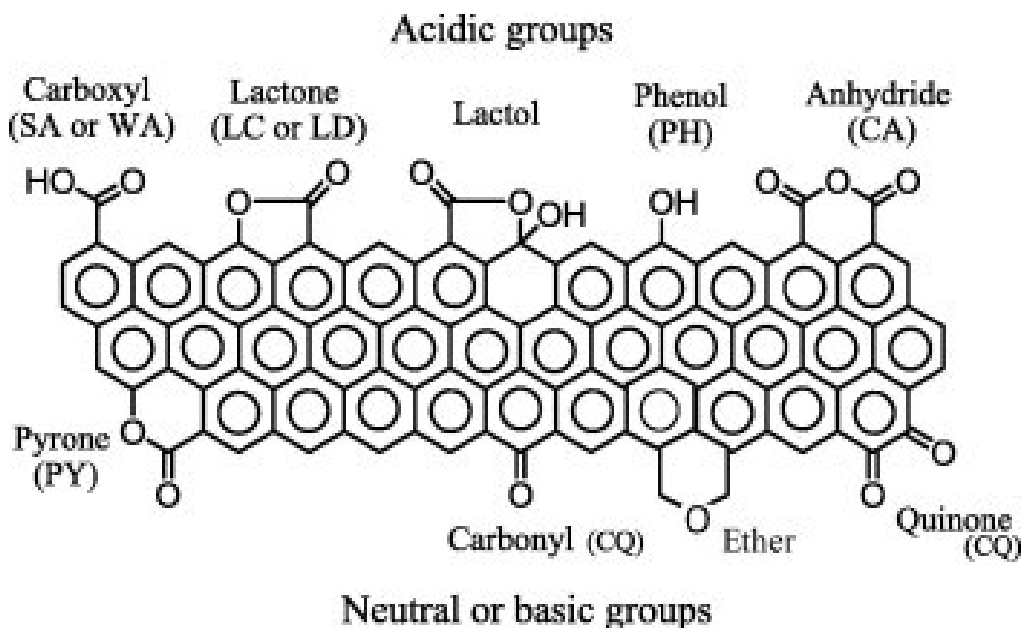


**Figure 11.** Carbon surface functional groups with basicity.<sup>[73]</sup>

### 2.5.2 Influential properties of adsorbate

Molecular weight and dimension, kinetic diameter, polarity, solubility, boiling point, and vapor pressure are properties of the adsorbate that can significantly impact the adsorption performance.

#### Molecular structure

Molecular weight and molecular dimensions (e.g. kinetic diameter) are closely correlated and usually they are proportional. Molecular dimension strictly refers to the cross-sectional area rather than any minimum dimension like width, length or thickness.<sup>[18]</sup> As a general behavior, small molecules are favorable to small pores and large size molecules are adsorbed in larger pores. In addition, it has been observed that the adsorbability deteriorates as the size difference between the pollutant and pore increases considerably.<sup>[18]</sup> The importance of molecular shape during adsorption can be easily explained in Figure 12, illustrating the adsorption of xylene isomers and

ethylbenzene. Figure 12 shows that ethylbenzene, o-xylene, p-xylene and m-xylene do not have the same adsorption tendency owing to their molecular structure. [18,74]

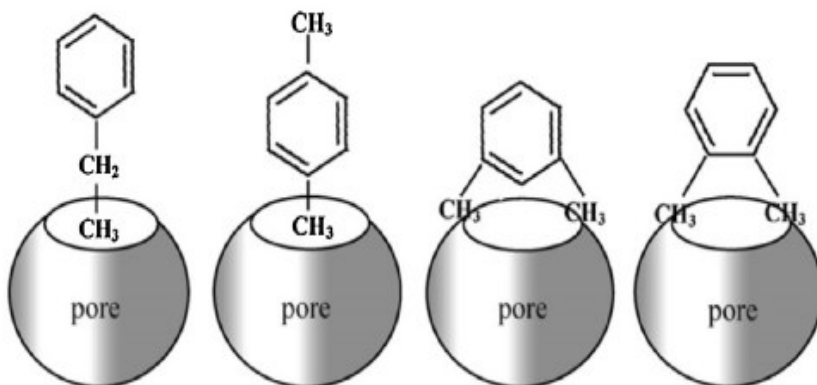


**Figure 12.** Preferential adsorption of ethylbenzene and p-xylene as compared to o-xylene and m-xylene.<sup>[18]</sup>

### Polarity

Polar VOCs preferentially adsorb on polar adsorbents and naturally non-polar ones better adsorb on non-polar porous materials. Inorganic impurities and surface acidic groups impart polarity to originally hydrophobic carbon substances. In some cases, carbons show highly polar activity either just after preparation or by further surface modification through oxidation (e.g. with ozone and HNO<sub>3</sub>). As already mentioned in section 2.1, about the Van der Waals attractive forces between neutral adsorbate molecules are of three types, namely induced-dipole/induced-dipole forces, dipole/induced-dipole forces and dipole-dipole forces. For non-polar molecules (such as propane, butane, toluene, n-hexane) induced-dipole/induced-dipole forces are the main reason for intermolecular attractive forces. In contrary, polar molecules engage in dipole/induced-dipole forces and dipole-dipole forces in addition to dispersion interactions (London forces) which govern their adsorption process.<sup>[75]</sup> Here, intramolecular potential energy might decline owing to

dipole-dipole interaction between adsorbent and polar adsorbate to facilitate adsorption process.<sup>[18]</sup> Qian et al. showed molecules with high dipole moment as well as high polarity like CH<sub>2</sub>CL<sub>2</sub> and CH<sub>3</sub>I (1.8 and 1.59 Debyes, respectively) exhibit higher capacity with micro spherical AC than molecules with lower dipole moment (CHCl<sub>3</sub> -1.1 and CCl<sub>4</sub> - 0 Debyes)).<sup>[18,76]</sup>

### **Volatility**

Highly volatile organic VOCs have lower intermediate forces compared to less volatile ones and consequently a lower probability of adsorption. This is valid with some mathematical correlations having 'R<sup>2</sup>' values close to 1 with a range of experimental analysis.<sup>[77,78]</sup> It is applicable to all kind of porous adsorbents due to the resemblance of physisorption with condensation.<sup>[79]</sup> High boiling point compounds possess superiority during competitive adsorption since they can replace highly volatile species. However, high boiling point VOCs face difficulties during regeneration and usually require higher temperature and higher energy input.<sup>[18]</sup>

### **Adsorption potential**

Adsorption potential gives quantitative description of physical adsorption of adsorbates on strongly heterogeneous surfaces, such as activated carbons. Theoretically, higher adsorption potential indicates higher possibility of adsorption and vice versa.<sup>[27]</sup> Thermodynamically, adsorption potential is defined by the amount of isothermal work done to compress one mole of adsorbate from equilibrium vapor pressure to the saturated vapor phase for completely liquefied adsorbate. According to Polanyi, adsorption potential can be expressed as<sup>[27]</sup> –

$$\varepsilon = RT \ln \frac{P_s}{P}$$

where  $R$  is the ideal gas constant,  $T$  is the temperature at which adsorption is taking place,  $P_s$  is the saturation vapor pressure of the liquid adsorbate at temperature  $T$ , and  $P$  is the equilibrium vapor pressure.<sup>[27]</sup>

For adsorbates with ideal homogenous energy sites, all the points at same distance from the adsorbent surface have the same adsorption potential  $\epsilon$  and virtually creates an equipotential plane. Adsorption potential of the parallel equipotential planes decreases as their distance from the surface increases and becomes zero at maximum distance. As the adsorbate molecules are compressed while approaching from equipotential planes of maximum distance (from zero adsorption potential plane) towards the active adsorption sites, their density tends to increase. Density of adsorbent molecules reaches its highest value at that equipotential plane with highest adsorption potential.<sup>[27]</sup>

### **2.5.3 Influential operating conditions during gaseous adsorption**

Operating conditions such as temperature, relative humidity of the gas, concentration of adsorbate, superficial gas flow rate and presence of other adsorbates also play vital role during adsorption process.

#### **Temperature**

Several studies reported that, increment in temperature brings about a reduction in adsorbed amount of VOC specially in case of physisorption.<sup>[18,80,81]</sup> To some extent, high temperature has some positive effects during adsorption by increasing molecular diffusion or facilitating interaction between VOCs and carbon materials typically in chemisorption.<sup>[18,81,82]</sup>

## Humidity

Though carbons are hydrophobic, still they adsorb water molecules at high relative humidity levels, exhibiting 'S' shape isotherms. This can be best explained by Dubinin-Serpinsky theory which assumes cooperative adsorption.<sup>[18]</sup> Surface oxygen functional groups serve as adsorption sites for water molecules and these adsorbed species connect more and more water molecules via hydrogen bonding, eventually leading to capillary condensation in the porous structure.<sup>[83,84]</sup>

## Concentration

Mass transfer phenomenon during adsorption depends on the concentration of adsorbate and it is important to understand the entire mass transfer process to interpret the effect of adsorbate concentration. Generally, mass transfer happens in three sequential steps namely film diffusion or external diffusion, internal diffusion and adsorption.<sup>[75,85,86]</sup> Film diffusion refers to the transport of adsorbate molecules from bulk fluid to the film surrounding the solid adsorbent matrix. Film diffusion is explained by the linear Ficks law,

$$N_A = h_m (C_b - C^*),$$

where,  $N_A$  is the mass flux ( $\text{mg}/\text{m}^2 \cdot \text{s}$ ),  $C_b$  is the gas concentration in the bulk phase ( $\text{mg}/\text{m}^3_{\text{air}}$ ),  $C^*$  is the gas phase concentration adjacent to the surface of the adsorbent particle in equilibrium with the adsorbed phase concentration ( $\text{mg}/\text{m}^3_{\text{air}}$ ) and  $h_m$  is the convective mass transfer coefficient in packed beds which can be estimated by empirical correlations.<sup>[75,85]</sup> Film diffusion is important to explain the low concentration adsorption because it considers the difference in concentration of adsorbate in the bulk flow and that in the vicinity of adsorbent's surface. Concentration gradient is the obvious driving force here, which is again controlled by the bulk phase concentration. In

case of low concentration of adsorbates, the driving force is not high enough to easily overcome the resistances during mass transfer.<sup>[75]</sup>

Film diffusion is followed by internal diffusion of adsorbates from this film to the adsorbent pores. Internal diffusion occurs in two parallel ways – pore diffusion (molecular diffusion in macropores and Knudsen diffusion in micropores)<sup>[75]</sup> and surface diffusion. High concentration facilitates the entire intraparticle diffusion stage by overcoming the diffusion resistance.<sup>[75,86]</sup> Finally, adsorption occurs at the active sites instantaneously which is an equilibrium step. However, high concentration is actually a favorable condition in overall to create enough driving force to overcome the mass transfer resistances.<sup>[86]</sup>

### **Gas flow rate**

Higher gas flow rate leads to faster breakthrough or saturation due to increase in the length of mass transfer zone. Longer mass transfer zone indicates poor bed utilization. In an ideal case, the length of mass transfer zone approaches nearly zero, indicating instant mass transfer without any resistance.<sup>[40,87]</sup> Lower gas velocity provides adsorbates with more time to be in contact with the adsorbents, resulting in a higher removal efficiency. Optimum velocity ensures enough residence time for adsorption bed utilization while keeping the pressure drop within an acceptable range.<sup>[87]</sup>

### **Presence of other adsorbates**

Multicomponent adsorption involves adsorbate-adsorbate and adsorbent-adsorbate interactions. Adsorbate-adsorbate interaction refers to the competition of adsorbates for active sites where compounds with stronger adsorption affinity preferentially adsorbed into the adsorbent. In some cases of multicomponent adsorption, the adsorbed molecules of adsorbates with lower affinity are replaced by compounds with higher affinity towards the adsorbent.<sup>[88]</sup> It is noteworthy



that compared to the single component adsorption, our understanding of multicomponent adsorption systems is limited primarily due to the complex diffusion processes.<sup>[89]</sup>

## 2.6 Adsorbent selection criteria

Selection of an adsorbent is very much case specific and depends on several key factors [35].

- Equilibrium isotherm at desired temperature and pressure.
- Adsorbent capacity for the target compound at specific concentration and operation conditions (temperature, pressure and acid-base medium).
- Length of unused bed at 5 %, 50 % and 100 % breakthrough time and throughput values.<sup>[90,91]</sup>
- Requirement of purity level of product.
- Relative humidity of air to be treated.

## 2.7 Adsorber types

Some of the most widely applied adsorber designs for VOC control<sup>[92]</sup> are summarized below.

- **Fixed regenerable beds** – They can handle over a wide range of batch, semi-batch, and continuous gas flow. They are applicable to flammable and toxic environments. They can also be used to treat air streams with extremely low concentrations of VOCs (~ ppbv level). A common problem with fixed bed adsorbers is improper mass transfer because of channeling or clogging. Some other drawbacks are potential hot zones, risk of bed fire, high pressure drop, and high operating cost.<sup>[92]</sup>
- **Fixed sacrificial beds** – These beds are quite similar to fixed beds and are usually employed to capture low concentration of VOCs remaining in the residual air stream after the main separation stage. Since regeneration is not a necessity for these adsorbers, after saturation, bed material is normally discarded.<sup>[12,92]</sup>

- **Cannisters, either disposable or regenerative** – When off-site regeneration is advantageous, these type of adsorbers are used. These adsorbers are typically small containers that can be easily handled and returned to the site after regeneration. They can exclusively control low volume and intermittent gas streams. <sup>[92]</sup>
- **Fluidized bed adsorbers** – They offer continuous and smooth operation with lower pressure drop, faster adsorption kinetics and steeper breakthrough curves even at high gas flow rates. <sup>[92,93]</sup>

## 2.8 Design of a sacrificial fixed bed

Design and cost of a sacrificial bed depend on several requirements imposed by the process conditions<sup>[92]</sup>:

- Volumetric flow rate of VOC contaminated gas,
- Input and output concentrations,
- Service life,
- Equilibrium capacity of adsorbent and
- VOC-laden stream conditions (e.g. humidity, corrosive nature, etc).

### 2.8.1 Estimating carbon requirement

Carbon requirement calculation for bench scale or scale up for sacrificial bed can be accomplished by using length of unused bed (LUB) approach. Despite being an empirical approach, it is validated by some other established models like Wheeler Jonas equation and Thomas model.

### 2.8.2.1 LUB method

LUB refers to the segment of carbon bed that is not saturated at the breakthrough time. A bench scale set-up is usually utilized to simulate the real scenario and generate relevant data. Figure 13 shows a typical breakthrough profile, which is simply a demonstration of VOC output concentration from an experimental bed against time. Up to a certain point, there is no upward response in the breakthrough profile. The breakthrough time depends on several parameters including adsorbate-adsorbent interaction, amount of adsorbent, operating conditions and adsorbate concentration. To rule out the dependency of breakthrough time on many parameters, slope of breakthrough curve is taken into consideration, which is almost constant for a specific adsorbate-adsorbent couple with a fixed adsorbate concentration.<sup>[94]</sup>

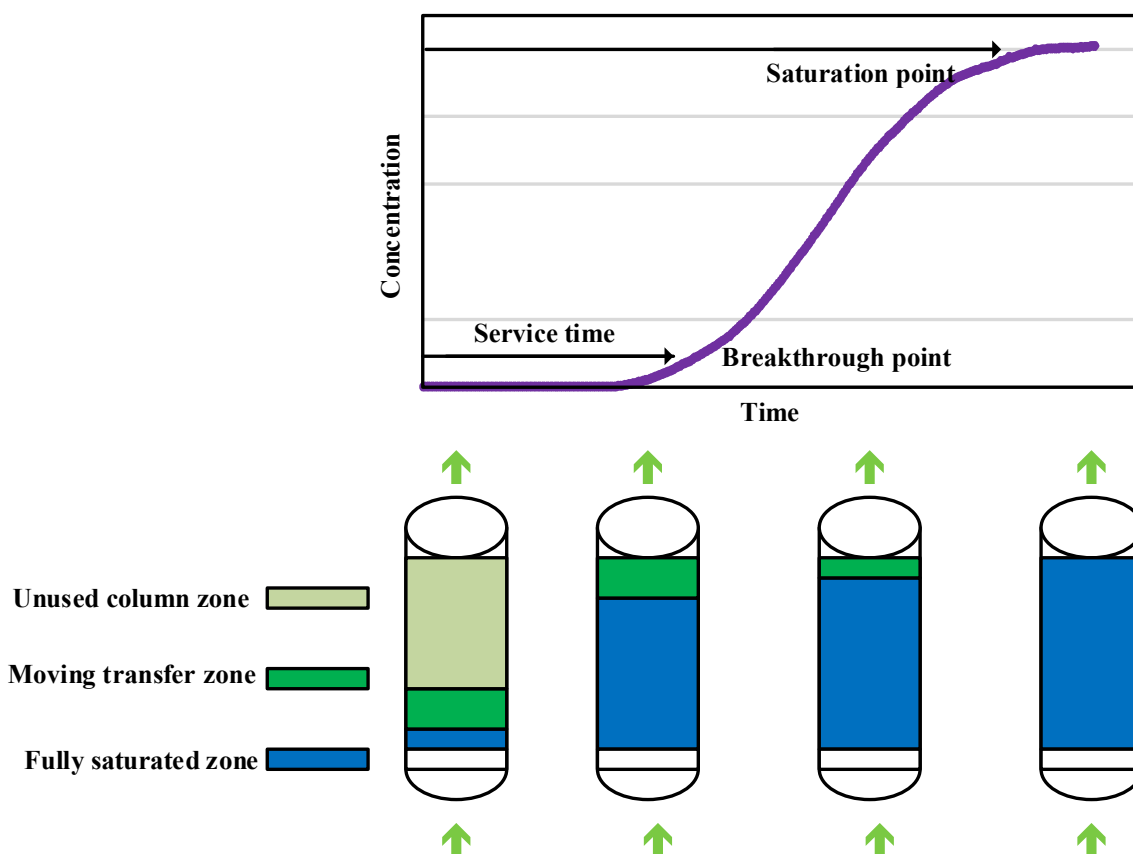


**Figure 13.** Typical breakthrough profile of adsorbents.<sup>[90,95]</sup>

Experimental LUB results are utilized to perform the scale up for large scale operations. The most important point during the scale up is to keep the superficial velocity at a constant value throughout the column to have a consistent mass transfer zone. It is also worth mentioning that the unused portion of the bed is constant for both bench scale and full scale since their breakthrough profiles have same slope. The detailed procedure to determine LUB is explained in Chapter 3.<sup>[84]</sup>

### 2.8.1.2 Model used to design sacrificial bed

#### Thomas model

This model is exclusively applicable to gaseous adsorption systems designed with activated carbons where feed flow is constant with negligible axial dispersion. The basic assumption is related to the Langmuir isotherm applied to a plug flow type reactor with second order reversible reaction kinetics.<sup>[96]</sup> This model is suitable for LUB method validation and the carbon requirement calculation. According to this model, effluent concentration at 5 % breakthrough time (BT) time can be calculated as follows:

$$\frac{C_{out}}{C_{in}} = \frac{1}{1 + \exp\left(\frac{K_{th} \times W_e \times W}{Q} - C_{in} \times K_{th} \times t_b\right)}$$

where,  $t_b$  is breakthrough time,  $W_e$  is adsorption capacity of carbon at saturation,  $W$  is carbon bed weight or carbon requirement,  $C_{in}$  is initial vapor concentration,  $C_{out}$  is breakthrough or effluent concentration,  $Q$  is airflow rate and  $K_{th}$  is Thomas rate constant.

#### Bohart-Adams model

This model assumes that adsorption rate depends on residual adsorbent capacity and remaining adsorbate concentration simultaneously. According to this model, the bed depth service time can be determined as follows:<sup>[97]</sup>

$$\text{BDST} = \frac{N^0 D}{v \cdot C_{in}} - \frac{1}{K_v C_{in}} \ln \left( \frac{C_{in}}{C_{out}} - 1 \right)$$

where  $N^0$  represents adsorption capacity of carbon,  $v$  is the superficial velocity of gas,  $D$  is depth of the bed and  $K_v$  is the adsorption rate coefficient.

### **Wheeler-Jonas equation**

This equation consists of two parts; the first one assumes ideal plug flow and provides the theoretical capacity of carbon material. The second part is related to the actual axial dispersion due to non-instantaneous adsorption kinetics and represents the width of mass transfer zone.<sup>[98]</sup> Due to the simplicity and availability of input parameters, Wheeler-Jonas equation has been used for a wide range of VOCs adsorption breakthrough specially with activated carbons.<sup>[99]</sup>

$$\text{Breakthrough Time, } t_b = \frac{W_e \cdot W}{Q \cdot C_{in}} - \frac{\rho_b W_e}{K_v C_{in}} \ln \left( \frac{C_{in}}{C_{out}} \right)$$

where,  $t_b$  is the breakthrough time,  $W_e$  is for adsorption capacity of carbon,  $W$  stands for carbon bed weight,  $C_{in}$  and  $C_{out}$  are challenge vapor concentration and breakthrough concentration, respectively,  $Q$  is for airflow rate,  $\rho_b$  stands for bulk density of carbon bed and  $K_v$  refers to adsorption rate coefficient.

## **Chapter 3. Materials & Methods**

### 3.1 Adsorbents

Eleven carbon samples belonging to major three categories of carbon-based adsorbents were investigated in this study - beaded activated carbon, activated carbon fiber cloth, and granular activated carbon. Experiments were conducted to find the best sacrificial adsorbents based on breakthrough analysis and adsorption capacity. All the samples were dried in an oven for 24 h at 140 °C and cooled down to room temperature in a desiccator prior to the adsorption and characterization tests. Screening was done using Fisher Scientific sieve series for crushed samples. Suppliers detail and physical properties claimed by suppliers are listed in Table 3 and 4.

**Table 3.** Description of tested adsorbents.

Types of adsorbents	Adsorbents (Trade name)	Type & shape	Supplier	Sources	Experimental form	Cost/kg
BACs <sup>[57]</sup>	Virgin BAC (BAC G -70R)	AC Beads (sphere)	Kureha Corporation	Petroleum pitch	As received	Medium
	Spent BAC (0.7AD)	Used BAC (sphere)				
ACFCs <sup>[100]</sup>	ACFC 10 (ACC-5092-10)	Twilled-weave fabrics	Gun Ei Chemical Industry	Phenol-formaldehyde resin precursor	1-inch split fiber	High
	ACFC 15 (ACC-5092-15)					
	ACFC 20 (ACC-5092-20)					
GACs <sup>[101,102,103,104]</sup>	OVC (4 × 8)	Granulated AC	Calgon	Coconut shell	Crushed (20 x 50)	Low
	BPL (4 × 10)		Carbon	Bitumen coal		
	VC48C (4 × 8)		Evoqua	Coconut shell		
	VCRSD (4 × 10)			Bitumen coal		
Pelleted GACs <sup>[105,106]</sup>	WV-A 1100 (8 × 25)	Granulated AC (pelleted)	Ingevity	Wood based	As received	Low
	WV-A 1500 (10 × 25)					

**Table 4.** Physical properties of tested adsorbents.

Adsorbents (Trade name)	Fill/ apparent density (g/cc)	Specific surface area (m <sup>2</sup> /g)	Residue on ignition/ Ash (wt %)	Hardness number (%)	Butane Activity (wt %)	Carbon Tetrachloride (wt %)				
							Weight (g/m <sup>2</sup> )	Thickness (mm)	Typical size/ Roll	
		Width (cm)	Length (m)							
BAC G-70R	0.6	1100 ~1300	0.05 %	95 %	-	-				
Spent BAC	-	-	-	-	-	-				
ACFC 10	-	> 800	-	-	-	-	200	0.65	115	35
ACFC 15	-	> 1300	-	-	-	-	170	0.60	110	35
ACFC 20	-	> 1800	-	-	-	-	135	0.55	105	35
OVC <sup>[101]</sup>	0.45 min	-	3 max	97 min	-	60 min				
BPL <sup>[102]</sup>	0.44 (min)	-	-	93 (min)	23.3 (min)	-				
VC48C <sup>[103]</sup>	0.45-0.52	-	-	95	23.5	60				
VCRSD <sup>[104]</sup>	0.45-0.56	-	-	-	19.5-23.5	50-60				
					ASTM BWC (g/100 ml)		Durability after 500 GWC cycles	GWC (g/L)	Pressure Drop at 15 cm/sec (kPa/cm)	
WV-A 1100 <sup>[105]</sup>	0.27	-	-	-	11.3	-	<10 % loss	55	0.040	
WV-A 1500 <sup>[106]</sup>	0.28	-	-	-	15.3	-	<10 % loss	70	0.040	



Some of the unique features of the activated carbon samples, according to their suppliers, are shortlisted -

**BACs** – Highly spherical and has some unique features along with adsorption performance like- high bulk density, high flowability, low carbon dust, high purity, high strength, high wear resistance and narrow particle size distribution.<sup>[57]</sup>

**Spent BACs** are Kureha BAC that have been utilized in industry for a significant period. They are also tested here as a low-cost alternate solution for using as sacrificial bed material.

**ACFCs (ACFC 10, ACFC 15 and ACFC 20)** are well etched, pliable and strong. Very sharp pore size distribution (uniform and straight) which is well correlated with specific surface area. Very efficient adsorption and desorption due to pore configuration and high surface to volume ratio.<sup>[100]</sup>

**GACs** –

**OVC** is made from specific grade of coconut shell and that is why its expected life is long with high hardness. It has high surface area, fine pore structure, high density, high-volume activity and potential for low pressure drop. Thermal reactivation is possible to reduce the disposal cost.<sup>[101]</sup>

**BPL** on the other hand, has low density, high pore volume, high surface area and low void fraction. It can quickly and strongly adsorb wide range of contaminants and concentrations. Reactivation and reuse are possible and pressure drop is low during adsorption due to their geometric shape.<sup>[102]</sup>

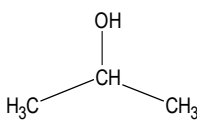
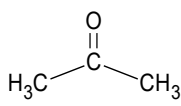
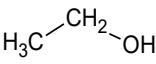
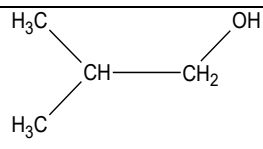
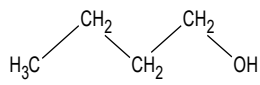
**VC48C** and **VCRSD** are highly active, having high surface and pore diffusion rates (specially for small molecules), a short contact time, low dust generation, and low pressure drop. They are cost effective, reusable and environment friendly.<sup>[103,104]</sup>

**WV-A 1100** and **WV-A 1500** have high gasoline working capacity, low density and excellent durability. Comparatively they are cheaper than other non-pelleted GACs (OVC, BPL).<sup>[105,106]</sup>

### **3.2 Adsorbates**

The exhaust stream coming from the fluidized bed mainly contains polar VOCs, because activated carbons favor non-polar adsorbates due to their hydrophobic natures. The target polar VOCs are 2-propanol, acetone, ethanol, 2-methyl-1-propanol, 1-butanol. All the breakthrough experiments were conducted for single compounds at low concentration. Table 5 lists all the relevant physical and chemical properties of target polar adsorbates. Here, adsorption potential is calculated according to the potential theory of adsorption introduced by Polanyi as described in Section 2.5.2 in Chapter 2.<sup>[27]</sup> The detailed sample calculation procedure to determine the adsorption potential of 10 ppmv 2-propanol is shown in appendix J.

**Table 5.** Physical and chemical properties of target adsorbates.

<b>Adsorbates</b>					
<b>Features</b>	<b>2-propanol<sup>[107]</sup></b>	<b>Acetone<sup>[108]</sup></b>	<b>Ethanol<sup>[109]</sup></b>	<b>Isobutanol<sup>[110]</sup></b>	<b>n-butanol<sup>[111]</sup></b>
<b>Chemical Formula</b>	CH <sub>3</sub> CHOHCH <sub>3</sub> (C <sub>3</sub> H <sub>8</sub> O)	CH <sub>3</sub> COCH <sub>3</sub> (C <sub>3</sub> H <sub>6</sub> O)	CH <sub>3</sub> CH <sub>2</sub> OH (C <sub>2</sub> H <sub>6</sub> O)	(CH <sub>3</sub> ) <sub>2</sub> CHCH <sub>2</sub> OH (C <sub>4</sub> H <sub>10</sub> O)	CH <sub>3</sub> (CH <sub>2</sub> ) <sub>3</sub> OH (C <sub>4</sub> H <sub>10</sub> O)
<b>Symbols</b>					
<b>Suppliers</b>	Fisher Scientific	Fisher Scientific	RICCA	Fisher Scientific	Fisher Scientific
<b>MW (g/mol)</b>	60.1	58.08	46.07	74.12	74.12
<b>Boiling Point (°C)</b>	80.37	56.05	78.24	107.89	117.7
<b>Kinetic Diameter (Å)</b>	4.7 <sup>[112]</sup>	4.6 <sup>[113]</sup>	4.5 <sup>[114]</sup>	-	5.5 <sup>[111]</sup>
<b>Water Solubility (% w/w)</b>	100	100	100	7	0.43
<b>Polarity<sup>[115]</sup></b>	0.546	0.355	0.654	0.552	0.586
<b>Relative vapor pressure at 10 ppmv</b>	$1.43 \times 10^{-7}$	$1.71 \times 10^{-8}$	$9.56 \times 10^{-8}$	$5.14 \times 10^{-7}$	$3.43 \times 10^{-7}$
<b>Adsorption Potential at 10 ppmv (kJ/mol)</b> [27,113]	29.27	44.10	39.96	37.38	36.33

### 3.3 Characterization tests

#### 3.3.1 Micropore surface analysis

All the virgin adsorbent samples were analyzed using a micropore surface analysis system (Autosorb iQ2MP, Quantachrome) to determine average pore width, BET surface area, micropore volume and total pore volume. Pore size distribution was obtained for all the virgin carbon samples and spent WV-A 1100 as the best performing adsorbent. To remove water vapor and other volatile compounds from the pores, 30 - 50 mg of carbon sample was placed in a 6 mm cell and was degassed at 120 °C for 5 hours before analysis. Nitrogen was used as probe molecule at  $10^{-7} < P/P_0 < 1$  and -196 °C (77.35 K). Micropore volume was determined using V-t model and quenched solid density functional theory (QSDFT) was used to measure pore width (median), pore size distribution (PSD) and total pore volume assuming slit-shaped pores. Specific surface area was calculated by the BET method (Brunauer et al., 1938). The relative pressure ranges were 0.01 to 0.07 and 0.2 to 0.5 respectively for BET surface area and micropore volume. Total pore volume was measured at a relative pressure of 0.99. The mesopore volume were calculated by subtracting the micropore volume from total pore volume (Quantachrome Autosorb 1 Operating Manual, 2006). By dividing the micropore volume by total pore volume, micro-porosity % is determined.

#### 3.3.2 XPS analysis

Surface elemental composition (C, O, and traces; except H) of virgin adsorbent samples were obtained by XPS analysis. XPS analysis was performed in an AXIS 165 spectrometer (Kratos Analytical) with monochromatized Al K $\alpha$  ( $h\nu = 1486.71$  eV) at room temperature with vacuum level lower than  $5 \times 10^{-10}$  torr. Binding energy at 840 eV of Au 4f $_{7/2}$  was used for calibration. Hemispherical electron energy analyzer with pass energy 20 eV was used for collecting core level spectra. Binding energy of survey spectra ranging from 1100 - 0 eV at 1 eV interval was collected

at analyzer pass energy of 160 eV. C1s peak at 284.8 eV was used as a reference. Nonlinear Marquardt Algorithm (Casa XPS) was used to find the peak model parameters and XPS core level lines in the peak were the product of Gaussian and Lorentzian functions. Elemental compositions were determined using survey spectra by major peaks and sensitivity factors.<sup>[116]</sup>

### 3.3.3 Boehm titration

Boehm titration was performed for all the virgin adsorbents to determine the concentration of different SOGs. 1 g BACs, 1 g GACs, or 0.3 g ACFCs (2-5 mm length) were dissolved in 50 ml of 0.05 M NaOH, NaHCO<sub>3</sub> and Na<sub>2</sub>CO<sub>3</sub> solution in a sealed glass vial. Before preparing these base solutions, nitrogen gas at 0.2 SLPM was passed through the demineralized water to eliminate CO<sub>2</sub>. All the sealed tubes with adsorbent-based solution were placed in a magnetic stirrer (Fisher Scientific; Model - 60100074) with the help of a stir bar for 24 h shaking. The solution was separated from the carbon using filter paper (Whatman, Dia-110 mm) and kept in a sealed vial to reduce the chance of CO<sub>2</sub> contamination. 10 ml from each base solution was titrated directly by adding methyl orange indicator with 0.05 M HCl solution. Then 10 ml base solution was taken in a glass beaker and mixed with excess 0.05 M HCl (2:1 volume ratio for monoprotic NaHCO<sub>3</sub> and NaOH, and 3:1 volume ratio for diprotic Na<sub>2</sub>CO<sub>3</sub>) to ensure enough acidity. After adding one or two drops of phenolphthalein indicator, acidified base solution is back titrated with 0.05 M NaOH solution. In direct titration a sharp change from orange to permanent faint pink color and in back titration from colorless to permanent faint pink color indicated titration end points.<sup>[117]</sup> The Boehm titration process is summarized in Figure 14.

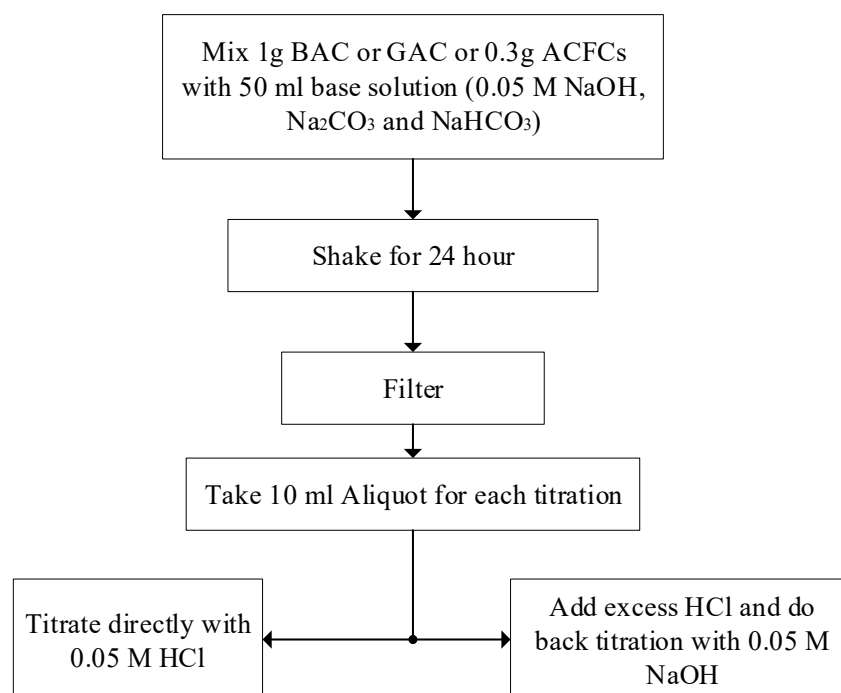


**Figure 14.** Boehm titration procedure (adapted from Goertzen et al.).<sup>[117,118,119]</sup>

NaOH solution was prepared before the titration and standardized daily using 0.05 M potassium hydrogen phthalate.<sup>[118]</sup>

The basic concept for the calculation of concentrations of various SOGs are<sup>[117]</sup> –

- $\text{NaHCO}_3$  (weak base) neutralizes carboxylic groups (including carboxylic anhydrides),
- $\text{Na}_2\text{CO}_3$  (moderate base) neutralizes carboxylic and lactone groups, and
- NaOH (strong base) neutralizes carboxylic, lactone and phenolic groups.

### 3.3.4 pH at point zero charge ( $\text{pH}_{\text{pzc}}$ ) determination

The  $\text{pH}_{\text{PZC}}$  was determined for all the virgin samples to determine the acidity or basicity when all the surface charge were neutralized by water.<sup>[44]</sup> Solutions were prepared by dissolving 540 mg carbon adsorbent in a glass tube with 27 ml demineralized water. These tubes were shaken

for 24 h and the solid particles in the solution were then allowed to settle. pH values were measured using pH meter (Oakton, model pH -700) thrice and the average was taken as  $\text{pH}_{\text{PZC}}$ .<sup>[59,117]</sup>

### 3.4 Experimental procedure

In this study, adsorption capacity towards single polar VOCs was evaluated and used to compare the performance of different adsorbents. For all the adsorption experiments, the same test-rig and experimental procedure were employed. Since these adsorbents were aimed to serve as sacrificial bed, no activation and regeneration was applied. Nevertheless, a 5-cycle adsorption-regeneration test was performed for the best adsorbent to study the regeneration performance and heel build-up.

Adsorption isotherm was also obtained for the best one to determine the adsorption capacity in the low concentration range. All the experiments were completed at least twice to ensure the reproducibility of data. As received GACs (OVC, BPL, VC48C and VCRSD) were initially tested for breakthrough experiments, however, channeling occurred (Appendix F). To avoid this problem, GACs were crushed and screened into  $20 \times 50$  mesh size (0.30 ~ 0.85 mm) to have similar particle dimension of BAC (0.70 mm) according to the ASTM E-11 Specification.<sup>[120]</sup>

#### 3.4.1 Adsorption test experiments

Figure 15 shows the lab scale adsorption-desorption set-up used for this project. It consists of an adsorption tube, a gas detection system, a heating system with variable transformer (Staco Energy Products Co.), a power application module, a data acquisition and control (DAC) system and a flame ionization detector (FID). Furthermore, Figure 16 depicts a schematic of the adsorption tube, showing the position of carbon adsorbent and the supporting material (i.e. glass wool).

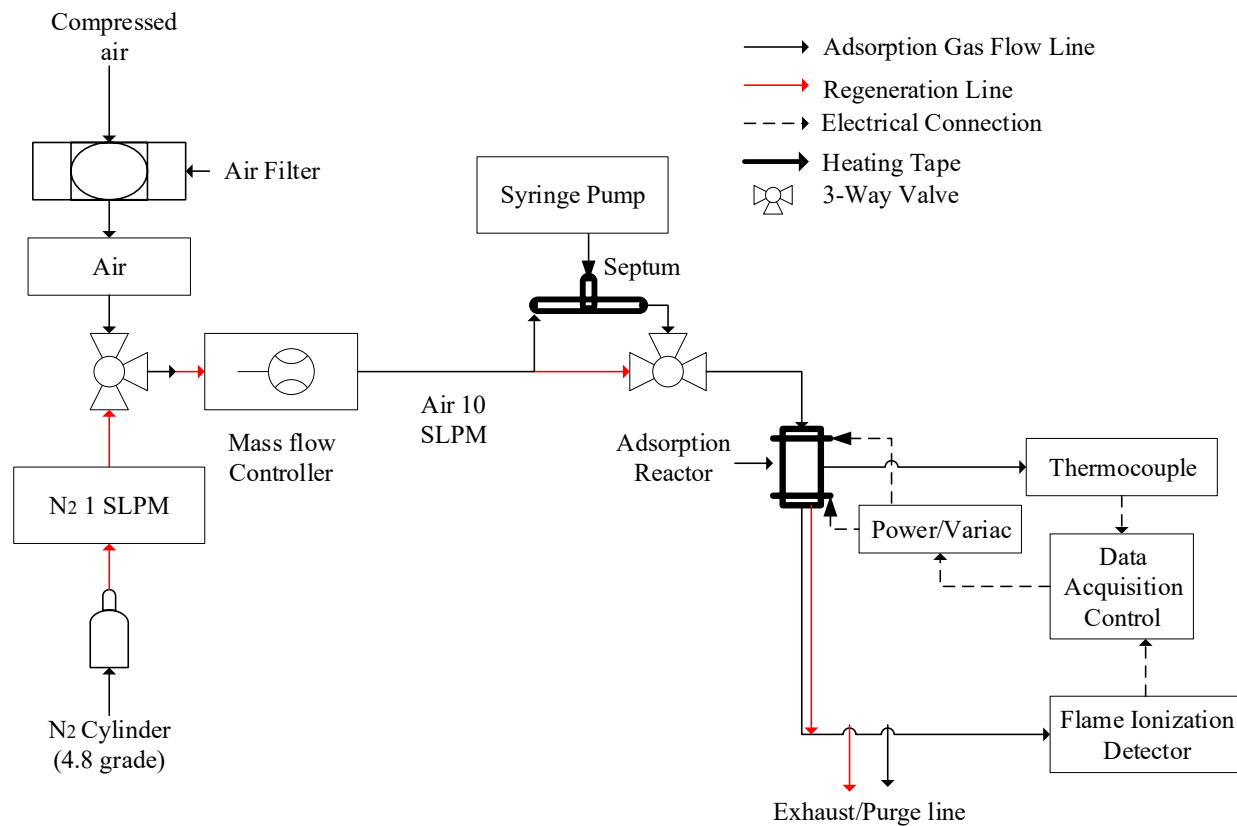


**Figure 15.** Flow diagram for adsorption-regeneration test.

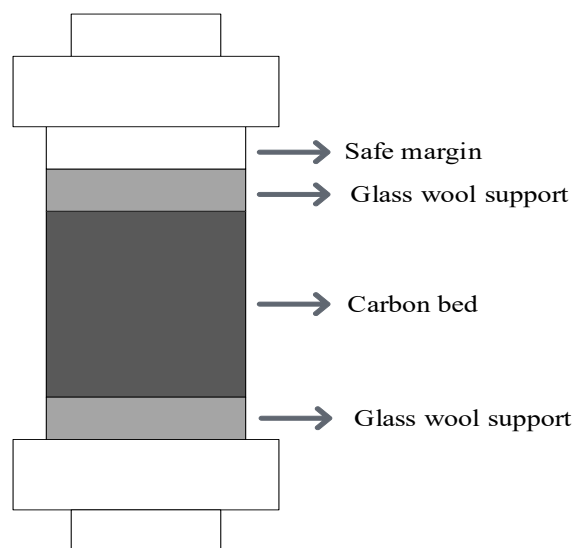


**Figure 16.** Inside view of adsorption regeneration tube.



The adsorption tube is a cylindrical stainless-steel tube with a length of 20 cm, outer diameter of 15 mm and thickness of 2 mm containing specific amount of the adsorbent ( $2 \pm 0.1$  g of GACs,  $2 \pm 0.1$  g of BACs,  $0.5 \pm 0.1$  g of ACFCs). The average bed length for BACs, ACFCs and GACs and pelleted GACs were 1 cm, 3 cm, 2 cm and 4.10 cm respectively. Before each experiment, the adsorbent was oven dried at  $140\text{ }^{\circ}\text{C}$  to remove the moisture and volatiles. Approximately 1.5 cm thick glass wool was used to support the adsorbent material at the bottom and top of the tube. Target challenge compound was injected into a 10 SLPM air stream using a syringe pump (Chemyx Inc, Model-Fusion 100) and a 500  $\mu\text{l}$  gas-tight glass syringe (Hamilton). Compressed air was first introduced into an air filter (Union Carbide) to remove water and other impurities. The flow rate of the air stream was controlled by a mass flow controller (Alicat Scientific). The injection rate was calculated using ideal gas law ( $PV = nRT$ ) with adsorbates' density and molecular weight and maintained at 10 ppmv for all the experiments. The outlet and inlet concentrations of VOC were measured with FID (Baseline Mocon, Series 9000). Ultrahigh purity hydrogen gas with flow rate of 35 cc/min and compressed air with flow rate of 175 cc/min were used for FID. Before each adsorption experiment, FID was calibrated using the same VOC injecting system with a bypass line to avoid the overflow.

During the entire experiment, VOC concentration at the adsorber's outlet was measured at a 1 min interval using the FID and continued till the saturation concentration (10 ppmv) is reached. A 'K' type thermocouple (Omega) inserted on the reactor and the probe of the thermocouple was placed in the center of the adsorbent bed during adsorption and regeneration to determine the temperature. The Data Acquisition and Control (DAC) system includes a LabVIEW program (National Instruments) and a data logger (National Instrument, Compact DAQ) with input-output

model which is interfaced with the thermocouple and FID to record temperature during adsorption and regeneration.

### **3.3.2 Adsorption-regeneration experiments**

For the 5-cycle adsorption-regeneration test, the adsorption part is the same as described in section 3.3.1. For thermal regeneration, heating and insulation tape (Omega; fiberglass-covered electrical resistive wire) were wrapped around the adsorption tube with the thermocouple. After 5 min purging with 1 SLPM N<sub>2</sub> to remove O<sub>2</sub>, regeneration was performed at 288 °C for 2 h to follow the industrial operation.<sup>[12,48,60]</sup> High purity nitrogen at a flowrate of 1 SLPM was used to purge the desorbed VOCs from the bed during regeneration. After the heating is stopped, the reactor tube was continuously purged with 0.1 SLPM N<sub>2</sub> gas for 1 h to reach the room temperature.

### **3.3.3 Adsorption isotherms**

Adsorption isotherm of 2-propanol with best adsorbent WV-A 1100 was performed using a digital recording microbalance (CAHN C -1000). Prior to each experiment, the microbalance is tared and calibrated. Samples (30 ~ 50 mg) were put in a stainless-steel basket sample holder. Ultrahigh purity N<sub>2</sub> was used during the experiment as carrier gas. The N<sub>2</sub> flow is divided into two separate streams and regulated via mass flow controllers (Alicat scientific). A 300 SCCM N<sub>2</sub> flow was used to carry the VOC injected by the syringe pump (Chemyx Inc, Model-Fusion 100) to a sealed chamber. N<sub>2</sub> and VOC mixture passed through the sample hang down assembly and over the adsorbent which is placed in the sample holder. The other N<sub>2</sub> flow (200 SCCM) passed through the weighing unit which is placed under a glass dome to create a positive pressure to prevent VOC contamination in glass dome.

### 3.5 Mass balance calculation

Through mass balance, we can obtain the adsorption and desorption amounts, adsorption capacity (%), heel formation (%), heel buildup after 1<sup>st</sup> cycle (%), cumulative heel buildup in 5 cycles (%), and total adsorption capacity loss. The employed equations for determining these indicators are listed below:

$$\text{Adsorption capacity, } W (\%) = \frac{\text{Adsorbent weight after adsorption} - \text{adsorbent weight before adsorption}}{\text{Weight of dry adsorbent}} \times 100$$

$$\text{Standard deviation (for population)} = \sqrt{\frac{\sum_{i=1}^n (W_i - \bar{W})^2}{n}}, \text{ where } n \text{ is the number of experiments}$$

$$\text{Heel formation } (\%) = \frac{\text{Adsorbent weight after desorption} - \text{adsorbent weight before adsorption}}{\text{Weight of dry adsorbent}} \times 100$$

$$\text{Total Capacity loss } (\%) = \frac{\text{Amount adsorbed after 1st cycle} - \text{Amount adsorbed after 5th cycle}}{\text{Amount adsorbed after 1st cycle}} \times 100$$

$$\text{Heel buildup after 1}^{\text{st}} \text{ cycle } (\%) = \frac{\text{Weight after 1st regeneration cycle} - \text{Weight before 1st adsorption cycle}}{\text{Weight of dry adsorbent}} \times 100$$

$$\text{Cumulative Heel buildup in 5 cycles } (\%) = \frac{\text{Weight after 5th regeneration cycle} - \text{Weight before 1st adsorption cycle}}{\text{Weight of dry adsorbent}} \times 100$$

100

### 3.6 Design of sacrificial bed

#### 3.6.1 LUB method

To design an adsorption packed bed, a test column to generate breakthrough curves (Figure 17) having the same superficial velocity as the full-scale operation is required. In both cases, the column is designed in a way that its length (L) is much larger (10 times) compared to its diameter (D) to minimize the wall effects. The tube diameter was at least 16 times the mean diameter of the largest carbon particles present.<sup>[120]</sup>

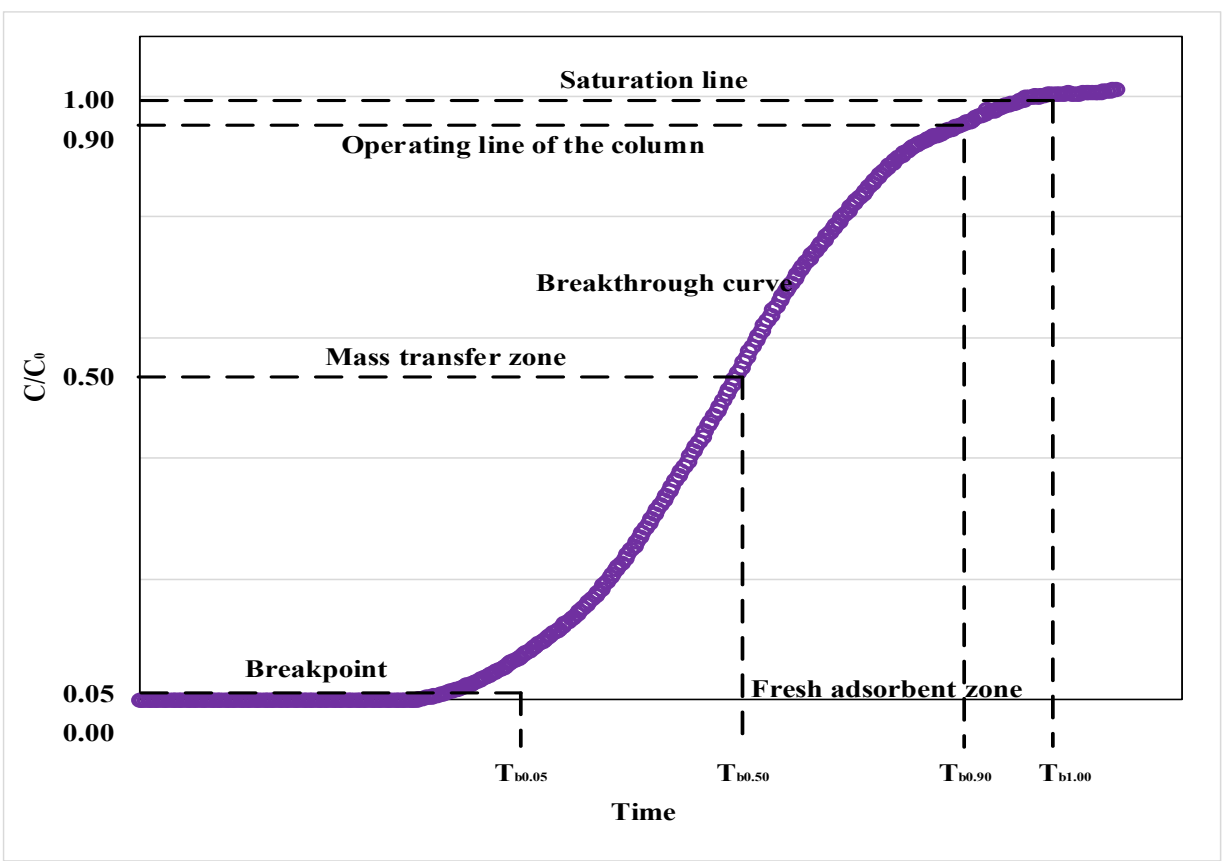


Figure 17. Typical breakthrough curve.<sup>[90,95]</sup>

The test column results were used for scaling up since the superficial velocity will be the same for the lab scale and the full-scale operations.<sup>[92,96,121,122]</sup> Important design parameters are briefly explained here:

### **Total length of the sacrificial bed during experiment (L)**

Total length of adsorption bed,  $l = LB + LUB$

$$\text{Length of used bed, } LB = l \frac{W_{b5}}{W_{sat}}$$

$$\text{Length of unused bed, } LUB = l \left(1 - \frac{W_{b5}}{W_{t100}}\right)$$

$W_{b5}$  = The amount of VOC adsorbed up to break point (usually 5 % breakthrough time)

$W_{t100}$  = The amount of VOC adsorbed up to saturation point.

### **Scale up for the sacrificial bed column in full scale**

Knowing the actual air flow rate, the following parameters can be calculated.

$$\text{Area of the column, } A = \frac{\text{Actual Air feed rate (Q)}}{\text{Superficial velocity (v)}}$$

$$\text{Diameter, } D = \sqrt{\frac{4A}{\pi}};$$

$$\text{Maximum bed depth of carbon} = \frac{\pi \times D}{12} \text{ [92]}$$

$$\text{Length of large-scale used bed at 5\% BT, } \overset{\circ}{L} = \frac{G_S \times t_b}{\rho_b \times W_{t100}} \text{ [121]}$$

where,

$G_s$  = Superficial flow rate of gas ( $\text{kgm}^{-2}\text{min}^{-1}$ )

$t_b$  = 5 % breakthrough time in large scale (min)

$\rho_b$  = bed bulk density, known from experiment ( $\text{kgm}^{-3}$ )

$W_{t100}$  = adsorbent's capacity from lab scale (kg VOC/kg adsorbent)

LUB from lab scale should be added to full scale used bed length as a mass transfer zone.

Total bed length for full scale at 5 % BT  $L = \overset{\circ}{L} + \text{LUB}$

### **Empty Bed Contact Time (EBCT/ $\tau$ )**

Empty bed contact time for full scale operation,  $\tau = \frac{\text{Area (A)} \times \text{Length (L)}}{\text{Air feed rate}}$

### **Carbon consumption at 5% BT**

Total mass of carbon required in sacrificial bed at 5 % BT = Volume  $\times$  bulk density =  $A \times L \times \rho_b$

Here,

A = Area of the sacrificial bed

L = Length/Height/Depth of sacrificial bed at 5 % BT

$\rho_b$  = bulk density of carbon adsorbent

Maximum carbon bed volume would be  $\frac{1}{3}$  of vessel volume.<sup>[92]</sup>

### **3.6.2 Thomas model**

Thomas model is applicable for adsorber columns with constant flow rate.<sup>[96]</sup>

$$\text{Effluent concentration at 5 \% BT time, } C_{\text{out}} = \frac{C_{\text{in}}}{1 + \exp\left(\frac{K_{\text{th}} \times W_e \times W}{Q} - C_{\text{in}} \times K_{\text{th}} \times t_b\right)}$$

Where,

$t_b$  = 5 % breakthrough time [sec]

$W_e$  = adsorption capacity of carbon at saturation [kg VOC/kg-carbon]

$W$  = carbon bed weight [kg]

$C_{\text{in}}$  = challenge vapor concentration [kg/m<sup>3</sup>]

$C_{\text{out}}$  = 5 % breakthrough concentration [kg/m<sup>3</sup>]

$Q$  = airflow rate [m<sup>3</sup>/s]

$K_{\text{th}}$  = Thomas rate coefficient [m<sup>3</sup>kg<sup>-1</sup>s<sup>-1</sup>]

After rearranging the above equation, we find the expression for Thomas rate coefficient –

$$K_{\text{th}} = \frac{\ln\left(\frac{C_{\text{in}}}{C_{\text{out}}} - 1\right)}{\frac{W_e \times W}{Q} - C_{\text{in}} t_b}$$

From the lab scale data 5 % breakthrough time, 5 % breakthrough concentration, adsorption capacity at saturation were obtained for a certain weight of carbon bed at specific VOC concentration and superficial gas velocity. These input values were used to determine the Thomas rate coefficient  $K_{\text{th}}$  from above expression.

To determine the carbon consumption for the full-scale system, air flowrate and 5 % breakthrough time at a specific VOC concentration are needed as additional input data from real

industrial operation. Carbon consumption value for up to 5 % breakthrough can be obtained by rearranging the Thomas equation as follows:

$$W = \frac{Q}{W_e} \left\{ \frac{1}{K_{th}} \ln \left( \frac{C_{in}}{C_{out}} - 1 \right) + C_{in} t_b \right\}$$

### 3.6.3 Wheeler-Jonas model

Due to the simplicity and availability of input parameters, the Wheeler-Jonas equation had been used for wide range of organic VOCs' adsorption breakthrough specially for activated carbons.<sup>[98,99]</sup>

$$\text{Breakthrough Time, } t_b = \frac{W_e \cdot W}{Q \cdot C_{in}} - \frac{\rho_b \cdot W_e}{K_v \cdot C_{in}} \ln \left( \frac{C_{in}}{C_{out}} \right)$$

where

$t_b$  = 5 % breakthrough time [min]

$W_e$  = adsorption capacity of carbon [g/g-carbon]

$W$  = carbon bed weight [g]

$C_{in}$  = challenge vapor concentration [g/cm<sup>3</sup>]

$C_{out}$  = 5 % breakthrough concentration [g/cm<sup>3</sup>]

$Q$  = airflow rate [cm<sup>3</sup>/min]

$\rho_b$  = bulk density of carbon [g/cm<sup>3</sup>]

$K_v$  = adsorption rate coefficient [min<sup>-1</sup>]



After rearranging the above equation, we find the expression for adsorption rate coefficient–

$$K_v = \left[ \frac{\ln \frac{C_{in}}{C_{out}}}{\left( W_{ads} - \frac{t_b \times Q \times C_{in}}{W_e} \right)} \right] Q \times \rho_b$$

Similarly using the lab scale data with additional bed bulk density value, it is possible to determine the adsorption rate coefficient  $K_v$  from above expression.

Carbon consumption value for up to 5 % breakthrough for full scale can be obtained by rearranging the Wheeler-Jonas equation as follows:

$$W_{ads} = \left[ \frac{t_b \times C_{in} \times Q}{W_e} + \frac{\rho_b \times Q}{K_v} \ln \frac{C_{in}}{C_{out}} \right]$$

## **Chapter 4. Result Analysis and Discussion**

This chapter is divided into two main sections. In the first part, adsorbents' characterization results are presented and analyzed. Adsorbents' textural properties such as BET surface area, micropore volume, total pore volume and micro-porosity were determined using N<sub>2</sub> adsorption analysis. Elemental composition, surface oxygen functional groups and acid functionalities were obtained using XPS analysis, Boehm titration and pH at point zero charge measurement, respectively. In the second part, adsorption performance of different activated carbons for the selected VOCs are determined and discussed. Afterwards, adsorber design and carbon consumption per day are studied as part of overall economic and operational feasibilities.

## **4 Adsorbents characterization**

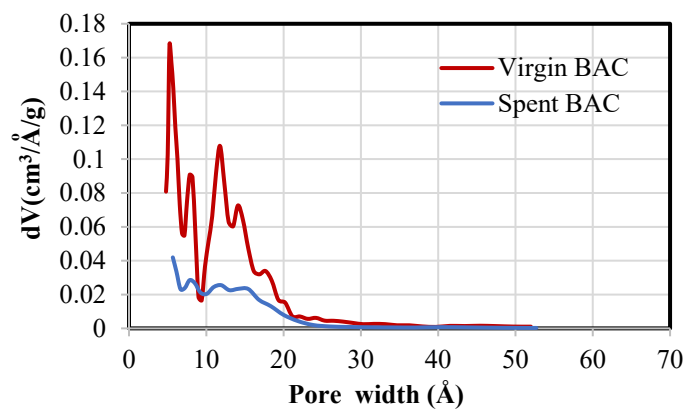
### **4.1 N<sub>2</sub> adsorption analysis**

Findings from N<sub>2</sub> adsorption analysis are summarized in Table 6. Virgin BAC possesses a highly microporous structure with large BET surface area, pore volume, and micro-porosity as compared to spent BAC. The pore width of Virgin BAC (11.0 Å) is smaller than that of spent BACs (11.8 Å). The reason is that for the latter, small micropores have been occupied by heel buildup during the previous use. BET surface areas, micropore volumes, and total pore volumes of Virgin BAC and coconut shell based GACs (OVC and VC48C) are close to those of ACFC 15. Coal-based carbons (BPL and VCRSD) showed smaller surface areas and pore volumes compared to Virgin BACs, which can be attributed to their activation conditions. WV-A 1100 and WV-A 1500 offer the highest BET surface areas and total pore volumes among all adsorbents despite their lower micro-porosities, suggesting presence of large amounts of mesopores within their structures. The pore size distributions of all eleven carbon samples are presented in Figure 18. All samples have substantial pores in the micropore region (< 20 Å). Virgin BAC and Spent BAC showed presence of small amount of mesopores in the range of 20-30 Å.

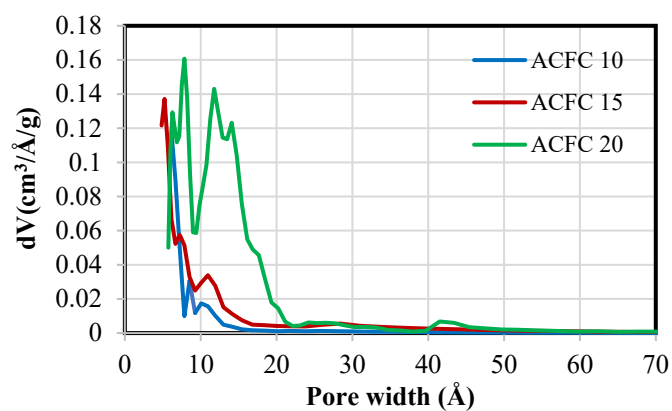
**Table 6.** Textural properties of adsorbents.

Adsorbents	Morphology	Particle/ fiber diameter	Average pore Width (Å)	BET surface area (m <sup>2</sup> /g)	Micropore volume (cm <sup>3</sup> /g)	Total pore volume (cm <sup>3</sup> /g)	Micro- porosity (%)
Virgin BAC	Beads (sphere)	~ 0.70	11.0±1.9	1340±19	0.50±0.00	0.54±0.00	92±0
Spent BAC		mm <sup>[57]</sup>	11.8±1.2	804±37	0.29±0.01	0.38±0.03	76±1
ACFC 10	Woven fabrics	10 µm <sup>[100]</sup>	6.1±0.01	1058±255	0.37±0.00	0.42±0.00	88±1
ACFC 15			8.2±0.7	1326±117	0.55±0.01	0.63±0.00	87±2
ACFC 20			11.9±2.0	1793±143	0.66±0.00	0.70±0.00	94±0
OVC	Granulated and crushed (20 × 50)	0.30 ~ 0.85 mm <sup>[101,102,103,104]</sup>	7.4±0.7	1311±61	0.48±0.01	0.54±0.03	89±3
VC48C			7.5±0.3	1194±6	0.44±0.00	0.49±0.00	90±1
BPL			9.3±1.2	1001±50	0.35±0.01	0.45±0.02	78±1
VCRSD			8.5±0.5	820±69	0.31±0.03	0.37±0.05	83±2
WV-A 1100	Granulated (pelleted)	1.2 mm	20.7±4.5	1466±10	0.25±0.03	1.09±0.03	23±1
WV-A 1500		(min) <sup>[105,106]</sup>	17.2±2.2	1964±18	0.42±0.00	1.29±0.04	32±0

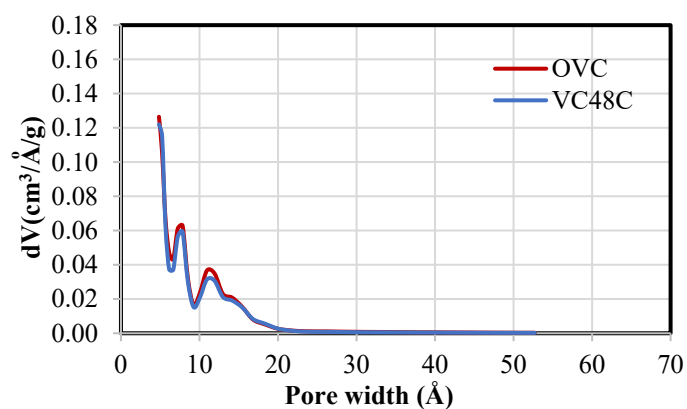
For ACFC 10 and ACFC 15, the majority of pores are in the 4.8-10 Å range, while ACFC 20 possesses a considerable amount of pores between 10-20 Å. There is no observable mesopore zone in wood based crushed GACs' (OVC and VC48C) pore size distributions. In contrary, coal based crushed GACs (BPL and VCRSD) show the presence of mesopores within 20 - 30 Å range. Among all adsorbents, pelleted GACs have a substantial mesopore contribution (> 68%). The mesopores size for WV- A 1100 and WV- A 1500 ranges between 20 and 70 Å.



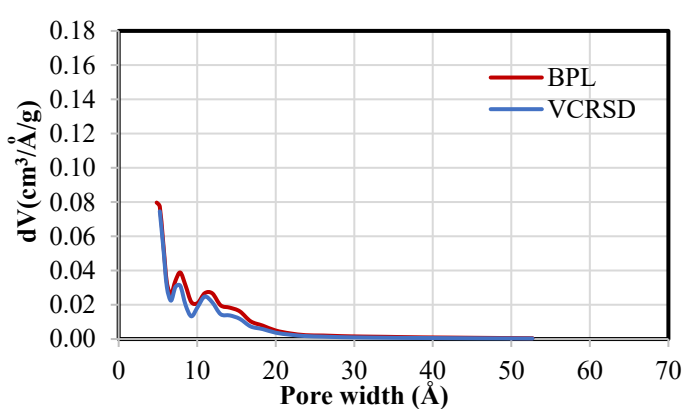
a. Virgin and Spent BAC



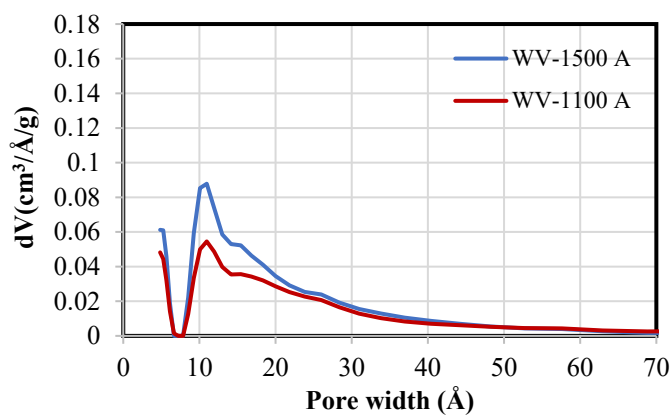
b. ACFCs



c. Wood-based crushed GACs (OVC and VC48C)



d. coal based crushed GACs (BPL and VCRSD)



e. Pelleted GACs (WV-A 1100 and WV-A 1500)

**Figure 18.** Pore size distribution of virgin carbon samples. **a.** Virgin and Spent BAC, **b.** ACFCs, **c.** Crushed GACs (wood-based), **d.** Crushed GACs (coal-based), **e.** Pelleted GACs.

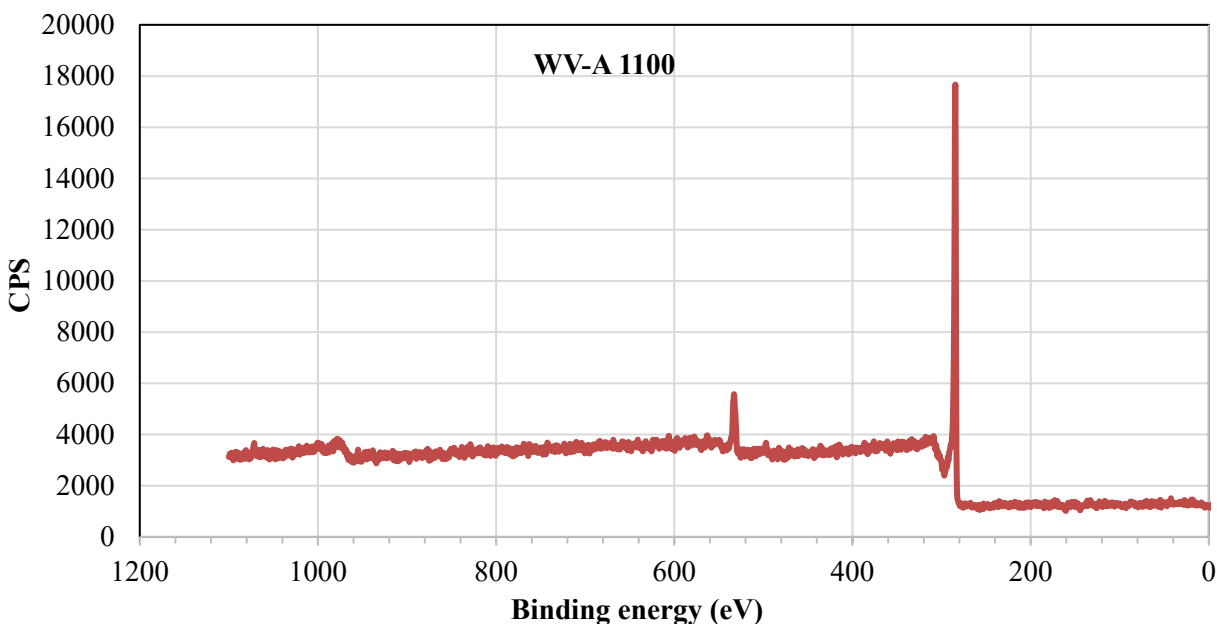
## 4.2 XPS analysis

Table 7 presents elemental analysis results from survey scans of all the carbon samples. In most cases, elemental analysis of virgin samples showed presence of only carbon (294 - 280 eV, C1s) and oxygen (530 - 540 eV, O1s). Individual chemical states of carbon and oxygen contribute to the entire C1s and O1s regions and atomic quantification developed from contribution of their relative areas to the total peak area of the survey scan.<sup>[123]</sup>

**Table 7.** Elemental composition of adsorbent samples by XPS analysis.

Adsorbents \ Elements	Atomic Concentration (%)		
	C	O	Others
<b>Virgin BAC</b>	93.09	6.91	0.00
<b>Spent BAC (0.7AD)</b>	94.88	5.12	0.00
<b>ACFC 10</b>	96.07	3.93	0.00
<b>ACFC 15</b>	97.34	2.66	0.00
<b>ACFC 20</b>	98.05	1.95	0.00
<b>OVC</b>	91.99	8.01	0.00
<b>VC48C</b>	94.55	5.45	0.00
<b>BPL</b>	94.79	5.21	0.00
<b>VCRSD</b>	92.44	7.56	0.00
<b>WV-A 1100</b>	91.34	8.37	0.28
<b>WV-A 1500</b>	93.11	6.61	0.29

A sample survey scan is reported in Figure 19 for WV-A 1100 to explain the elemental analysis. The largest peak is at 280 - 300 eV which represents the C1s spectrum while the second largest peak at 530 eV is assigned to O1s.



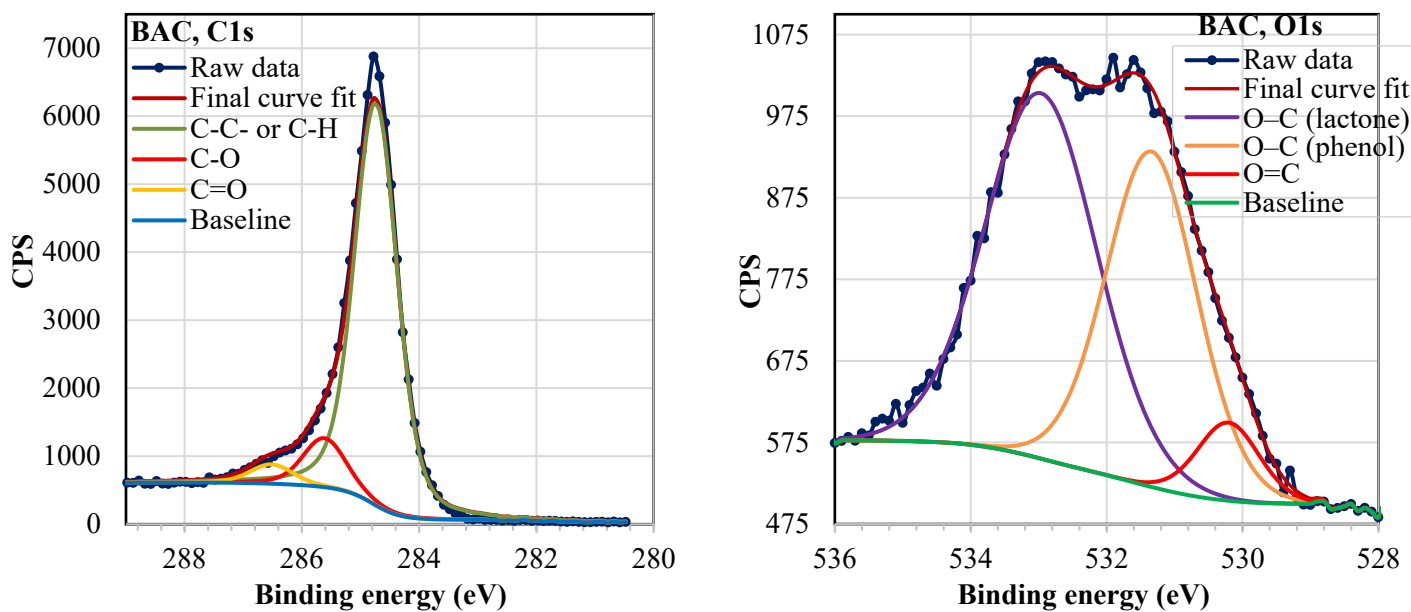
**Figure 19.** Full range survey spectrum for WV-A 1100.

Depending on the adsorbent, carbon and oxygen contents vary between 91-98 % and 2-8.5 %, respectively. At 978.5 eV, both WV-A 1100 and WV-A 1500 show a very small peak, indicating the presence of trace amount of sodium, which might come from either the source material or the way carbons were activated (usually with  $\text{Na}_2\text{SO}_4$ ,  $\text{Na}_2\text{CO}_3$  or  $\text{NaOH}$ ).<sup>[18,124,125]</sup> Virgin BAC has a higher oxygen and a lower carbon content compared to spent BAC. For carbon clothes, oxygen concentration decreases with activation level in the order of ACFC 10 (3.93 %) > ACFC 15 (2.66 %) > ACFC 20 (1.95 %), while the carbon content increases in the opposite order. In general, the oxygen content of ACFCs is much lower than that of other samples. Furthermore, most of the GACs (e.g. OVC and WV-A 1100) have a lower carbon content in comparison to

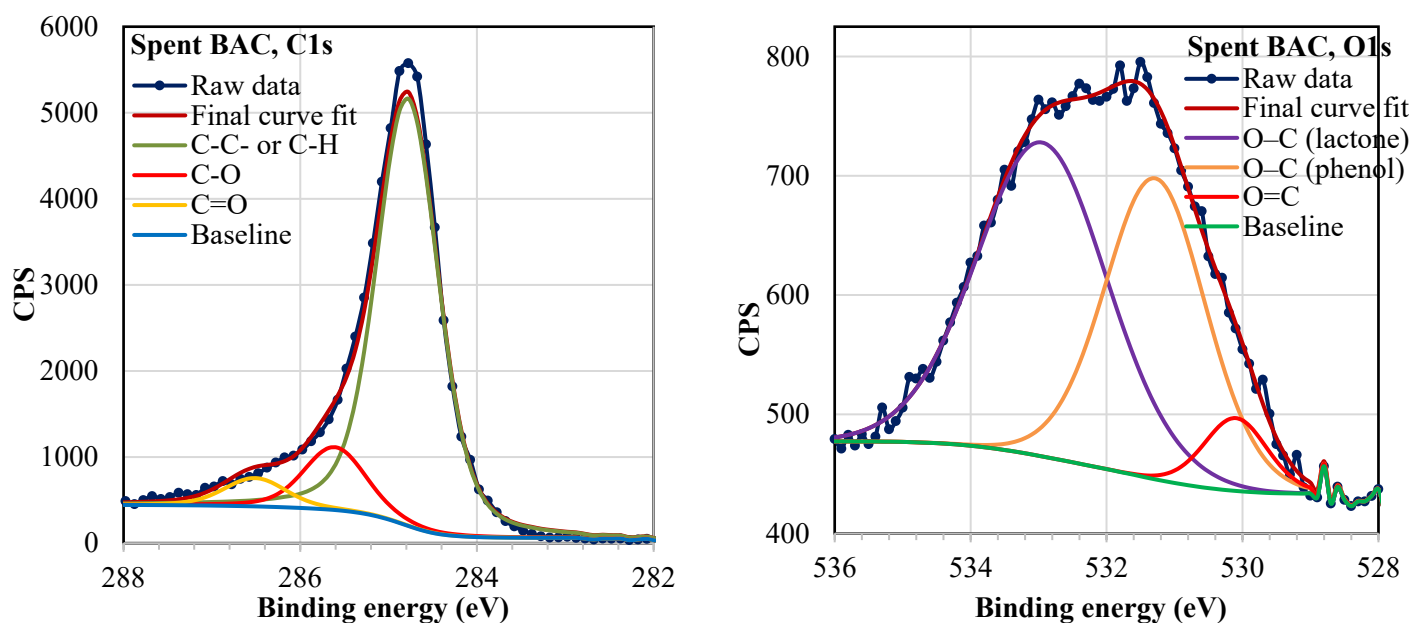
Virgin BAC. Nonetheless, there is no correlation between the oxygen content of activated carbons and their source material (bituminous or wood based) or activation process.

C1s and O1s high resolution spectra provide valuable information about the chemical states of carbon and oxygen surface functional groups as well as the sources of acidic properties of activated carbons.<sup>[126]</sup> Non-linear least square optimization method was followed to analyze the high-resolution survey scans in relevant spans. The functional groups come with individual Gaussian arcs but ensembled under a main peak. The curves associated with functional groups were varied to fit the main C1s or O1s spectrum (shown in Figures 20 to 24). Binding energy value and standard deviation (between 0 and 1) dictate the quality of curve fitting. The vertical axis in XPS spectrum represents count per second of responses, which are basically function of kinetic energy interrelated with the excitation of core level electron. Data analysis was accomplished after background subtraction to acquire more accurate curve fittings.



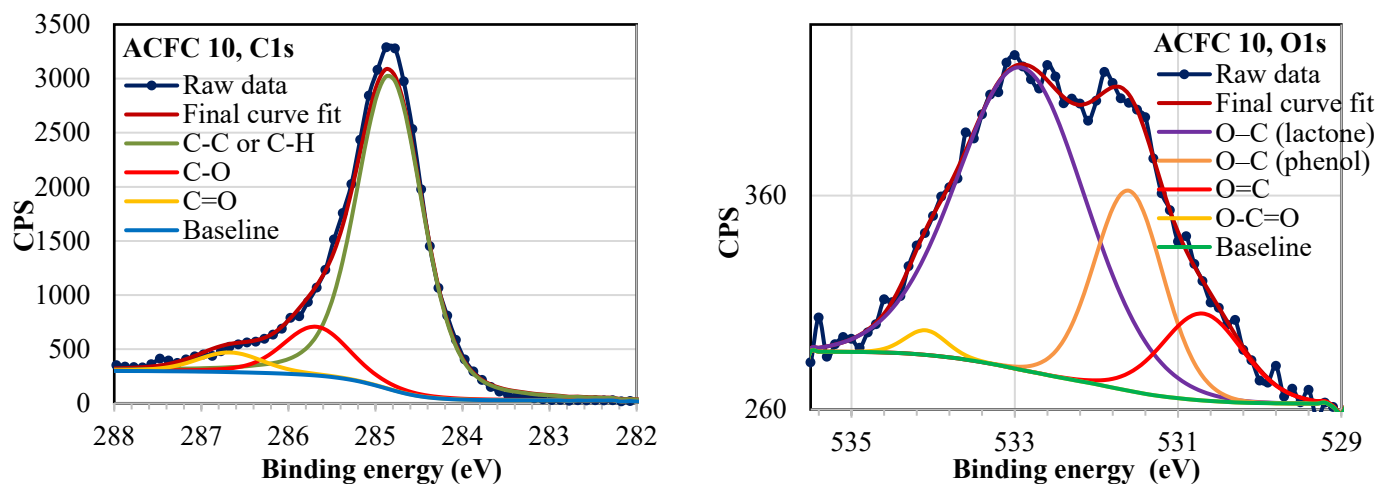


a. virgin BAC (C1s and O1s respectively).

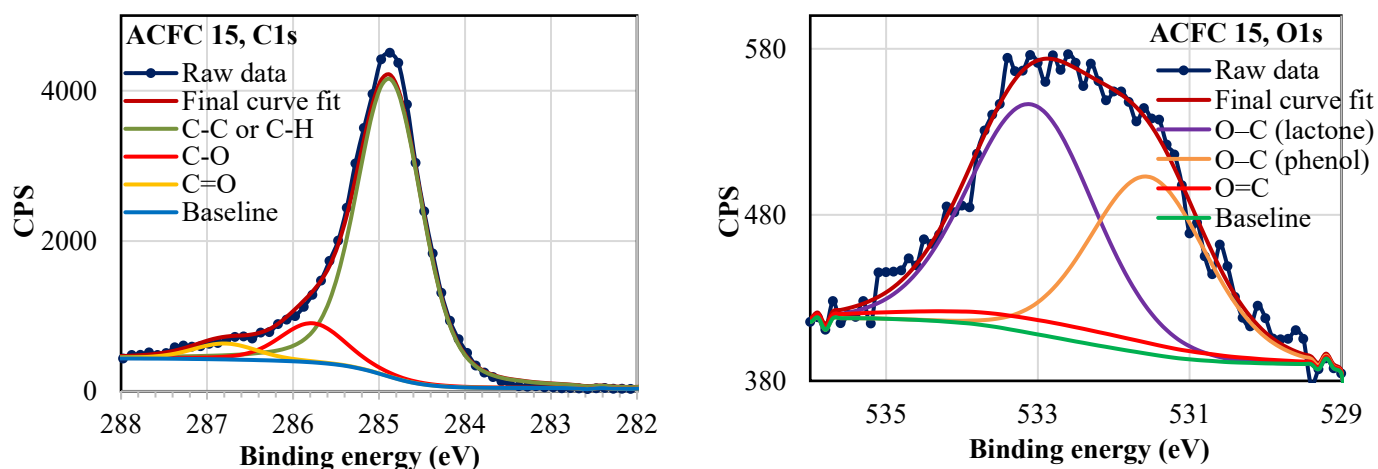


b. spent BAC (C1s and O1s respectively).

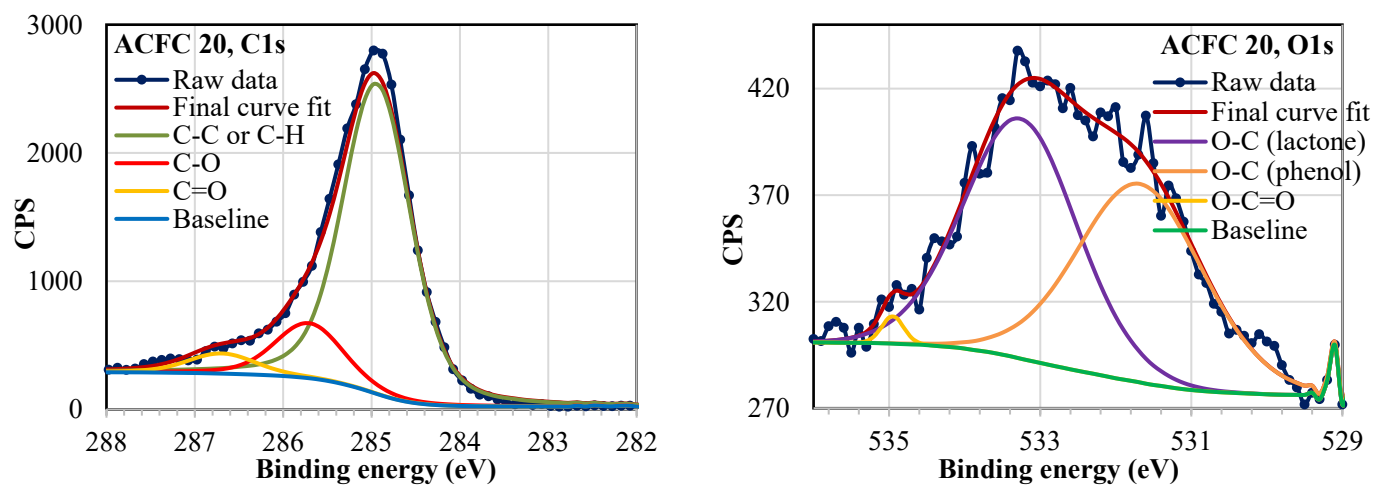
**Figure 20.** Survey scan deconvolution for **a.** virgin BAC (C1s and O1s respectively) and **b.** spent BAC (C1s and O1s respectively).



a. ACFC 10 (C1s and O1s respectively).

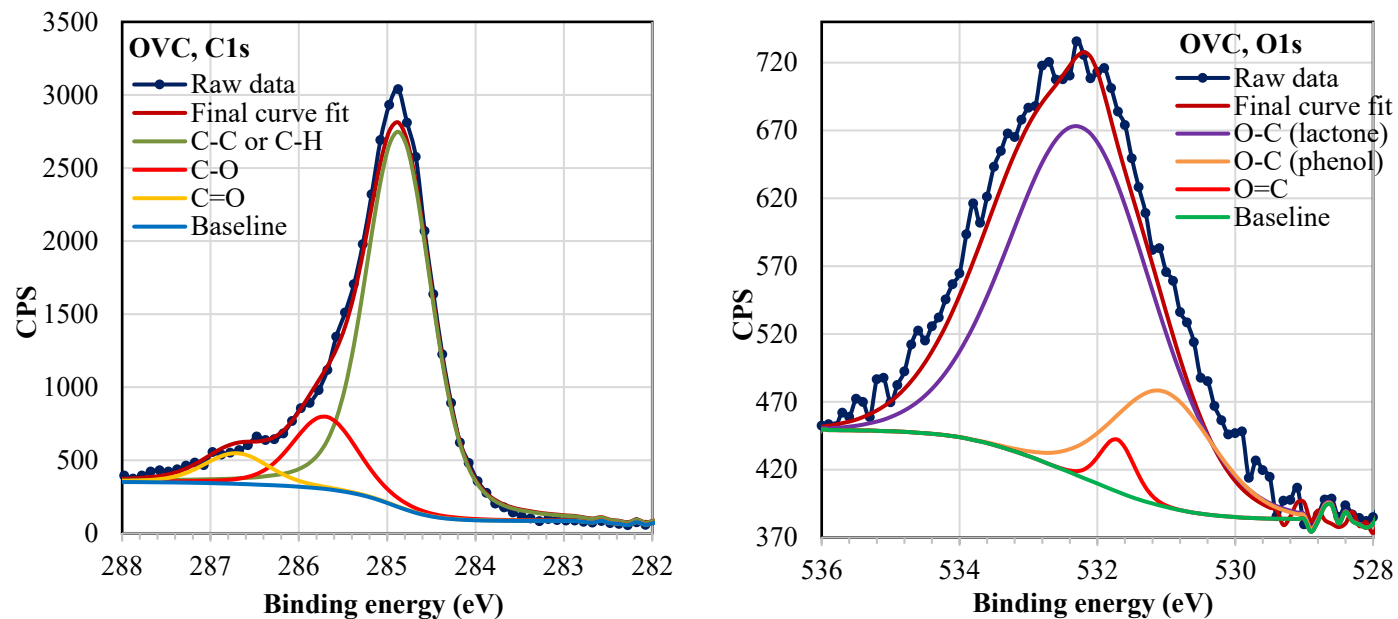


b. ACFC 15 (C1s and O1s respectively).

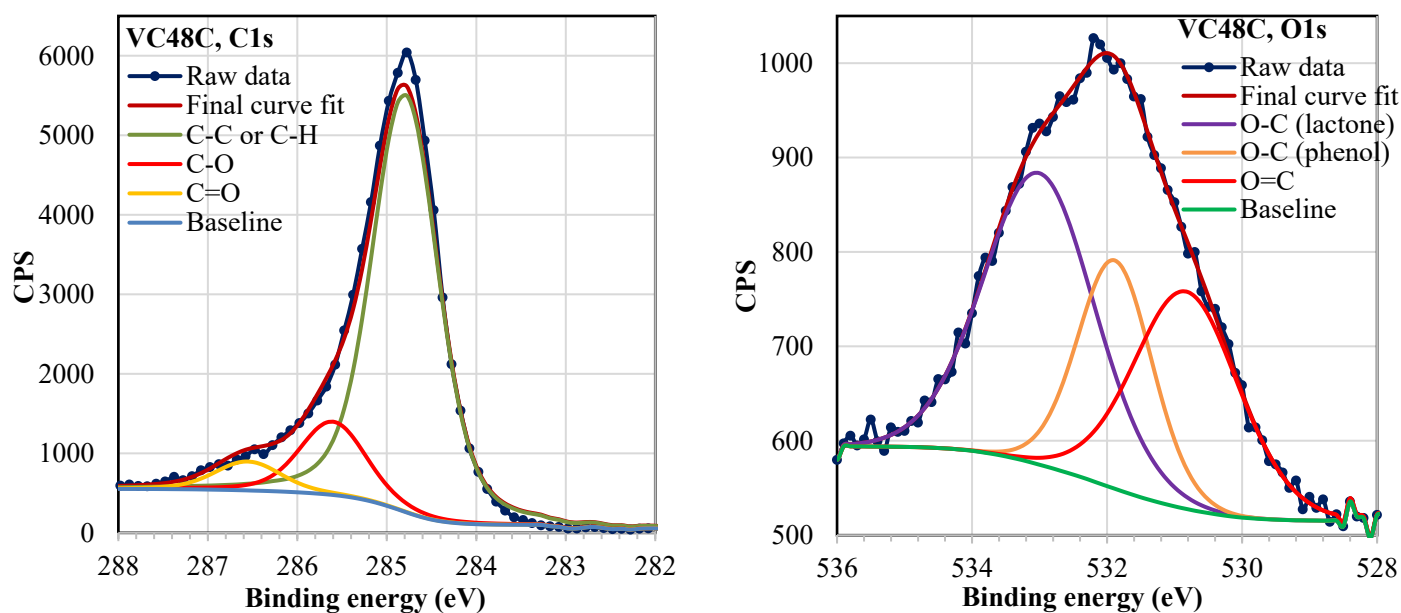


c. ACFC 20 (C1s and O1s respectively).

Figure 21. Survey scan deconvolution for a. ACFC 10, b. ACFC 15 and c. ACFC 20.

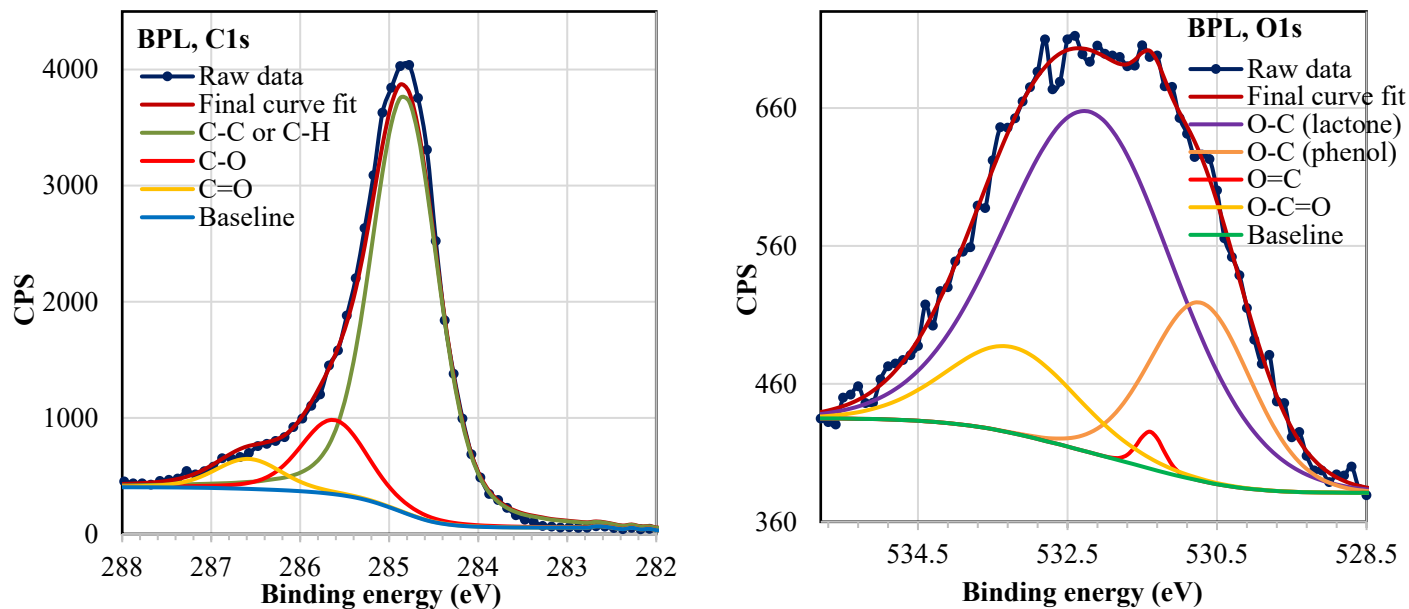


a. OVC (C1s and O1s respectively).

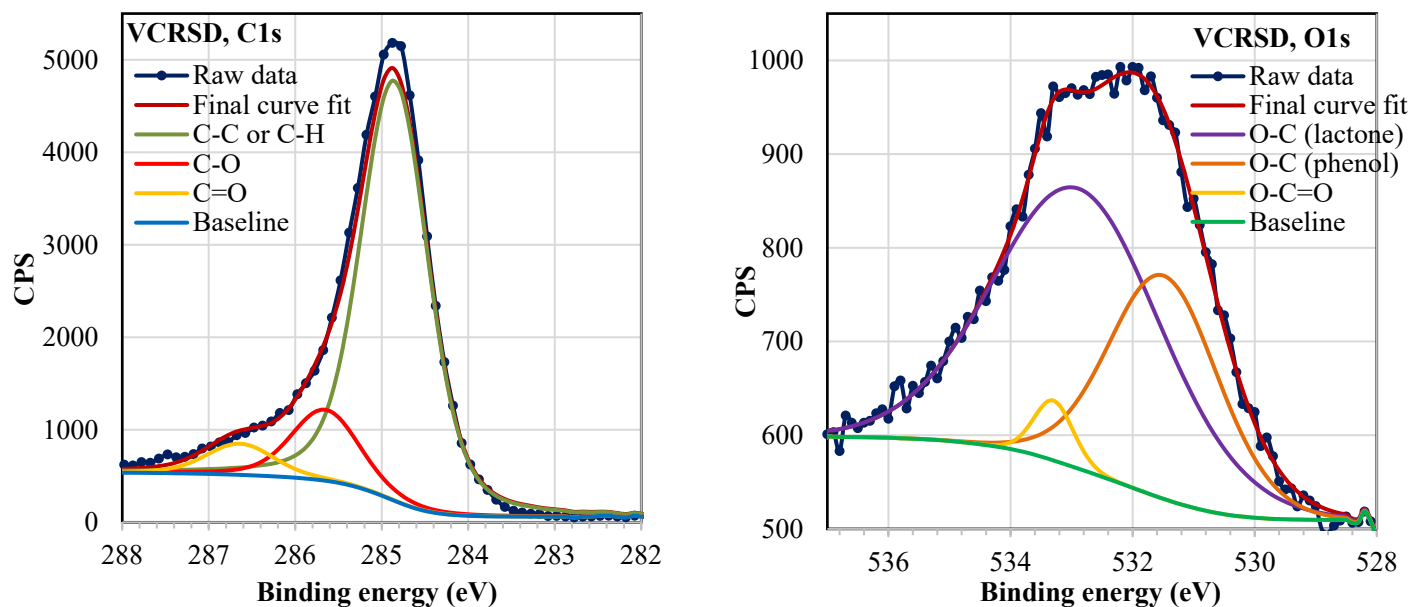


b. VC48C (C1s and O1s respectively).

**Figure 22.** Survey scan deconvolution for wood-based non-pelleted GACs, **a.** OVC (C1s and O1s respectively) and **b.** VC48C (C1s and O1s respectively).

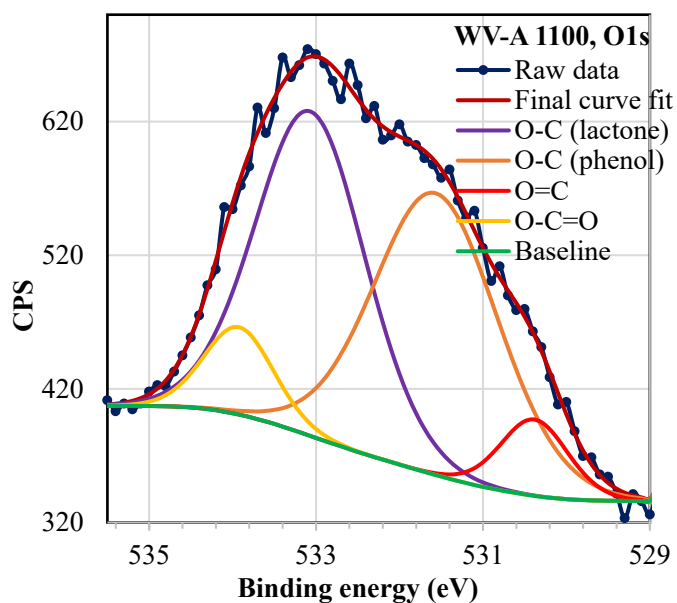
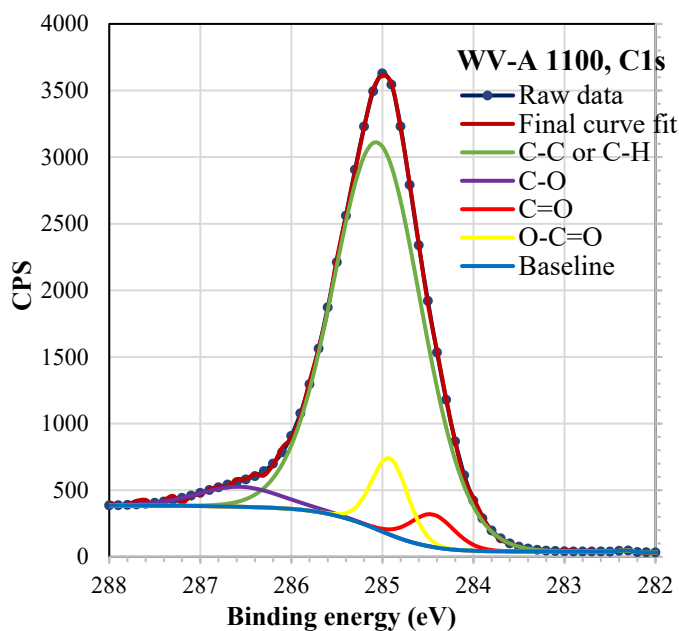


a. BPL (C1s and O1s respectively).

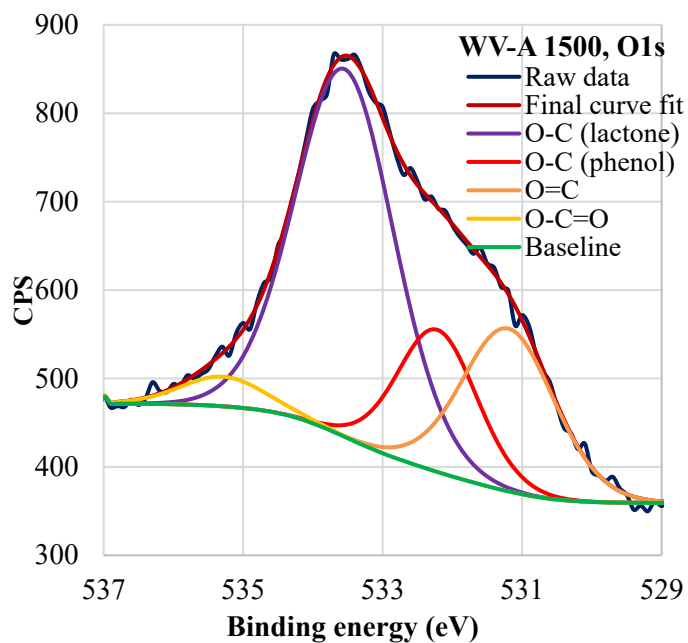
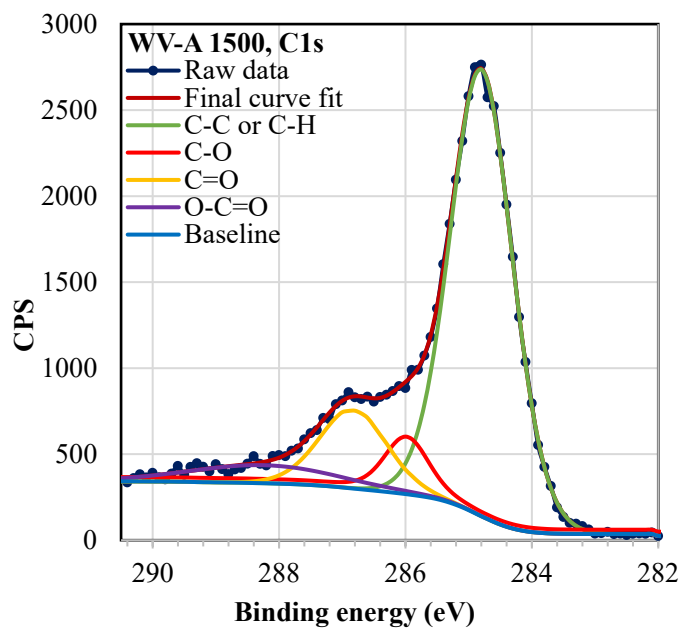


b. VCRSD (C1s and O1s respectively).

**Figure 23.** Survey scan deconvolution for coal-based non-pelleted GACs, **a.** BPL (C1s and O1s respectively) and **b.** VCRSD (C1s and O1s respectively).



a. WV-A 1100 (C1s and O1s respectively).



b. WV-A 1500 (C1s and O1s respectively).

**Figure 24.** Survey scan deconvolution for wood-based pelleted GACs, **a.** WV-A 1100 (C1s and O1s respectively) and **b.** WV-A 1500 (C1s and O1s respectively).

In general, C1s spectra deconvolution provides information about five peaks originated from carbon core electron binding energy area.<sup>[126,127,128]</sup>

- Peak 1 for indistinguishable hydrocarbon and graphitic carbon (C-H and/or C-C) at  $284.8 \pm 0.2$  eV.
- Peak 2 for hydroxyl, ethers, alcoholic or phenolic groups (C-O) at  $285.7 \pm 0.2$  eV.
- Peak 3 for carbonyl or quinone groups (C=O) at  $286.7 \pm 0.7$  eV.
- Peak 4 for carboxyl, ester or lactone groups (O-C=O) at  $288.7 \pm 0.7$  eV and
- Peak 5 denotes any oxygen contamination at surface such as adsorbed CO and/or CO<sub>2</sub> as well as carbonates.

C1s peak spanned in the range of 284 - 290 eV and the 284.8 eV peak was used to calibrate as well as to correct any charge effect. All the binding energies were referenced to the C1s peak at 284.8 eV of the surface adventitious carbon. Adventitious carbon is a thin layer of various relatively short chain polymeric hydrocarbons species that usually forms on the surface of air exposed samples.<sup>[129]</sup> Though the peak position of all the chemical states of carbon are already well documented in plenty of early works, still they shift to some extent. For this study, this deviation is roughly within  $\pm 0.65$  % for all the samples as compared to the analogous carbon materials reported in literature. This deviation is partly due to the chemical environment altered by neighboring atoms on the surface.

O1s survey scan is less intense in comparison to C1s and it includes four peaks. It is difficult to discriminate the individual peaks for O1s specifically because most of them tend to overlap. O1s peaks are <sup>[126,127,128]</sup>:

- Peak 1 - carbonyl groups or quinone (O=C) at  $530 \pm 0.2$  eV.

- Peak 2 - anhydrides and lactones with carbonyl O, phenol or ether groups' O (O-C) at  $532 \pm 0.5$  eV.
- Peak 3 - lactones with ether O or anhydrides (O-C) at  $533 \pm 0.5$  eV and
- Peak 4 - carboxylic acid group (O-C=O) at  $534 \pm 0.2$  eV.

Some peaks are asymmetric due to merging with other high energy small peaks, resulting in the formation of shoulders. For instance, presence of moisture, chemisorbed oxygen, or oxygen in pyrone like structures can lead to shoulder formation. The shoulder in C1s spectrum is due to bonded oxygen, which tends to advance its energy level ( $> 288$  eV) to high energy region due to its own higher binding energy ( $< 530$  eV).<sup>[126]</sup>

Fractional compositions of functional groups are directly proportional to each subordinate curves' contribution to the total area under the main peak. Degree of oxidation ( $C_{ox}/C_{gr}$ ) is represented by the ratio of sum of all types of carbon oxidation states to the overall graphitic carbon from C1s spectrum.<sup>[127]</sup> It can be useful to also investigate the results of O1s deconvolution to verify the type and population of each functional group determined based on the C1s spectra. Standard deviations for curve fittings were around 0.6-0.8 % for all functional groups for both C1s and O1s.

Tables 8 and 9 report the population of surface functional groups determined based on C1s and O1s deconvolutions, respectively. Virgin BAC has the highest percentage of graphitic carbon among all samples. Given that Spent BAC already adsorbed some VOCs from other applications and might contain chemisorbed oxygen, its degree of oxidation is slightly higher than Virgin BAC. Among ACFCs, ACFC 20 exhibited the highest share of solid carbon segment and hence the lowest degree of oxidation. GAC samples showed lower shares of carbon content, which directly

signifies their higher degree of oxidation. Evidently, pelleted GACs have been oxidized to the highest level. For all the carbon samples, carbonyl content is lower than phenol content and carboxylic group content is very small.

**Table 8.** Distribution of carbon functional groups based on C1s deconvolution.

<b>Functional groups (%)</b> <b>Adsorbents</b>	<b>Graphitic carbon</b> <b>(C-C- or C-H)</b>	<b>Phenol</b> <b>(C-O)</b>	<b>Carbonyl</b> <b>(C=O)</b>	<b>Carboxylic acid</b> <b>(O-C=O)</b>	<b>C<sub>ox</sub>/C<sub>gr</sub></b> <b>(%)</b>
<b>Virgin BAC</b>	85.5	10.4	4.1	0.0	17
<b>Spent BAC</b>	82.4	12.1	5.5	0.0	21
<b>ACFC 10</b>	81.9	12.8	5.3	0.0	22
<b>ACFC 15</b>	84.7	11.0	4.3	0.0	18
<b>ACFC 20</b>	85.4	10.7	3.9	0.0	17
<b>OVC</b>	80.6	13.9	5.5	0.0	24
<b>VC48C</b>	80.3	14.1	5.6	0.0	25
<b>BPL</b>	78.8	14.8	6.4	0.0	28
<b>VCRSD</b>	81.3	12.9	5.8	0.0	23
<b>WV-A 1100</b>	73.8	9.4	9.9	6.9	35
<b>WV-A 1500</b>	72.8	9.8	13.5	4.0	37



**Table 9.** Distribution of oxygen functional groups based on O1s deconvolution.

<b>Functional groups (%)</b> <b>Adsorbents</b>	<b>Carbonyl (O=C)</b>	<b>Phenol (O-C)</b>	<b>Lactones (O-C)</b>	<b>Carboxylic acid (O-C=O)</b>
<b>Virgin BAC</b>	6.4	39.9	53.6	-
<b>Spent BAC</b>	6.1	40.1	53.8	-
<b>ACFC 10</b>	11.6	22.9	41.7	3.0
<b>ACFC 15</b>	7.1	38.6	54.2	-
<b>ACFC 20</b>	-	41.6	58.8	1.9
<b>OVC</b>	2.9	18.9	78.3	-
<b>VC48C</b>	23.9	31.7	44.6	-
<b>BPL</b>	1.8	20.6	62.8	15.5
<b>VCRSD</b>	-	33.3	63.6	3.2
<b>WV-A 1100</b>	14.7	32.1	47.5	5.7
<b>WV-A 1500</b>	15.6	11.9	65.4	7.1

Though useful information could be extracted from the XPS analysis regarding the nature and concentration of various functional groups, some of the findings were inconsistent with previous reports in the literature.<sup>[126,127,128]</sup> In C1s deconvolution, the carboxylic and lactone groups are missing from almost all the samples except WV-A 1100 and WV-A 1500. This might be due to their low population or the merging of carboxylic/lactone peak with that of carbonyl groups (Figure 24). Similarly, O1s peak has overlapping in the case of phenol and carbonyl groups, and lactone and carboxylic groups. Though lactones and phenols are visibly distinguishable in O1s

peaks, they also share a common area which is quite significant for all the samples. This is due to the fact that both these peaks possess anhydrides and carbonyl/ether oxygen. It is quite difficult to have distinguishable peaks for all the surface functional groups within C1s and O1s narrow spans of binding energy in XPS analysis. Consequently, further characterization was performed by Boehm titration to acquire more insight about the surface functional groups on various activated carbons.

### 4.3 Boehm titration analysis

The acidic characteristics, which are related to hydrophilicity, in carbon materials are usually introduced by oxide species present on the surface. Acid functional groups are mostly polar and can strongly affect the adsorption of polar VOCs on activated carbons. In this regard, Boehm titration can be used to investigate the surface functional groups as well as acidity. As can be noted in Figures 25 and 26, phenolic and lactone groups are the most abundant on all samples, which is in good agreement with the XPS results for O1s deconvolution. Nevertheless, it should be highlighted that in contrast to the Boehm titration results, the XPS analysis revealed that the lactone group is more prominent than phenol for all activated carbons. Although carboxylic group was not observed in XPS analysis, it was clearly detected by Boehm titration. The amount of carboxylic group ranged from 4 % to 20 % of total acidity. WV-A 1100 and WV-A 1500 (wood based pelleted GACs) exhibited the highest amounts of carboxylic content (nearly 0.2 mmol/g), which agrees with the XPS analysis.

Surprisingly, spent BAC only possesses phenolic group and in a very small quantity (0.07 mmol/g acidity). The highest total acidity belongs to ACFC 15 with 1.11 mmol/g acidity, while for other ACFCs and wood based pelleted GACs total acidity ranges between 0.84 and 0.99 mmol/g. All non-pelleted GACs showed lower values for each functional group and total acidity

with respect to Virgin BAC, ACFCs, and pelleted GACs. Virgin BAC has a total acidity of 0.66 mmol/g, which is much lower than ACFCs and wood based pelleted GACs.

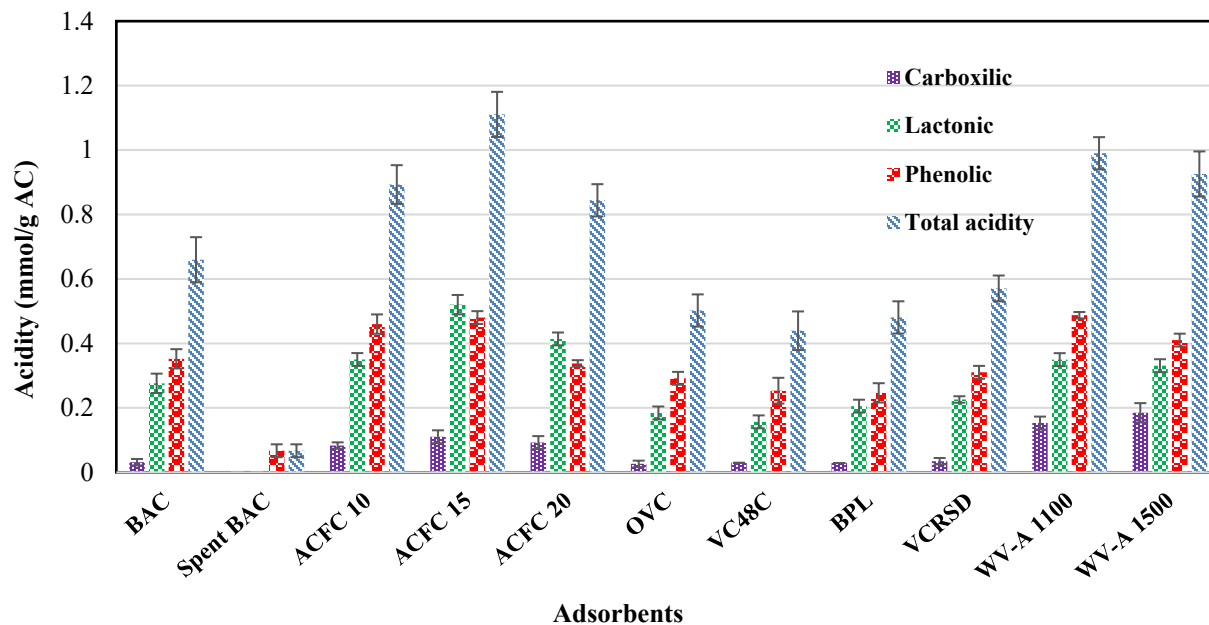


**Figure 25.** Contribution of SOFG to total acidity derived from Boehm titration.

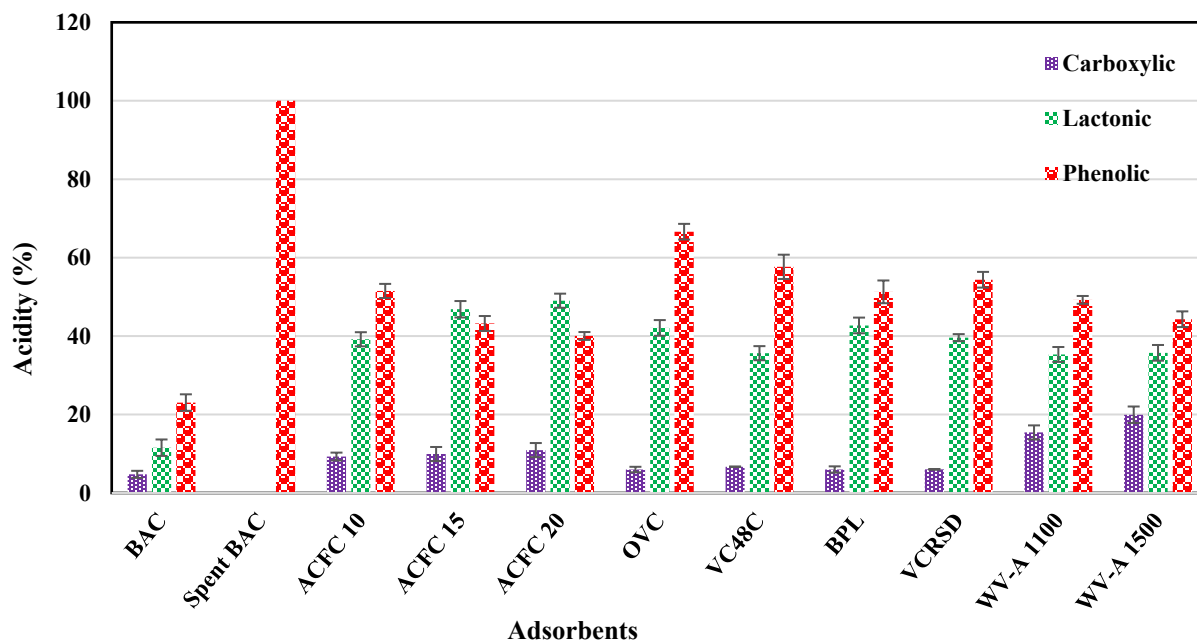


**Figure 26.** Relative amount of acidity originated from SOFGs.

#### 4.4 pH at point zero charge determination

The pH value at point zero charge ( $\text{pH}_{\text{pzc}}$ ) is related to the extent of acidity when all the surface charge is neutralized. This parameter indicates the carbon sample's inherent acidic and/or basic nature and the degree of oxidation. In Table 10, the experimental results for  $\text{pH}_{\text{pzc}}$  are summarized and compared to the overall oxygen content and degree of oxidation estimated from XPS analysis, and total acidity obtained from Boehm titration.

**Table 10.**  $\text{pH}_{\text{pzc}}$ , overall oxygen content (%), degree of oxidation ( $\text{C}_{\text{ox}}/\text{C}_{\text{gr}}$ , %), and total acidity for carbon samples.

Adsorbents	$\text{pH}_{\text{pzc}}^*$	Overall oxygen content (%)	Degree of oxidation, $\text{C}_{\text{ox}}/\text{C}_{\text{gr}}$ (%)	Total acidity mmol/g AC
Virgin BAC	5.72±0.0	6.91	17	0.66±0.07
Spent BAC	5.02±0.1	5.12	21	0.07±0.02
ACFC 10	5.56±0.0	3.93	22	0.89±0.06
ACFC 15	5.42±0.3	2.66	18	1.11±0.07
ACFC 20	5.92±0.2	1.95	17	0.84±0.05
OVC	8.40±0.0	8.01	24	0.50±0.05
VC48C	8.15±0.0	5.45	25	0.44±0.06
BPL	6.68±0.1	5.21	28	0.48±0.05
VCRSD	6.90±0.2	7.56	23	0.57±0.04
WV-A 1100	5.60±0.0	8.37	35	0.99±0.05
WV-A 1500	5.76±0.0	6.61	37	0.93±0.07

\*Values appear as their mean of all the duplicates ± standard deviation.

From this table, it can be easily deduced that the obtained values for pH at point zero charge for the activated carbons are consistent with our findings (total acidity) from Boehm titration analysis with a high coefficient of determination ( $R^2 \approx 0.70$ ) values. In general, wood based crushed GACs with comparatively lower total acidity (OVC, VC48C) had pH values in the basic range, and BACs, ACFCs, coal based crushed GACs (BPL, VCRSD) and pelleted GACs had pH values in the acidic range. Crushed GACs are either fully basic or close to neutral, which is also in agreement with their lower acidic content witnessed in Boehm titration.

However, findings from Boehm titration are not fully consistent with XPS analyses. For instance, Spent BAC showed lower pH value and higher degree of oxidation but negligible total acidity. This might be due to the presence of oxygen species (from Spent BAC previous use) that contribute to the degree of oxidation but not to oxygen surface functionality. XPS analyses revealed that crushed GACs had high oxygen contents and high degrees of oxidation, which is in contrary to their basic pH and low total acidity found in Boehm titration and  $\text{pH}_{\text{pzc}}$  analyses. This observation is probably due to the fact that some oxygen functional groups such as pyrone, ether, quinone or carbonyl in GACs structure can result in basicity.<sup>[58,73]</sup> Both C1s and O1s deconvolution results confirmed the presence of a considerable percentage of carbonyl groups either in individual peaks or in peaks which are merged with phenol or lactone groups. Total acidity from Boehm titration,  $\text{pH}_{\text{pzc}}$  and overall oxygen content and degree of oxidation from XPS analysis are all in good agreement for pelleted GACs (WV-A 1100 and WV-A 1500).

#### 4.5 Adsorption breakthrough study

The outlet flow from the fluidised bed adsorber mainly contains aliphatic polar compounds such as 2-propanol, acetone, ethanol, iso-butanol and n-butanol. In this section, the results for single component breakthrough experiments are presented and discussed in details. A breakthrough curve demonstrates the variation of effluent concentration with time, starting from an initially clean bed (free of any adsorbate) to the saturation point. Data generated from breakthrough tests are essential to select a suitable adsorbent and to have a reliable technical design.<sup>[35,96,122]</sup>

The performance of adsorbents is typically represented by parameters such as VOC removal capacity and breakthrough time. The adsorption performance of activated carbon samples for polar VOCs is closely connected with both adsorbent and adsorbate properties. Surface area, micro-porosity, and surface chemistry of adsorbents exert great influence on the capacity and breakthrough profile for organic compounds. On the other hand, adsorbate's properties such as molecular weight, molecular structure, kinetic diameter, polarity, solubility, and boiling point greatly impact the adsorption process.<sup>[18]</sup> Figures 27 to 37 summarize the experimental breakthrough curves for all the tested adsorbates.

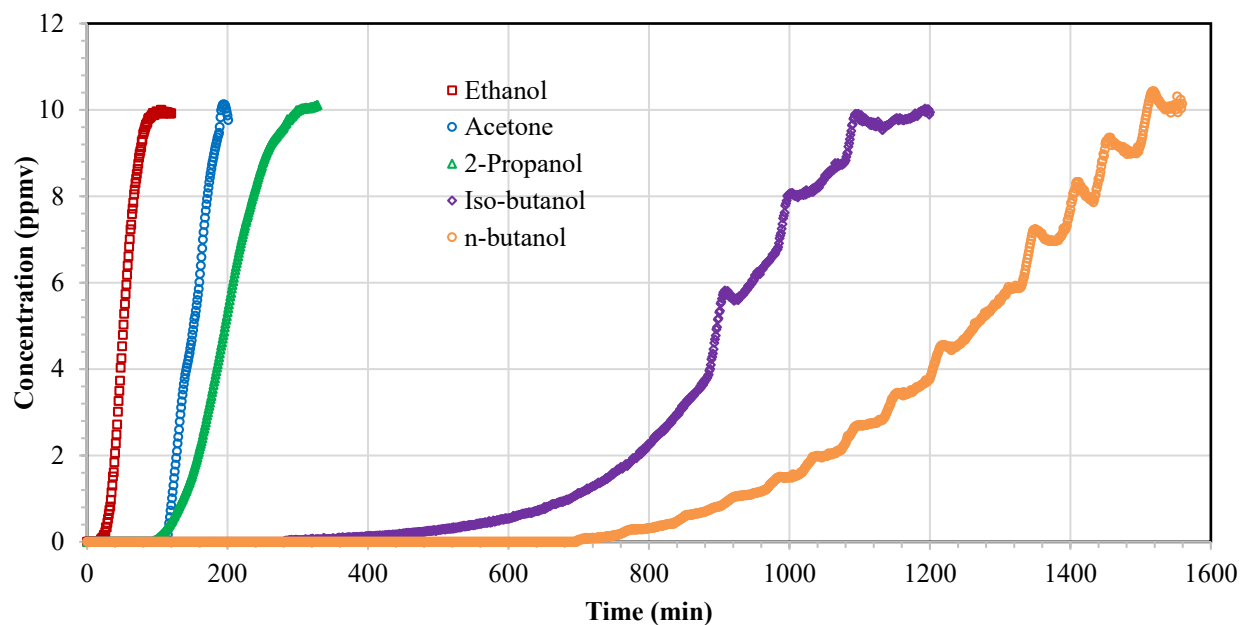


**Figure 27.** Single-component adsorption breakthrough profiles of 10 ppmv 2-propanol, acetone, ethanol, iso-butanol and n-butanol on 2 g virgin BAC at 22 °C.

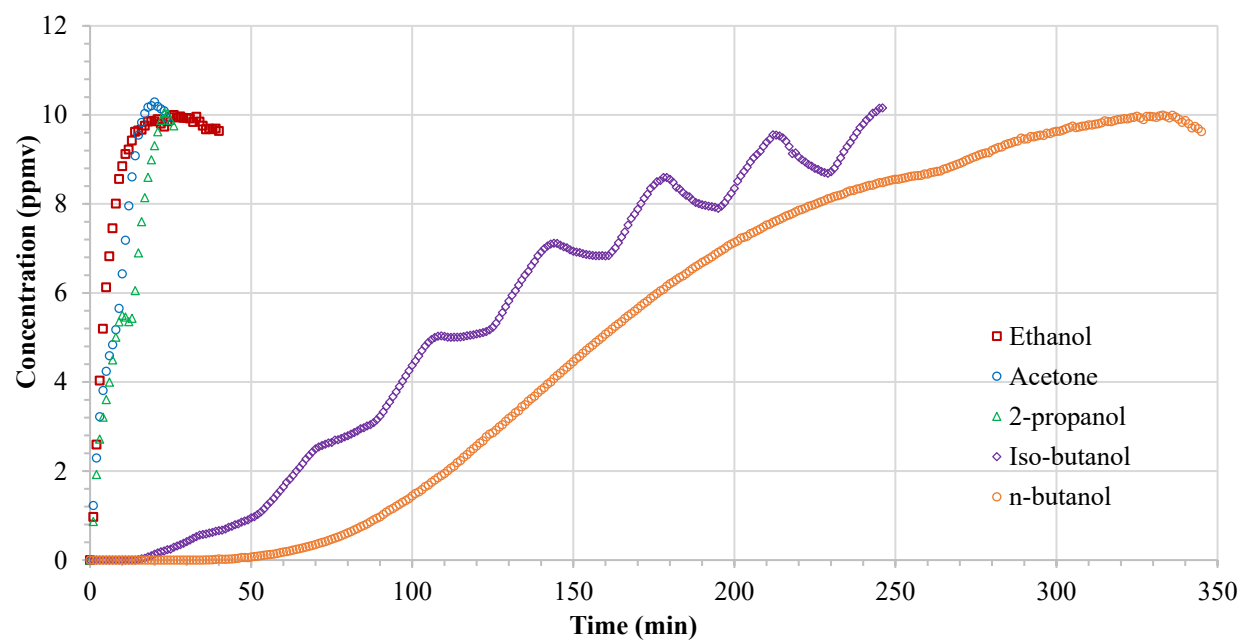


**Figure 28.** Single-component adsorption breakthrough profiles of 10 ppmv 2-propanol, acetone, ethanol, iso-butanol and n-butanol on 4 g spent BAC at 22 °C.

Among the selected VOCs, ethanol is the smallest molecule with the lowest molecular weight and dimensions. In spite of the fact that small molecular dimension facilitates penetration of ethanol molecules into the pores, the adsorption capacity for ethanol is very small compared to other adsorbates for all the adsorbents.<sup>[130]</sup> The highest adsorption capacity and 5 % breakthrough time for ethanol were 2.1 % and 62 minutes over WV-A 1100, respectively. Apart from pelleted GACs (i.e. WV-A 1100 and WV-A 1500), only ACFC 10 possessed an adsorption capacity over 1 % for ethanol. For ethanol, 5 % breakthrough time was below 1 h for most adsorbents and occurred instantaneously for spent BAC (Figures 28).

This observation is mainly due to the high polarity and low molecular weight of ethanol. Regarding the adsorption of polar VOCs on activated carbons, it is suggested that surface oxygen groups dominate the adsorption at low relative pressures or concentrations.<sup>[131]</sup> At high concentration, porosity is the governing factor for polar and non-polar adsorbates.<sup>[131]</sup> There are three types of Van-der Waals attractive forces among neutral molecules (i.e. molecules with no net charge or permanent dipole moment): induced-dipole/induced-dipole forces, dipole/induced-dipole forces and dipole-dipole forces.<sup>[75]</sup> Among Van der Waals attractive forces, dipole/induced-dipole and dipole-dipole forces control the adsorption of polar molecules such as ethanol at low concentration.<sup>[75,132]</sup> These two forces mainly result from the carboxyl and anhydride functional groups on activated carbon. This is supported by the fact that wood-based pelleted GACs (WV-A 1100 and WV-A 1500), which possess the highest amount of carboxylic groups, performed best for ethanol.

Compared to ethanol, acetone has higher molecular weight and lower polarity, which are both favorable for adsorption onto activated carbons. In contrast, the higher volatility and water-solubility of acetone with respect to ethanol can adversely affect the adsorption capacity of



acetone. On the other hand, the higher adsorption potential of acetone compared to ethanol (Table 5) leads to stronger Van der Waals attractive forces and better physisorption.<sup>[35]</sup> The highest acetone adsorption capacity was 4.6 % over ACFC 10 and the longest 5 % breakthrough time was 134 min over VC48C. Except for ACFC 10 and Spent BAC, acetone adsorption capacity was around 2 % for all other adsorbents.

2-propanol has a higher molecular weight, higher vapor pressure, and similar adsorption potential compared to ethanol. However, since it is less polar, it showed a greater affinity towards activated carbon samples.<sup>[107]</sup> The highest adsorption capacity for 2-propanol, 6.4 %, was achieved by ACFC 10. An adsorption capacity of 4 % was observed for wood based GACs (OVC, VC48C, WV-A 1100 and WV-A 1500), ACFC 15 and ACFC 20. The adsorption capacity and 5 % breakthrough time for 2-propanol varied between 0.1 - 6.4 % and 28 - 205 min, respectively, depending on the adsorbent.

Following 2-propanol, heavier molecules (iso-butanol and n-butanol) with larger molecular sizes, higher boiling points, and lower polarities were investigated. There was a substantial increase in the adsorption capacity and breakthrough time for iso-butanol and n-butanol even though these compounds have larger kinetic diameters and lower adsorption potentials (Table 5).

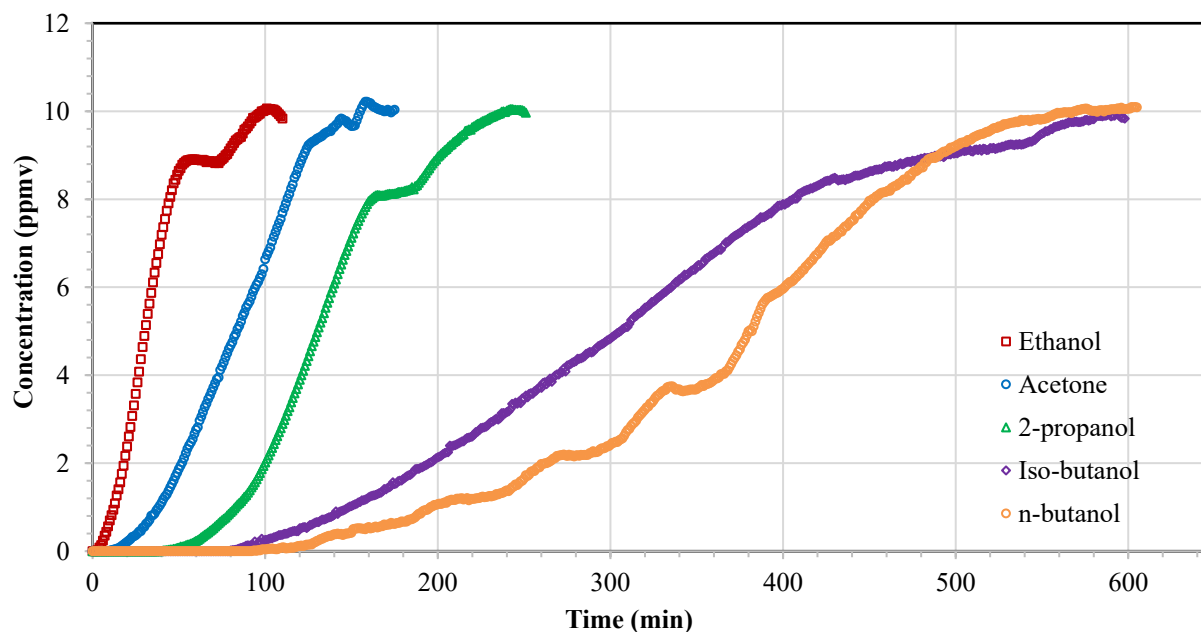


**Figure 29.** Single-component adsorption breakthrough profiles of 10 ppmv 2-propanol, acetone, ethanol, iso-butanol and n-butanol on 0.5 g ACFC 10 at 22 °C.

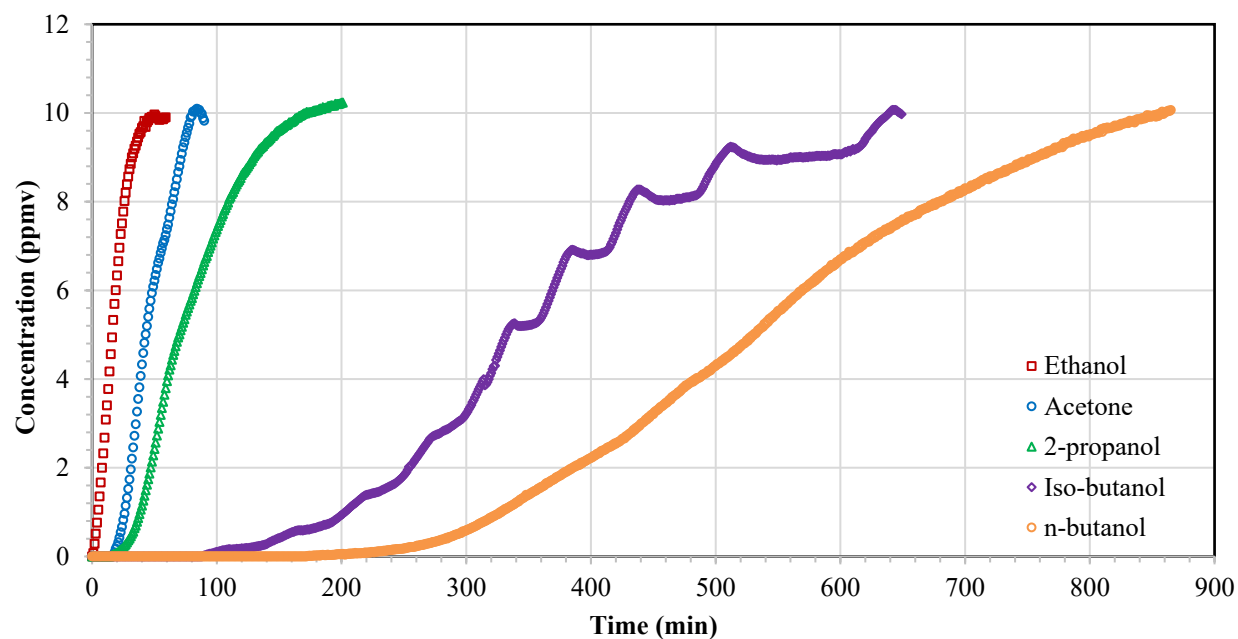


**Figure 30.** Single-component adsorption breakthrough profiles of 10 ppmv 2-propanol, acetone, ethanol, iso-butanol and n-butanol on 0.5 g ACFC 15 at 22 °C.

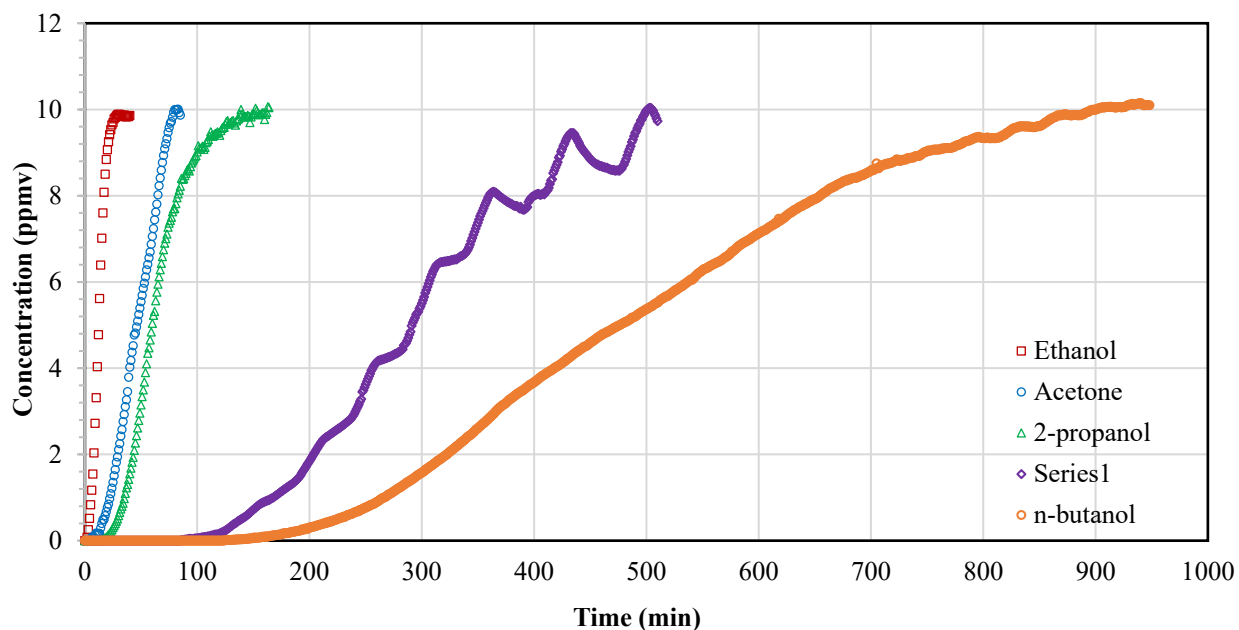


**Figure 31.** Single-component adsorption breakthrough profiles of 10 ppmv 2-propanol, acetone, ethanol, iso-butanol and n-butanol on 0.5 g ACFC 20 at 22 °C.

All carbon samples showed lower adsorption capacity for iso-butanol than n-butanol although iso-butanol has a slightly higher adsorption potential. This is mainly due to the higher water solubility and lower boiling point of iso-butanol. For iso-butanol, ACFC 20 exhibited the highest adsorption capacity (26 %) and for n-butanol most carbon samples achieved around 30 % adsorption capacity. For iso-butanol, the 5 % breakthrough time was around 10 h for Virgin BAC, OVC and VC48C, and for n-butanol, it was above 1000 min for OVC and VC48C.

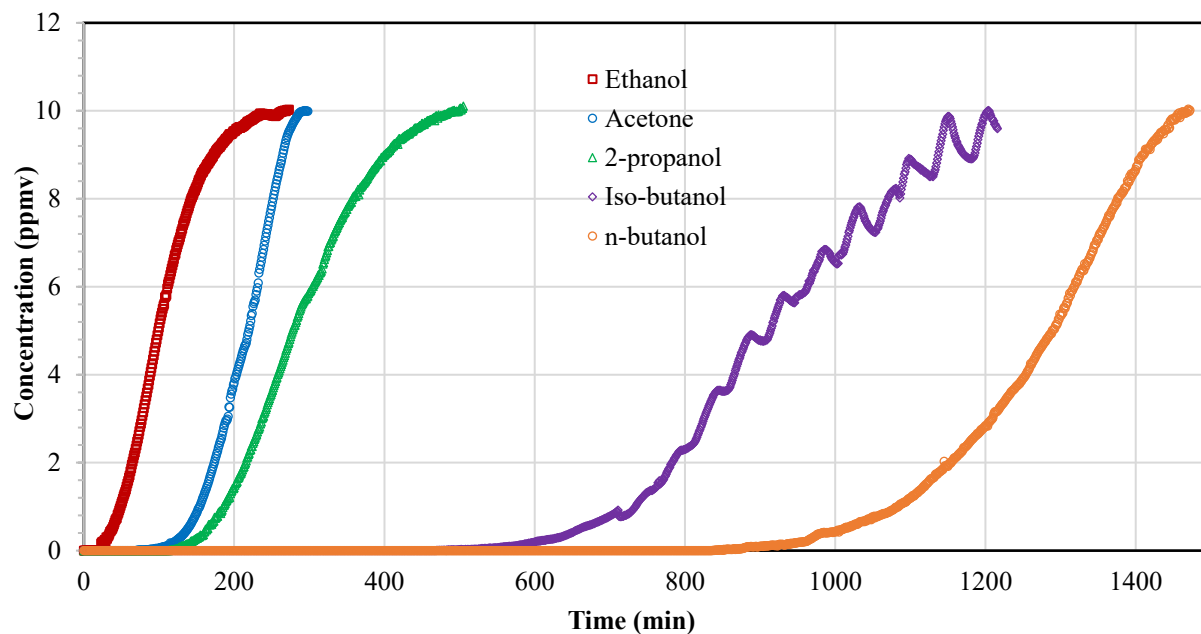


**Figure 32.** Single-component adsorption breakthrough profiles of 10 ppmv 2-propanol, acetone, ethanol, iso-butanol and n-butanol on 2 g OVC at 22 °C.

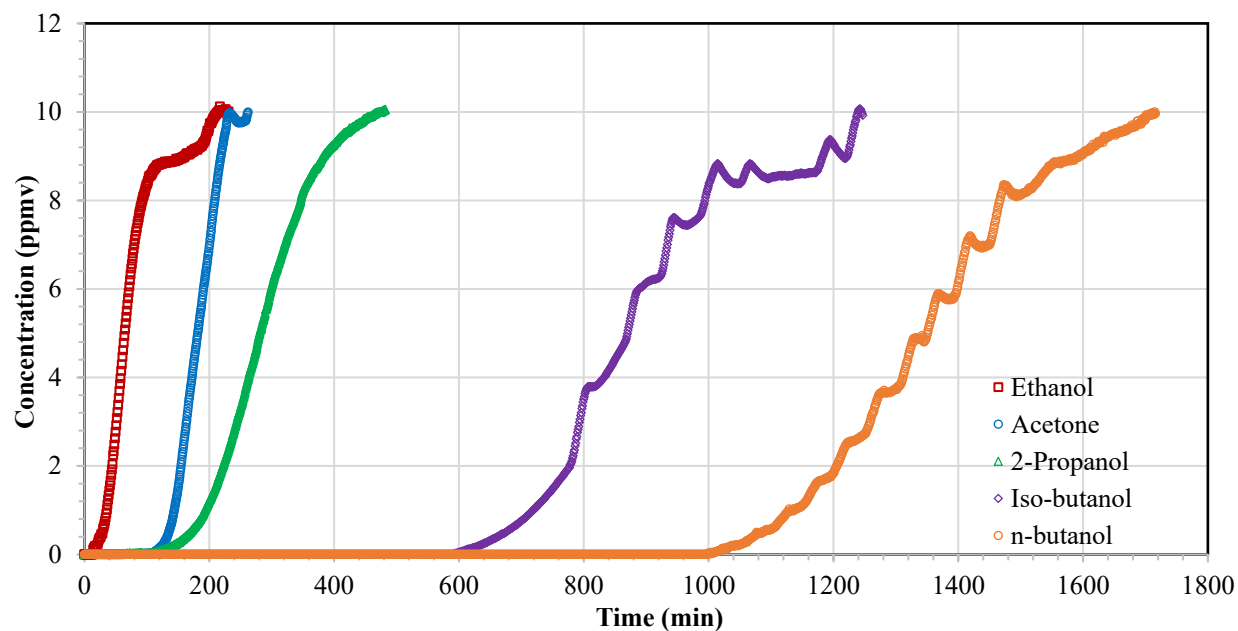


**Figure 33.** Single-component adsorption breakthrough profiles of 10 ppmv 2-propanol, acetone, ethanol, iso-butanol and n-butanol on 2 g VC48C at 22 °C.

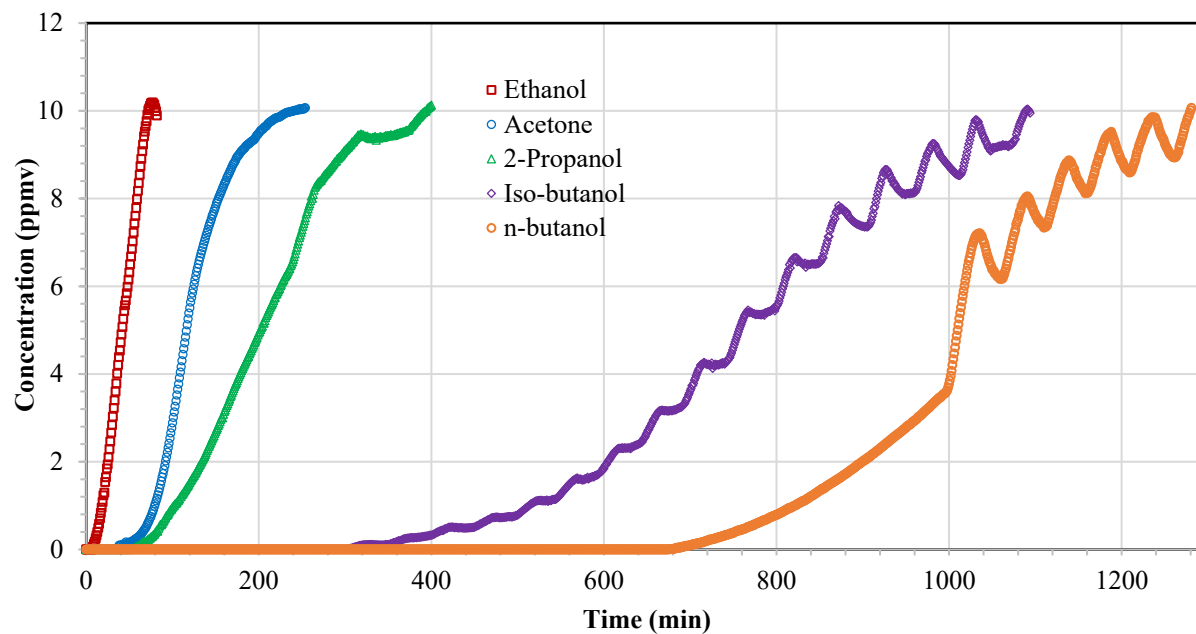


**Figure 34.** Single-component adsorption breakthrough profiles of 10 ppmv 2-propanol, acetone, ethanol, iso-butanol and n-butanol on 2 g BPL at 22 °C.

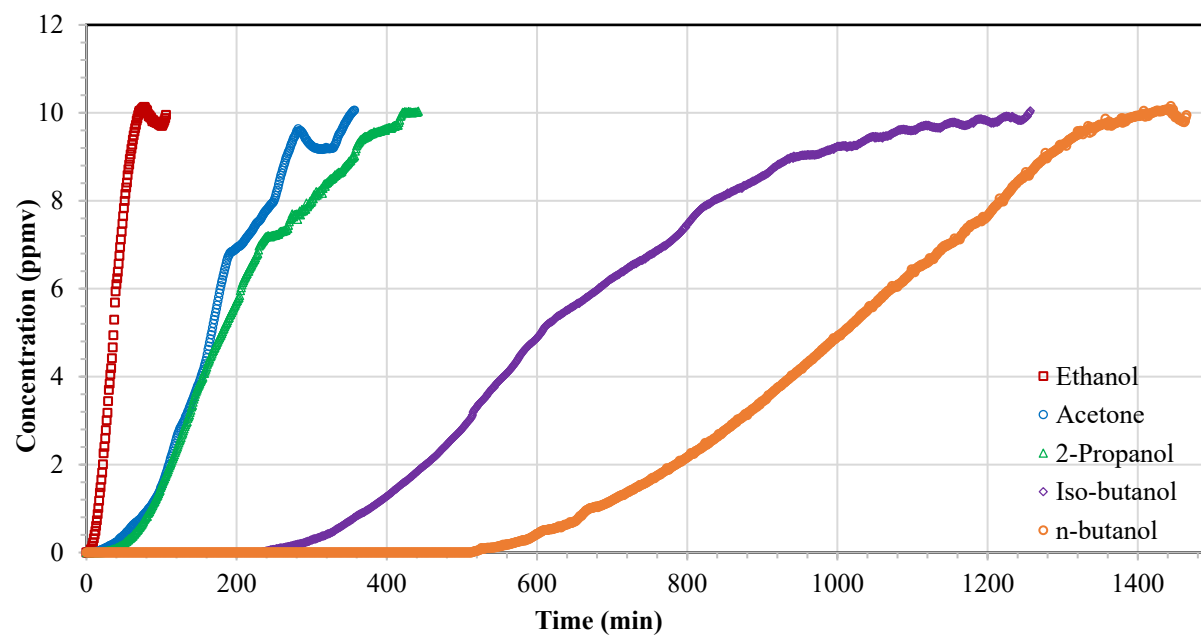


**Figure 35.** Single-component adsorption breakthrough profiles of 10 ppmv 2-propanol, acetone, ethanol, iso-butanol and n-butanol on 2 g VCRSD at 22 °C.

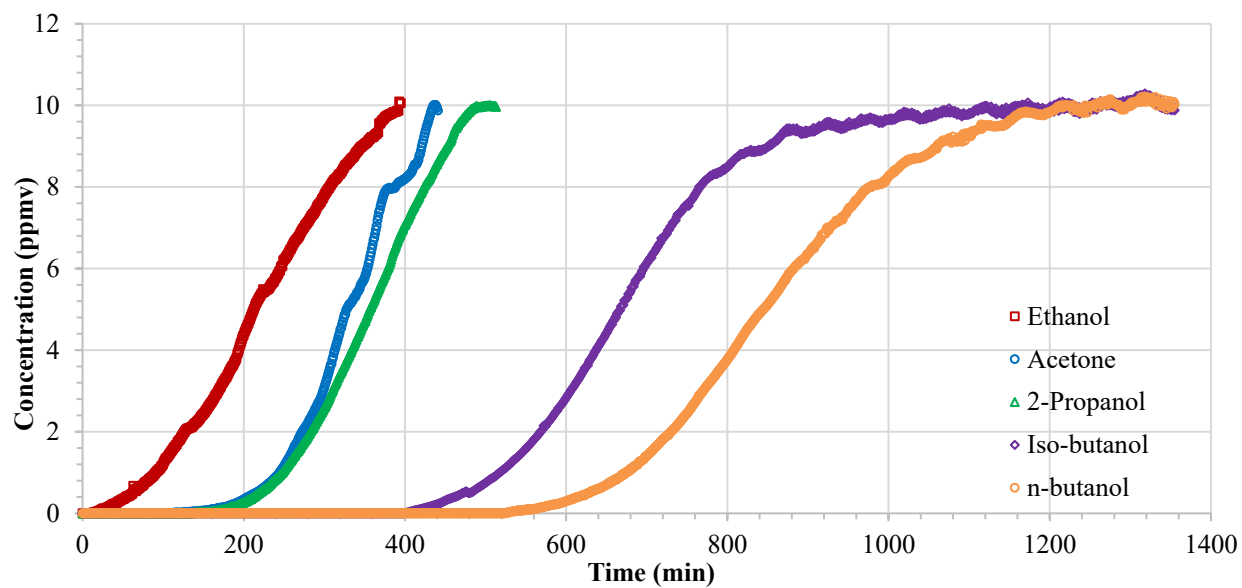


**Figure 36.** Single-component adsorption breakthrough profiles of 10 ppmv 2-propanol, acetone, ethanol, iso-butanol and n-butanol on 2 g WV-A 1100 at 22 °C.

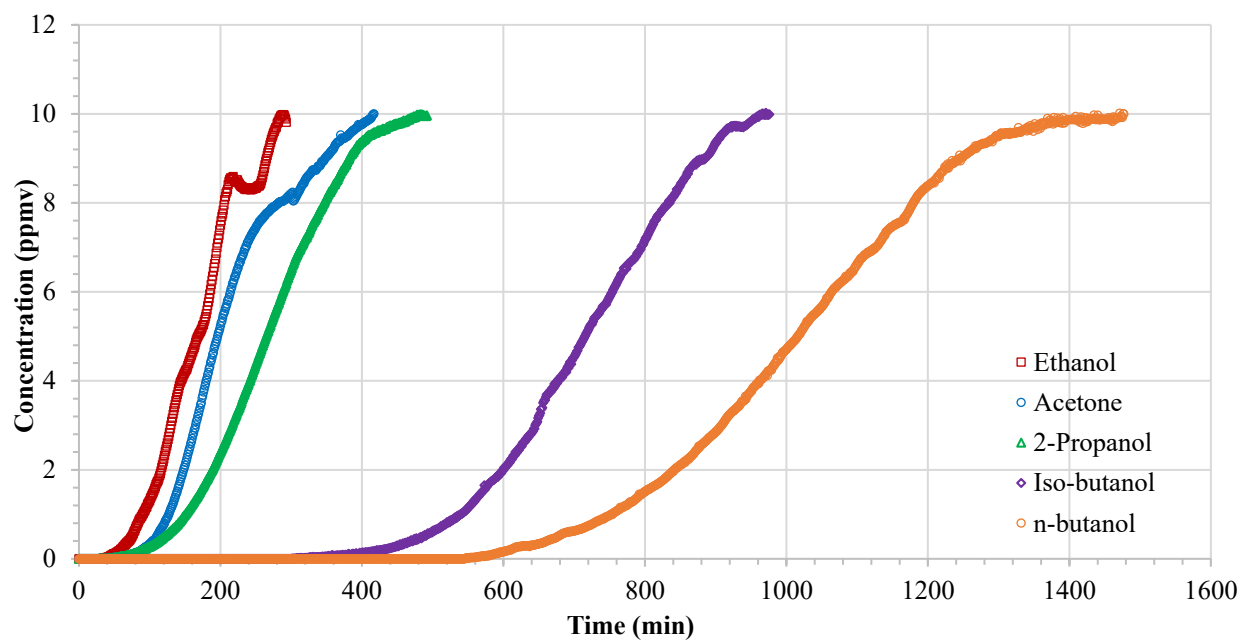


**Figure 37.** Single-component adsorption breakthrough profiles of 10 ppmv 2-propanol, acetone, ethanol, iso-butanol and n-butanol on 2 g WV-A 1500 at 22 °C.

In order to study the trend in adsorption capacity from adsorbent perspective, it would be advantageous to elucidate the adsorbents' behavior according to a broader classification: BACs, ACFCs, crushed GACs (wood and coal base) and pelleted GACs. It should be highlighted that the performance evaluation of Spent BACs was not conducted for adsorbates with high polarity and low molecular weight since the adsorption capacity and breakthrough time were negligible.

For easier comparison, adsorption capacities and properties of carbon samples are summarized in Tables 11 and 12. Adsorption capacity of adsorbents depends on the adsorbents' textural and chemical properties. In general, at low concentration, adsorption capacity of less polar or non-polar adsorbates (i.e. iso-butanol and n-butanol) is controlled by adsorbent's physical properties such as pore size, BET surface area, micropore volume, narrow micropore volume and micro-porosity.<sup>[131]</sup> Table 11 summarizes the adsorption capacity of n-butanol and iso-butanol. It can be noted that the trend of adsorption capacity of BACs, ACFCs, crushed GACs (wood and coal base) and pelleted GACs matches the trend of these adsorbent's surface area and pore volume (total and micropore). For instance, BET surface area, micropore volume, total pore volume and micro-porosity values are close for Virgin BAC and wood based crushed GACs (OVC and VC48C). As shown in Table 11, adsorption capacities of these three carbons for iso-butanol and n-butanol are also close. OVC and VC48C possess high micro-porosity, which can enhance their performance to a great extent. Coal or bitumen based GACs (BPL and VCRSD) showed lower adsorption capacities compared to Virgin BAC due to their lower BET surface area and total pore volume. It is worth mentioning that in our study, a marginal increase in surface area is not so influential because at low concentration of 10 ppmv, adsorption mainly involves micropore volume not the total pore volume.<sup>[75,84,128]</sup> It is known that adsorption occurs preferentially at micropores due to their higher adsorption energy. Nonetheless, crushing the GAC samples was

advantageous because it reduces the diffusion path and resistances during external and internal mass transfers.<sup>[74,75]</sup>

**Table 11.** Adsorbents textural properties and adsorption capacity for iso-butanol and n-butanol.

Adsorbents	BET surface area (m <sup>2</sup> /g)	Micropore Volume (cm <sup>3</sup> /g)	Narrow Micropore Volume (cm <sup>3</sup> /g)	Total Pore Volume (cm <sup>3</sup> /g)	Micro-porosity (%)	Adsorption capacity (weight %)	
						Iso-butanol	n-butanol
Virgin BAC	1340	0.50	0.19	0.54	92	18.9	26.7
Spent BAC	804	0.29	0.09	0.38	76	0.2	0.8
ACFC 10	1058	0.37	0.30	0.42	88	14.9	21.5
ACFC 15	1326	0.55	0.31	0.63	87	25.0	29.7
ACFC 20	1793	0.66	0.35	0.70	94	26.0	32.5
OVC	1311	0.48	0.29	0.54	89	18.3	27.4
VC48C	1194	0.44	0.27	0.49	90	16.1	26.0
BPL	1001	0.35	0.19	0.45	78	12.7	19.2
VCRSD	820	0.31	0.17	0.37	83	12.3	19.4
WV-A 1100	1466	0.25	0.08	1.09	23	13.5	19.7
WV-A 1500	1964	0.42	0.09	1.29	32	13.1	17.9

Similarly, the adsorption capacities and breakthrough times for ACFCs follow the sequence of ACFC 20 > ACFC 15 > ACFC 10, confirming that for these two pollutants micro-porosity and surface area are the determining factors.



Regarding the porous structure of GACs and BACs, it is reported that their micropores are somehow branched from their larger pores and are not readily available at the surface as beneficial adsorption sites.<sup>[44]</sup> This along with their particle size can explain why the breakthrough curves of GACs are not comparatively sharp especially for heavy compounds. Smaller particle size offers more compaction in the fixed bed, less void volume and higher bulk density, which are important to prevent channeling and improper mass transfer. Heavier molecules (iso butanol and n-butanol) at first occupy micropores and then adsorption continues in mesopores until saturation is reached. In contrary, smaller molecules occupy mainly the micropores and quickly reach to saturation, showing a comparatively steeper curve. Possessing micropores comparable in size to the molecular diameter of the challenge compound is beneficial for adsorbents to reach higher adsorption capacity and steeper breakthrough curves.<sup>[48,96]</sup> Slopes of breakthrough curves for OVC and VC48C are roughly similar to that of Virgin BAC and higher than other coal-based GACs (BPL and VCRSD), indicating lower mass transfer resistances for these samples.

Wood-origin pelleted GACs (WV-A 1100 and WV-A 1500) have higher BET surface areas and larger total pore volumes compared to all other samples, which can improve the adsorption performance. However, their micropore volume and micro-porosity are clearly lower than most selected adsorbents. This feature of WV-A 1100 and WV-A 1500 can, to a great extent, justify their inferior adsorption performance in comparison to Virgin BAC, ACFCs, OVC and VC48C for less polar (iso-butanol) and non-polar (n-butanol) compounds.

Among correlations of adsorption capacities of iso-butanol and n-butanol with all the textural properties, best suited correlation was found with micropore volume with high coefficient of determination ( $R^2 \approx 0.8$ ) as shown in Figure 38.

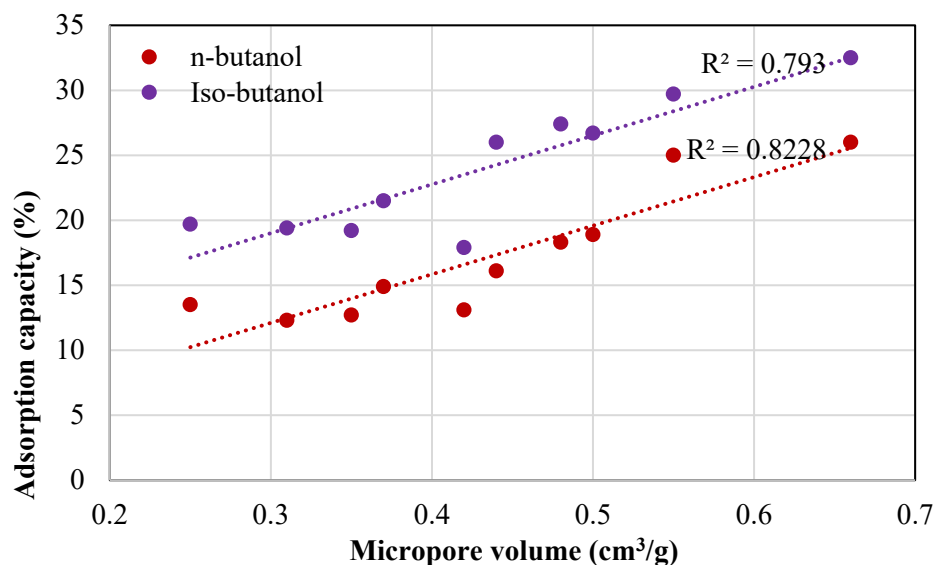


**Figure 38.** Correlations to micropore volume of the carbon samples with adsorption capacity of Iso-butanol and n-butanol.

On the other hand, chemical properties of adsorbent materials such as elemental composition, percentage of total oxygen, presence of functional groups, degree of oxidation and total acidity control adsorption capacity of polar components at low concentration.<sup>[131]</sup> Table 12 summarizes the adsorption capacity of ethanol, acetone and 2-Propanol along with adsorbent's chemical properties.

Depending on the adsorbate, oxygen surface functional groups and micro-porosity of ACFCs affected the adsorption capacity differently. For n-butanol and iso-butanol, the adsorption capacity followed the order ACFC 20 > ACFC 15 > ACFC 10. For smaller and highly polar molecules (i.e. ethanol, acetone and 2-propanol), ACFC 10 outperformed ACFC 15 and ACFC 20. This can be explained by the total oxygen content and degree of oxidation of ACFCs, which follows the order ACFC 10 > ACFC 15 > ACFC 20. The ACFCs adsorption trend for light VOCs can also be justified by considering the fact that at low concentration narrower pores of ACFC 10

lead to better VOC adsorption. In an experimental work, Foster et al.<sup>[133]</sup> evaluated three different types of ACFCs namely ACFC 15, ACFC 20 and ACFC 25 for acetone adsorption at 10.3 ppmv. They also observed that the adsorption capacity followed the sequence of ACFC 15 > ACFC 20 > ACFC 25.

**Table 12.** Adsorbent's chemical properties and adsorption capacity of ethanol, acetone and 2-propanol.

Adsorbents	pH <sub>PZC</sub>	Overall Oxygen Content (%)	Degree of oxidation, C <sub>ox</sub> /C <sub>gr</sub> (%)	Total Acidity mmol/g AC	Adsorption capacity (weight %)		
					Ethanol	Acetone	2-propanol
Virgin BAC	5.72	6.91	17	0.66	0.5	2.0	2.5
Spent BAC	5.02	5.12	21	0.07	0.0	0.1	0.1
ACFC 10	5.56	3.93	22	0.89	1.2	4.6	6.4
ACFC 15	5.42	2.66	18	1.11	0.5	2.8	4.6
ACFC 20	5.92	1.95	17	0.84	0.4	2.4	3.4
OVC	8.40	8.01	24	0.50	0.9	2.4	4.4
VC48C	8.15	5.45	25	0.44	0.9	2.4	4.0
BPL	6.68	5.21	28	0.48	0.5	1.6	2.2
VCRSD	6.90	7.56	23	0.57	0.5	2.3	2.5
WV- A 1100	5.60	8.37	35	0.99	2.1	2.2	4.5
WV- A 1500	5.76	6.61	37	0.93	1.3	2.0	3.5

As evidenced in their characterization, WV-A 1100 and WV-A 1500 possess all the surface functional groups with acidic character. Among all the activated carbons, only these adsorbents

demonstrated the presence of carboxylic acid functionalities. These functional groups are suggested to be crucial for the physical adsorption of polar VOCs at low concentration range.<sup>[128]</sup> Therefore, higher adsorption capacity and longer breakthrough times for these carbon samples are attributed to larger surface area, higher total pore volume, acidic pH and the presence of carboxylic groups.

Among correlations of adsorption capacities of ethanol, acetone and 2-propanol with all the chemical properties, best suited correlation was found with total acidity with high coefficient of determination ( $R^2$ ) as shown in Figure 39. In case of 2-propanol  $R^2$  value is highest ( $\sim 0.51$ ) followed by acetone ( $\sim 0.41$ ) and ethanol ( $\sim 0.31$ ).

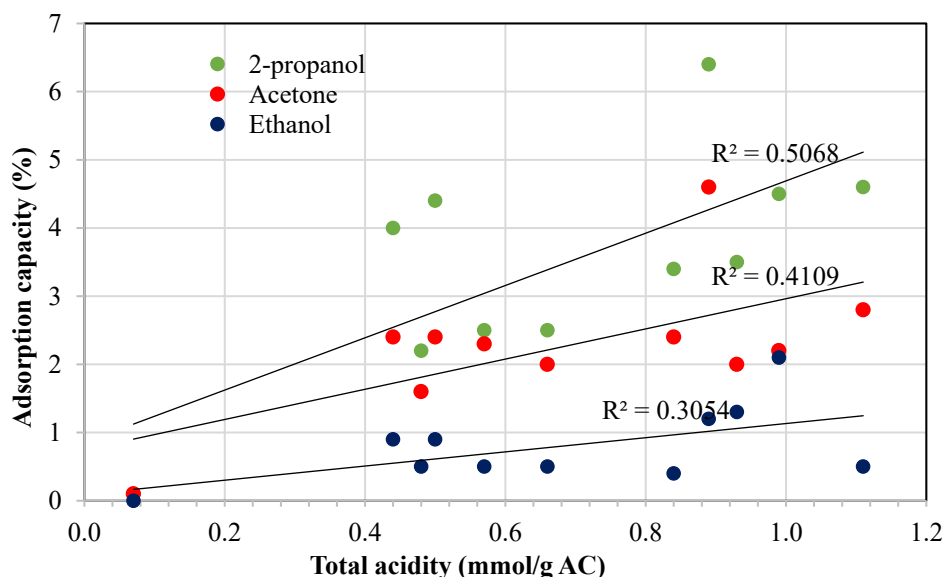


**Figure 39.** Correlations to total acidity (mmol/g AC) of the carbon samples with adsorption capacity of 2-propanol, acetone and ethanol.

The adsorption capacity was determined by mass balance (formulas brought in Chapter 3) as well as by breakthrough curve integration. It should be noted that some discrepancies were observed in these two approaches in our work (tolerance up to  $\pm 5\%$ ). The second approach,

breakthrough curve integration, is considered more accurate because the gravimetric approach is more susceptible to human errors. Table 13 presents the values of adsorption capacity (calculated based on the results of breakthrough experiments) and standard deviation of adsorption capacities for all eleven activated carbons challenged with five adsorbates.

**Table 13.** Adsorption capacity in weight % (with standard deviation) based on breakthrough curves for various ACs.

<b>Adsorbents \ Adsorption Capacity*</b>	<b>Ethanol (wt %)</b>	<b>Acetone (wt %)</b>	<b>2-Propanol (wt %)</b>	<b>Iso-butanol (wt %)</b>	<b>n-butanol (wt %)</b>
<b>Virgin BAC</b>	0.5±0.0	2.0±0.3	2.5±0.2	18.9±0.6	26.7±0.5
<b>Spent BAC</b>	0.0±0.0	0.1±0.0	0.1±0.0	0.2±0.0	0.8±0.1
<b>ACFC 10</b>	1.2±0.1	4.6±0.2	6.4±0.2	14.9±0.2	21.5±0.4
<b>ACFC 15</b>	0.5±0.3	2.8±0.0	4.6±0.1	25.0±0.2	29.7±0.2
<b>ACFC 20</b>	0.4±0.0	2.4±0.0	3.4±0.3	26.0±0.1	32.5±0.0
<b>OVC</b>	0.9±0.1	2.4±0.2	4.4±0.3	18.3±0.3	27.4±0.2
<b>VC48C</b>	0.9±0.0	2.4±0.1	4.0±0.3	16.1±0.3	26.0±0.3
<b>BPL</b>	0.5±0.0	1.6±0.1	2.2±0.1	12.7±0.6	19.2±0.2
<b>VCRSD</b>	0.5±0.0	2.3±0.3	2.5±0.3	12.3±0.4	19.4±0.4
<b>WV-A 1100</b>	2.1±0.0	2.2±0.1	4.5±0.2	13.5±0.6	19.7±0.1
<b>WV-A 1500</b>	1.3±0.2	2.0±0.0	3.5±0.3	13.1±0.3	17.9±0.4

\* Values appear as their mean of all the duplicates ± standard deviation.

All the experiments were reproduced at least twice to ensure the consistency of data. Standard deviation of these values varies from 0 to 0.59 (less than 1), which confirms the reliability of experimental works. Further information regarding the single component adsorption tests

including the adsorption capacities based on both gravimetric analysis and breakthrough profile, saturation time, and breakthrough time are provided in Appendix A to E.

In summary, all activated carbon samples showed the lowest adsorption capacity for ethanol, mostly below 1 %. ACs exhibited greater capacities for acetone and 2-propanol compared to ethanol. The best adsorption capacities were for iso-butanol and n-butanol with capacities as high as 26.0 % and 32.5 %, respectively.

Some performance indicators such as the throughput ratio (TPR) and the length of unused bed (LUB) can be extracted from the breakthrough profiles.<sup>[96]</sup> TPR is defined as the ratio between 5 and 50 % breakthrough times, which are respectively the times at which the outlet concentration equals 5 and 50 % of the inlet concentration.<sup>[122]</sup> Steeper breakthrough curves have higher TPR values, signifying enhanced mass transfer. Length of unused bed is a dimensionless indicator of the length of unused portion of adsorbent bed at 5 % breakthrough time (shown in Figure 13).<sup>[96]</sup>

In the present study, sacrificial fixed bed is designed based on the concept of LUB, which is explained in detail in Appendix I. In an adsorber design, TPR value should be higher than 70 % and LUB should vary around 30 % or less. However, in some cases (e.g. adsorbers using GACs), values up to 50 % are acceptable for LUB.<sup>[96]</sup> Table 14 lists the 5 % breakthrough time, TPR, and LUB values for all eleven adsorbents and five adsorbates investigated in this study. All the experimental cases can be categorized in 3 groups:

- Totally feasible (indicated by green color), where  $LUB \leq 50\%$  for GACs and  $\leq 30\%$  for other ACs, and  $TPR \geq 70\%$ .
- Not feasible (indicated by red color), where TPR and LUB are far outside the acceptable ranges.

- Potentially feasible (indicated by blue color), where TPR, LUB or both are close to safe margins.

Among 55 scenarios, there are nine totally feasible cases for which both TPR and LUB values are satisfactory. In 31 not feasible cases, the adsorbent-adsorbate system can not overcome the limitations related to mass transfer and/or adsorption affinity. In the other 15 potentially feasible scenarios, TPR and/or LUB values are out of acceptable range. Based on Table 14, Virgin BAC is technically the most feasible adsorbent for the sacrificial bed as it offers promising design conditions with all the adsorbates (5 cases). However, Virgin BAC's high cost puts some constraints on its application as a sacrificial material. Likewise, ACFCs are not suitable because of their cost, which is almost 10 times higher than Virgin BAC. Wood based crushed GACs (OVC and VC48C) allowed totally feasible scenarios for all adsorbates except ethanol. Employing coal based crushed GACs (BPL and VCRSD) as sacrificial bed resulted in fewer feasible cases compared to the wood-based ones (in total 4 cases). It is noteworthy that in general, crushing and screening operations to achieve desired particle size are costly and energy intensive. WV-A 1100 and WV-A 1500 offered roughly the same number of totally feasible and potentially feasible scenarios as wood based GACs (7 cases). Taking into account all the performance parameters and cost, WV-A 1100 is selected as the best adsorbent for sacrificial bed design in our study. Therefore, further studies on detailed adsorber design and cyclic adsorption-regeneration were only conducted for this sample.

**Table 14.** Summary of performances parameters calculated based on single-VOC breakthrough curves.

VOCs Adsorbents	Ethanol			Acetone			2-propanol			Iso-butanol			n-butanol			Overall
	5% BT (min)	TPR (%)	LUB (%)	5% BT (min)	TPR (%)	LUB (%)	5% BT (min)	TPR (%)	LUB (%)	5% BT (min)	TPR (%)	LUB (%)	5% BT (min)	TPR (%)	LUB (%)	Feasibility
Virgin BAC	28	64	47	123	80	21	123	63	37	607	66	45	824	71	50	5
Spent BAC	IB	-	-	1	20	-	IB	-	-	81	48	85	27	31	97	0
ACFC 10	7	26	71	15	26	83	66	54	47	133	42	54	153	41	64	0
ACFC 15	2	15	81	22	46	59	34	49	62	141	54	71	295	54	49	0
ACFC 20	3	17	62	16	36	65	28	46	57	122	38	76	150	32	75	0
OVC	36	38	42	112	61	38	168	60	49	680	74	48	1020	77	49	4
VC48C	31	46	52	134	72	26	181	62	43	664	73	29	1074	79	37	4
BPL	15	29	56	77	59	37	86	56	35	429	58	56	755	73	47	3
VCRSD	15	38	55	53	35	70	61	34	69	353	55	63	605	61	54	1
WV - A 1100	62	29	56	106	58	38	205	63	42	486	73	48	618	73	49	4
WV- A 1500	45	30	54	93	57	40	119	42	56	462	64	50	655	67	48	3
*Cases	G - 0, B - 1, R - 10			G - 2, B - 4, R - 5			G - 0, B - 5, R - 6			G - 3, B - 2, R - 6			G - 4, B - 3, R - 4			

\* Green (G) – Feasible, Blue (B) - Potentially feasible, Red (R) – Not feasible. IB-Initial breakthrough; the number appears after the letters (G, B, or R) refers to the number of relevant cases for each VOC.



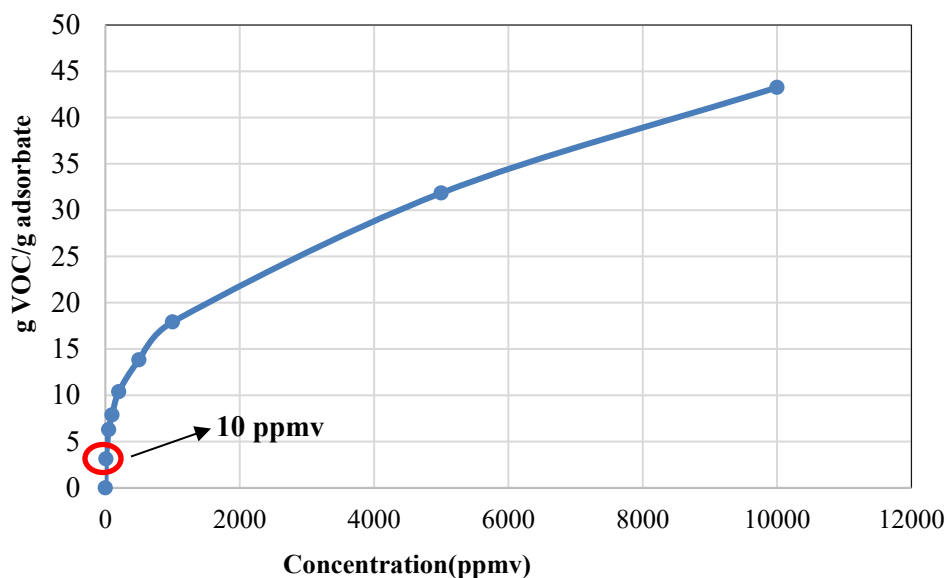
The detailed design of sacrificial bed using WV-A 1100 A is summarized in Table 15 and the design calculations are provided in Appendix I. In the lab scale set-up, the unused fraction of bed is about 42 %, which is within the safe margin for adsorber columns using GACs. The same value for unused fraction of bed at 5 % breakthrough was considered in the full-scale system calculations. Based on that, the amount of activated carbon was estimated to be around  $1400 \pm 50$  kg at 5 % breakthrough time by LUB method. Using lab scale data Thomas rate coefficient and Wheeler-Jonas adsorption coefficient were  $147.22 \text{ kg}^{-1}\text{m}^3\text{s}^{-1}$  and  $17892 \text{ min}^{-1}$ , respectively. Moreover, the total bed length for full scale system was 0.192 at 5 % breakthrough time. Cross sectional area of the full-scale bed, maximum bed depth and used volume were  $14.22 \text{ m}^2$ , 1.12 m and  $2.77 \text{ m}^3$ , respectively. Thomas model and wheeler Jonas equation also provided close values for per day carbon consumption (1363 and 1348 kg/day), confirming consistency between the LUB method and widely used models for adsorber design.

**Table 14.** Full-scale sacrificial bed designed with WV-A 1100 for 2-propanol adsorption.

<b>Bench Scale data</b>			
<b>Given Data</b>		<b>Calculated Values</b>	
Length of adsorber Bed = 0.041 m		LUB at @ 5% = 0.0178 m	
Bed Bulk density = 522.2 kgm <sup>-3</sup>		Fraction unused = 42%	
Air feed rate = 10 SLPM		Cross sectional area of the adsorber = $9.36 \times 10^{-5}$ m <sup>2</sup>	
Superficial Velocity = 1.78 ms <sup>-1</sup> = 107 mmin <sup>-1</sup>		Volume of the adsorber = $3.83 \times 10^{-6}$ m <sup>3</sup>	
5% BT time = 206 min		Superficial gas flow rate = $2.88 \times 10^{-3}$ kgm <sup>-2</sup> min <sup>-1</sup>	
Capacity = 0.045 kg VOC/Kg AC		Thomas rate coefficient K <sub>th</sub> = 147.22 kg <sup>-1</sup> m <sup>3</sup> s <sup>-1</sup>	
Column length to diameter ratio, $\frac{L}{D} = 10$		Adsorption rate coefficient K <sub>v</sub> = 17892 min <sup>-1</sup> (Wheeler-Jonas model)	
<b>Full Scale System</b>			
<b>Provided Data</b>		<b>Calculated Values</b>	
Actual feed flow rate = 55000 ft <sup>3</sup> min <sup>-1</sup>		Cross sectional area of the bed = 14.57 m <sup>2</sup>	
5% BT time = 1 day = 1440 min		Diameter of the Bed = 4.31 m	
Column length to diameter ratio, $\frac{L}{D} = 5$ (thumb rule)		Maximum bed depth = 1.12 m	
Superficial gas flow rate = $2.88 \times 10^{-3}$ kgm <sup>-2</sup> min <sup>-1</sup>		LUB % = 42 %	
		LUB at @ 5% = 0.175 m	
		Total LB = 0.192 m	
		Empty bed contact time = 24 s	
		Used Volume = 2.77 m <sup>3</sup>	
<b>Carbon consumption comparison</b>			
	LUB	Wheeler-Jonas model	Thomas model
Carbon consumption @5%	1446 kg	1363 kg	1348 kg

#### 4.6 Adsorption isotherms

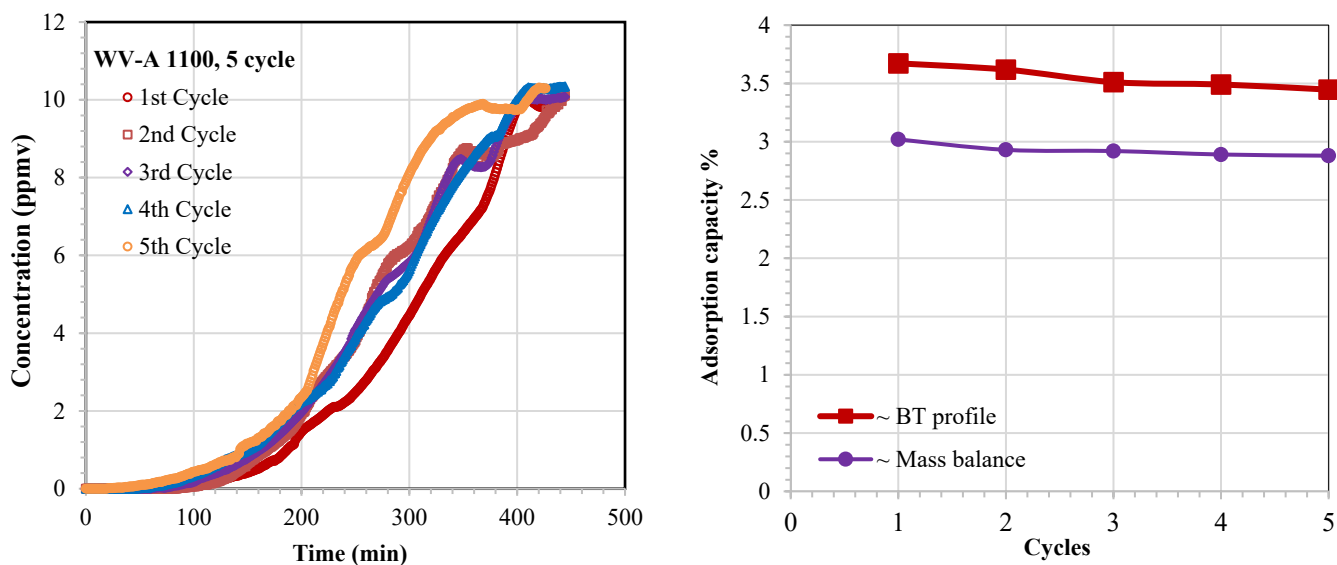
In all breakthrough experiments, VOC concentration was 10 ppmv, which is quite low to overcome all the mass transfer resistances during external and internal diffusions. In this regard, it is important to acquire the adsorption isotherm for WV-A 1100A and 2-propanol system to understand the performance of selected adsorbent in a wider concentration range.<sup>[40]</sup> Figure 40 shows the adsorption isotherm of WV-A 1100 for 2-propanol. In the low concentration range (<1000 ppmv), the steep rise in VOC uptake indicates the suitability of this adsorbent for low concentration. At 10000 ppmv, capacity reaches 43% and the isotherm curve reaches a plateau, signifying utilization of mesopores. As confirmed by the shape of obtained isotherm (type II isotherm), WV-A 1100 is suitable for application as a sacrificial bed. The reason is that WV-A 1100 high adsorption capacity at low concentration is crucial and its regeneration efficiency is not considered a relevant parameter in this project.



**Figure 40.** Adsorption Isotherms of 2-propanol on WV-A 1100 at 20 °C.

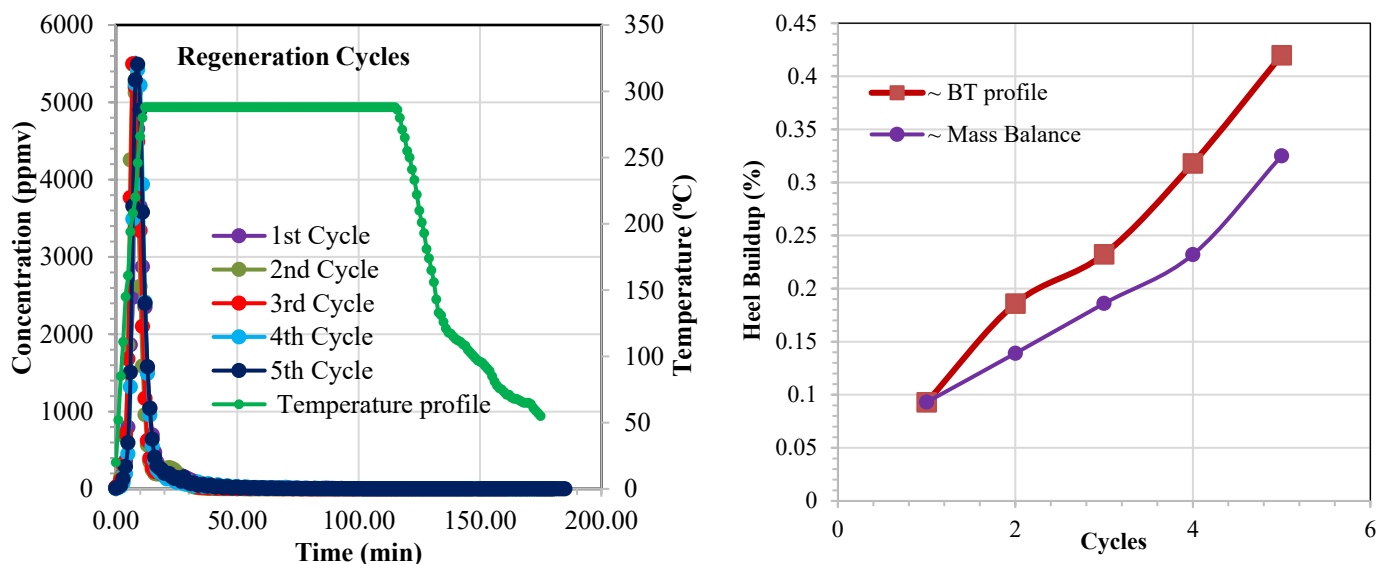
#### 4.7 Cyclic adsorption-desorption

Even though regeneration of a sacrificial bed is not a common practice, considering the high cost of tested carbon samples, it was decided to investigate the feasibility of regeneration of the adsorbents. In this regard, the regenerability of WV-A 1100, as the best performing sample, was evaluated. To investigate the adsorption performance and regeneration characteristics of the adsorbent, a 5-cycle adsorption-regeneration test was conducted using WV-A 1100 and 2-propanol. Figure 41a presents adsorption breakthrough profiles for five consecutive cycles, indicating that the reduction in 5% breakthrough time is not significant. In addition, the adsorption capacities for each cycle calculated based on the mass balance and integration of breakthrough curve are depicted in Figure 41b. It is evident that the WV-A 1100 relative capacity loss during the first five cycles (defined as  $(1^{\text{st}} \text{ cycle capacity} - 5^{\text{th}} \text{ cycle capacity}) \times 100 / 1^{\text{st}} \text{ cycle capacity}$ ) is less than 6 %.



**Figure 41.** a. Adsorption breakthrough profiles of 2-propanol on 2 g WV-A 1100 at 20 °C and  
b. Adsorption capacity for 2-propanol on 2 g WV-A 1100 at 20 °C.

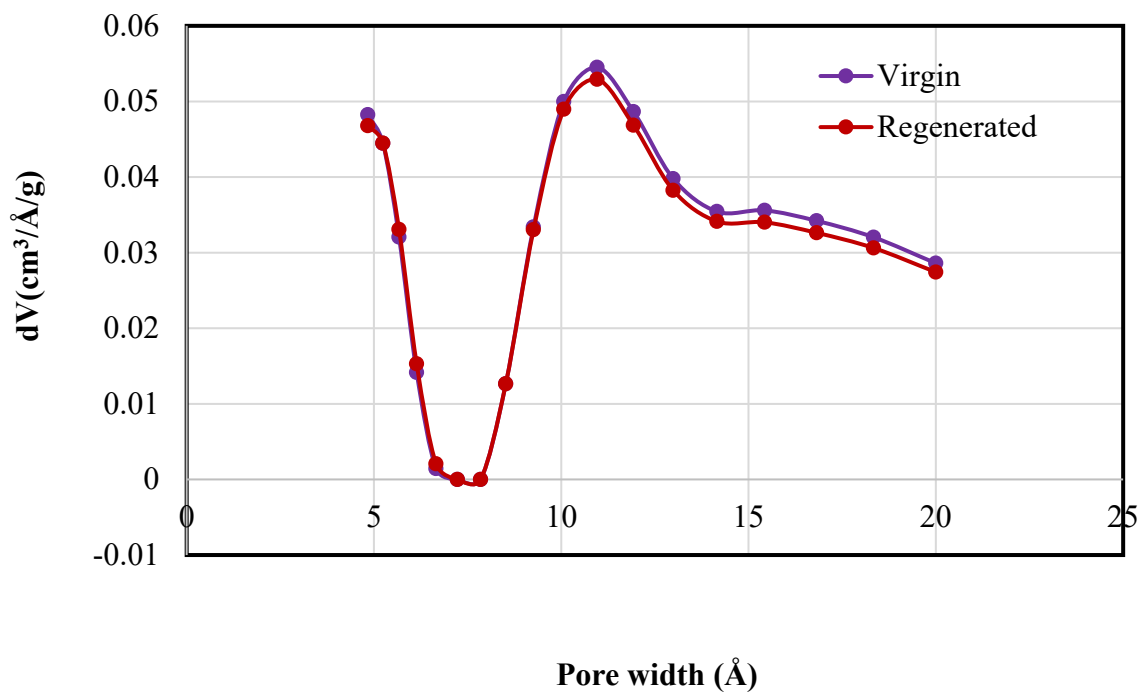
Figure 42a presents 2-propanol concentration profiles and the temperature of the bed during the regeneration stage. As temperature was raised, 2-propanol concentration at the outlet of the adsorber sharply increased and reached its maximum, 5500 ppmv, after 10 min of starting the regeneration. It is interesting to note that the concentration peaked roughly when the reactor reached the desired regeneration temperature of 288 °C. In about 20 min, almost all of the adsorbed 2-propanol was desorbed from the bed and the outlet concentration approached zero.



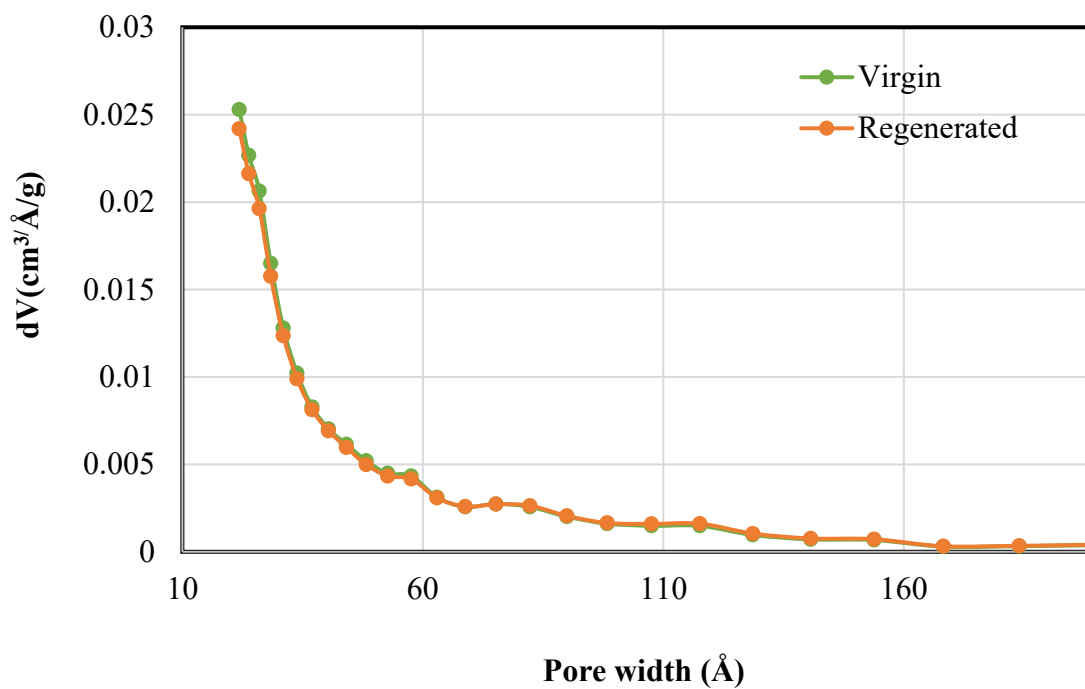
**Figure 42. a.** Desorption concentration and temperature profiles of 2-propanol on 2 g WV-A 1100 and **b.** Desorption efficiency for 2-propanol on 2 g WV-A 1100 at 288 °C.

Figure 42b shows the desorption efficiency determined both by mass balance and breakthrough integration for all cycles. The area under the desorption curve (Figure 42a) gives the amount of VOC desorbed. This value is then subtracted from the quantity of VOC adsorbed (Figure 40a) to obtain the amount of heel. Based on both mass balance and breakthrough calculations, the cumulative heel after 5 cycles is less than 0.45 %.

Figures 43 and 44 compare the pore size distributions of virgin and regenerated samples after 5 cycles of adsorption-desorption. The changes in pore size distribution in micro- and mesopore regions before and after 5 cycles can help to study heel build-up. Considering Figure 43, for both fresh and spent samples, in the micropore region, pore sizes are mainly in the range of 5-7 Å and 8-20 Å. Judging from the downward shift of the pore size distribution curve for regenerated sample between 10 and 20 Å, it is suggested that large micropores contribute to heel formation. As evidenced in Figure 44, the difference in pore size distributions for fresh and regenerated samples in the mesopore region (20-50 nm) is much less significant, indicating that WV-A 1100 mesopores play an important role in 2-propanol adsorption but not in heel build-up. Desorption of adsorbed 2-propanol from micropores with higher adsorption energy compared to mesopores is harder and requires more energy. Consequently, under the employed regeneration conditions (288 °C), 2-propanol molecules are easily desorbed from the mesopores but not completely from the micropores, resulting in heel formation. Therefore, larger micropores are responsible for most of the heel build-up due to the higher share of high energy adsorption sites.<sup>[134]</sup>



**Figure 43.** Micropore size distribution of virgin and spent WV-A 1100.



**Figure 44.** Mesopore size distribution of virgin and spent WV-A 1100.

## **Chapter 5. Conclusion & Recommendation**



## 5.1 Conclusion

The central goal of this research work was to investigate the applicability and efficiency of various activated carbon adsorbents in a sacrificial carbon bed for removal of low concentration of polar VOCs from paint booth air. The objective was to find the best adsorbent in terms of adsorption capacity and cost to capture ethanol, acetone, 2-propanol, 2-methyl-1-propanol, and 1-butanol at very low concentration (10 ppmv). In the first step, Virgin Kureha BAC and three types of activated carbon clothes were investigated and showed satisfactory performances; however, owing to their very high cost, they were considered as last candidates for the sacrificial bed design. Focusing on less costly commercially available carbon adsorbents, coal based (BPL and VCRSD) and coconut shell based GAC adsorbents (OVC and VC48C) were examined. On the basis of the results obtained from adsorption experiments (i.e. adsorption capacity and breakthrough time) with different pollutants and cost of various adsorbents, it was proposed that pelleted GACs (WV-A 1100 and WV- A 1500) are the most viable candidates for the sacrificial bed.

Some of the major findings of this project work are listed below.

- Adsorption capacity for highly polar species like ethanol, acetone and 2-propanol were around 1, 2 and 3 %, respectively with almost all the adsorbents. Adsorption capacity for ethanol was very poor (maximum 1 %), while the adsorption capacity for 2-propanol was satisfactory (maximum 6 %). Adsorbates with higher molecular weight and lower polarity performed better in terms of capacity (starting around 13 % and reached up to 30 %). Adsorbents' physical properties control the performance for less polar components while chemical properties dominated the polar compounds adsorption process.

- Among adsorbents, coal based GACs' (BPL and VCRSD) performance was poor as compared to other adsorbents. BAC, ACFCs, non-pelleted GACs (OVC and VC48C) and pelleted GACs (WV-A 1100 and WV-A 1500) all exhibited acceptable capacities and breakthrough profiles.
- In general, compared to other adsorbents, GAC (both crushed and pelleted) samples possessed better LUB and TPR values. Most of the experiments (GACs challenged with various VOCs) were feasible and potentially feasible (TPR, LUB or both close to safe margins). So sacrificial bed design would be theoretically feasible if activated carbon is selected from this family of carbon adsorbents.
- Sacrificial bed design using WV-A 1100 for adsorption of 2-propanol suggests per day carbon consumption of around 1300 - 1400 kg. The amount of carbon requirement from LUB method showed consistency with the estimations determined by Thomas and Wheeler Jonas models.

## 5.2 Recommendations

In this research, the overall performance of various activated carbons has been investigated to select a suitable material (i.e. low cost and high capacity) for a sacrificial bed. Carbon samples were thoroughly characterized to highlight possible connections between their properties and performances. Finally, theoretical design of the sacrificial bed was discussed for the best performing adsorbent. Still, further research in the following areas are recommended to achieve more feasible carbon adsorbents for the sacrificial bed.

- Surface oxygen functional groups are responsible for adsorption of polar compounds on activated carbons. Acid treatment (with  $\text{HNO}_3$ <sup>[127]</sup>) can be carried out to further functionalise the carbon adsorbents and to increase the acidic percentage specially the carboxylic content.

- Design based on the lab scale data cannot assure flawless and valid results for large scale applications. Similar experiments can be performed in pilot scale to obtain more relevant and reliable data for adsorber design.
- Multicomponent adsorption experiments can be carried out to investigate the competitive adsorption between various VOCs as well as breakthrough profiles at low concentration range.
- Effect of relative humidity on the adsorption performance of activated carbon can be studied for both polar and non-polar compounds.

## References

---

- 1 Environmental Protection Agency. 2016. Technical Overview of Volatile Organic Compounds. Accessed on March 2019 from <https://www.epa.gov/indoor-air-quality-iaq/technical-overview-volatile-organic-compounds>
- 2 Volatile organic compounds in products overview. Accessed on March 2019 from <https://www.canada.ca/en/environment-climate-change/services/managing-pollution/sources-industry/volatile-organic-compounds-consumer-commercial/overview.html>
- 3 Common air pollutants: Volatile Organic Compounds (VOCs). Accessed on March 2019 from <https://www.ec.gc.ca/air/default.asp?lang=En&n=15B9B65A-1>.
- 4 Guenther, A., C. N. Hewitt, D. Erickson, R. Fall, C. Geron, T. Graedel, P. Harley, L. Klinger, M. Lerdau and W. McKay (1995). "A global model of natural volatile organic compound emissions." *Journal of Geophysical Research: Atmospheres* 100 (D5): 8873 - 8892.
- 5 Piccot, S. D., Watson, J. J., & Jones, J. W. (1992). A global inventory of volatile organic compound emissions from anthropogenic sources. *Journal of Geophysical Research*, 97 (D9), 9897 - 9912.
- 6 Bari, M.A., Kindzierski, W.B., and Spink, D. 2016. Twelve-year trends in ambient concentrations of volatile organic compounds in a community of the Alberta Oil Sands Region, Canada. *Environment International*, 91: 40 - 50.
- 7 Khan, F. I.; Ghoshal, Kr. A. Removal of Volatile Organic Compounds from polluted air. *Journal of Loss Prevention in the Process Industries* 2000, 13, 527- 545.

---

8 Zhao, L., Huang, S., and Wei, Z. 2014. A demonstration of biofiltration for VOC removal in petrochemical industries. *Environmental Science: Processes & Impacts*, 16 (5): 1001-1007.

9 Golovoy, A. and J. Braslaw (1981). "Adsorption of automotive paint solvents on activated carbon: I. Equilibrium adsorption of single vapors." *Journal of the Air Pollution Control Association* 31 (8): 861-865.

10 Lu, Q. and G. A. Sorial (2004). "Adsorption of phenolics on activated carbon—impact of pore size and molecular oxygen." *Chemosphere* 55 (5): 671- 679.

11 Yu, F. D., L. Luo and G. Grevillot (2007). "Electrothermal swing adsorption of toluene on an activated carbon monolith: Experiments and parametric theoretical study." *Chemical Engineering and Processing: Process Intensification* 46 (1): 70 - 81.

12 Kim, B. R. (2011). VOC Emissions from Automotive Painting and Their Control: A Review. *Environmental Engineering Research*, 16 (1), 1–9.

13 Ramos, M.E., Bonelli, P.R., Cukierman, A.L., Ribeiro Carrott, M.M.L., and Carrott, P.J.M. 2010. Adsorption of volatile organic compounds onto activated carbon cloths derived from a novel regenerated cellulosic precursor. *Journal of Hazardous Materials*, 177(1-3): 175-182.

14 Canada's air pollutant emissions inventory report 2019: chapter 2.4. Accessed on March 2019, from

<https://www.canada.ca/en/environment-climate-change/services/airpollution/publications/emissions-inventory-report-2019/chapter-2-4.html>

15 Chang, C., & Lee, C. (2002). Assessment of the strategies for reducing volatile organic compound emissions in the automotive industry in Taiwan, 34, 117–128.

- 
- 16 Kim, B. R., Kalis, E. M., Dewulf, T., Andrews, K. M., Kim, B. R., Kalis, E. M., Andrews, K. M. (2000). Henry's Law Constants for Paint Solvents and Their Implications on Volatile Organic Compound Emissions from Automotive Painting.' 72 (1), 65 –74.
- 17 Katyal, A.; Morrison, D. R.; 'Forensic applications of contaminant transport models in the subsurface.' Introduction to Environmental Forensics (Second Edition) 2007,513-575
- 18 Zhang, X.; Gao, B'; Creamer, A.E.; Cao, C; Li.; Li, Y.; 'Adsorption of VOCs onto engineered carbon materials: A review.' Journal of Hazardous Materials 338 (2017), 102 -123.
- 19 Leslie, G. B. (2000). "Review: Health risks from indoor air pollutants: public alarm and toxicological reality." Indoor and Built Environment 9 (1): 5-16.
- 20 Kampa, M. and E. Castanas (2008). "Human health effects of air pollution." Environmental Pollution 151(2): 362 - 367.
- 21 Pariselli, F., M. G. Sacco, J. Ponti and D. Rembges (2009). "Effects of toluene and benzene air mixtures on human lung cells (A549)." Experimental and Toxicologic Pathology 61 (4): 381- 386.
- 22 Huang, C.; Wang, H.L.; Li,L.; Wang, Q.; Lu, Q.; De Gouw, J. A.; Zhou, M.; Jing, S. A.; Lu, J.; Chen, C. H.; 'VOC species and emission inventory from vehicles and their SOA formation potentials estimation in Shanghai, China.' Atmospheric Chemistry and Physics, Volume 15, issue 19, 6 October 2015; 11081-11096.
- 23 C.D. Cooper, F.C. Alley, Air pollution control: a design approach, in: F.C. Alley (Ed.) Waveland Press, Long Grove, Ill, 2011.
- 24 Parmar, G. R.; Rao, N. N. Emerging control technologies for volatile organic compounds. Critical Reviews in Environmental Science and Technology 2009, 39, 41-78.

---

25 Berenjjan, A.; Chan, N.; Malmiri, H. J. Volatile Organic Compounds removal methods: A review. *American Journal of Biochemistry and Biotechnology* 2012, 8, 220 - 229.

26 <https://en.wikipedia.org/wiki/Adsorption>, Accessed on July 2019.

27 Bansal, R. C., & Goyal, M. (2005). *Activated carbon adsorption*. New York: Taylor & Francis, 67-143.

28 Slejko, F.L. 1985. *Adsorption technology: a step-by-step approach to process evaluation and application*. M. Dekker, New York.

29 Bottani, E. J.; Tascón, J. M. D. *Adsorption by carbons*. Amsterdam; London: Elsevier, 2008, 53-72.

30 Dimotki, E.D.; Cal, M.P.; Economy, J.; Rood, M.J.; Larson, S.M.; 'Chemically treated activated carbon cloths for removal of volatile organic carbons from gas steams: evidence for enhanced physical adsorption.' *Environmental Science and technology*, 1955, 29, 1876 -1880.

31 Suzuki, M. *Adsorption engineering*. Amsterdam; New York: Elsevier, 1990.

32 Kenneth S. W. Sing.; 'Characterization of porous solids: An introductory survey.' Elsevier B.V. Volume 62, 1991, 1- 9.

33 Do, D.D. 1998. *Adsorption analysis: equilibria and kinetics*, Imperial College Press, London.

34 Singh, K. P.; Mohan, D.; Tandon, G. S.; Gupta, G. S. D. Vapor-phase adsorption of hexane and benzene on activated carbon fabric cloth: Equilibria and rate studies. *Industrial and Engineering Chemistry Research* 2002, 41, 2480 - 2486.

35 Yang, R. T. *Gas separation by adsorption processes*. London: Imperial College Press, 1997.

---

36 Artioli, Y.; 'Adsorption', Encyclopedia of ecology, 2008, 60 - 65.

37 Foo, K.Y., and Hameed, B.H. 2010. Insights into the modeling of adsorption isotherm systems. Chemical Engineering Journal, 156 (1): 2 - 10.

38 Huang, H.; Haghghat, F.; Blondeau, P. 'Volatile organic compound (VOC) adsorption on material: influence of gas phase concentration, relative humidity and VOC type.' Indoor air, 2006 June. Vol 16: 236–247

39 Brunauer, S., Deming, L.S., Deming, W.E., Teller, E. 'On a Theory of the van der Waals Adsorption of Gases(Article).' Journal of the American Chemical Society, Volume 62, Issue 7, 1 July 1940, 1723-1732.

40 Alan Gabelman, P.E., 'Adsorption Basics: part 1.' American Institute of Chemical Engineers (AIChE), July 2017, 48-53.

41 J.-H. Tsai, H.-M. Chiang, G.-Y. Huang, H.-L. Chiang, Adsorption characteristics of acetone chloroform and acetonitrile on sludge-derived adsorbent, commercial granular activated carbon and activated carbon fibers, Journal of Hazardous Materials. 154 (2008) 1183 –1191.

42 Burg, P.; Cagniant, D. 'Characterization of carbon surface chemistry.' Chemistry and physics of carbon. Volume 30, chapter 3, 130 – 175.

43 Zhang, G.; Liu, Y. Zheng, S.; Hashisho, Z. 'Adsorption of volatile organic compounds onto natural porous minerals.' Journal of Hazardous Materials., 364 (2019), 317 - 324.

44 Lu, Q.; Sorial, G. A. The role of adsorbent pore size distribution in multicomponent adsorption on activated carbon. Carbon 2004, 42, 3133 - 3142.



---

45 Ahmad, A.A., and Idris, A. 2014. Preparation and characterization of activated carbons derived from bio-solid: a review. *Desalination & Water Treatment*, 52 (25 - 27): 4848 - 4862.

46 Ahmadpour, A., and Do, D.D. 1997. The preparation of activated carbon from macadamia nutshell by chemical activation. *Carbon*, 35 (12): 1723 - 1732.

47 Salvador, F., Martin-Sanchez, N., Sanchez-Hernandez, R., Sanchez-Montero, M., and Izquierdo, C. 2015. Regeneration of carbonaceous adsorbents. Part I: thermal regeneration. *Microporous & Mesoporous Materials*, 202: 259 - 276.

48 Lashaki, M.J., Atkinson, J.D., Hashisho, Z., Phillips, J.H., Anderson, J.E., and Nichols, M. 2016. The role of beaded activated carbon's pore size distribution on heel formation during cyclic adsorption/desorption of organic vapors. *Journal of Hazardous Materials*, 315: 42 – 51.

49 <https://envirosupply.net/products/powdered-hardwood-carbon>, Accessed on March 2019.

50 [https://www.123rf.com/photo\\_36862276\\_granular-activated-carbon-for-water-filter-on-white-background.html](https://www.123rf.com/photo_36862276_granular-activated-carbon-for-water-filter-on-white-background.html). Accessed on March 2019.

51 <https://www.deltaadsorbents.com/activated-carbon-bulk> Accessed on March 2019.

52 <https://www.acarbons.com/bead-activated-carbon/> Accessed on March 2019.

53 <https://newatlas.com/carbon-cloth-removes-pollutants/16803/> Accessed on March 2019.

54 <https://www.aliexpress.com/item/32386794748.html> Accessed on March 2019.

55 Bhatnagar, A. Application of adsorbents for water pollution control. *Chemical engineering journals*, Oak Park 2013, 219, pp. 499-511.

---

56 Kwiatkowski, J.F. 2012. Activated carbon. Nova Science Publishers, New York.

57 Product specification Beaded shaped activated carbon by Kureha corporation.

58 Le Cloirec, P. 2012. Adsorption onto activated carbon fiber cloth and electrothermal desorption of volatile organic compound (VOCs): a specific review. *Chinese Journal of Chemical Engineering*, 20 (3): 461 - 468.

59 Lu, Q.; Sorial, G. A. The role of adsorbent pore size distribution in multicomponent adsorption on activated carbon. *Carbon* 2004, 42, 3133 - 3142.

60 Lashaki, M. J., Atkinson, J. D., Hashisho, Z., Phillips, J. H., Anderson, J. E., & Nichols, M. (2016). The role of beaded activated carbon's surface oxygen groups on irreversible adsorption of organic vapors. *Journal of Hazardous Materials*, 317(317), 284 – 294.

61 Liu, P., Long, C., Li, Q., Qian, H., Li, A., & Zhang, Q. (2009). Adsorption of trichloroethylene and benzene vapors onto hyper crosslinked polymeric resin. *Journal of Hazardous Materials*, 166, 46 – 51.

62 Stelzer, J., Paulus, M., Hunger, M., & Weitkamp, J. (1998). Hydrophobic properties of all-silica zeolite beta1. *Microporous and Mesoporous Materials*, 22, 1 – 8.

63 K.-J. Kim, C.-S. Kang, Y.-J. You, M.-C. Chung, M.-W. Woo, W.-J. Jeong, N.-C. Park, H.-G. Ahn, Adsorption-desorption characteristics of VOCs over impregnated activated carbons, *Catalyst. Today* 111 (2006) 223 – 228.

64 Q. Qian, C. Gong, Z. Zhang, G. Yuan, Removal of VOCs by activated carbon microspheres derived from polymer: a comparative study, *Adsorption* 21 (2015) 333 – 341.

- 
- 65 W. Su, Y.-p. Zhou, L.-f. Wei, Y. Sun, L. Zhou, Effect of microstructure and surface modification on the hydrogen adsorption capacity of active carbons, *New Carbon Material*. 22 (2007) 135 – 140.
- 66 W. Qiao, Y. Korai, I. Mochida, Y. Hori, T. Maeda, Preparation of an activated carbon artifact: oxidative modification of coconut shell-based carbon to improve the strength, *Carbon* 40 (2002) 351 – 358.
- 67 F. Villacañas, M.F.R. Pereira, J.J.M. Órfão, J.L. Figueiredo, Adsorption of simple aromatic compounds on activated carbons, *J. Colloid Interface Science* 293 (2006) 128 – 136.
- 68 L. Li, S. Liu, J. Liu, Surface modification of coconut shell based activated carbon for the improvement of hydrophobic VOC removal, *Journal of Hazardous Materials* 192 (2011) 683 – 690.
- 69 J. Jaramillo, P.M. Álvarez, V. Gómez-Serrano, Preparation and ozone-surface modification of activated carbon. Thermal stability of oxygen surface groups, *Applied Surface Science* 256 (2010) 5232–5236.
- 70 M. Abe, K. Kawashima, K. Kozawa, H. Sakai, K. Kaneko, Amination of activated carbon and adsorption characteristics of its aminated surface, *Langmuir* 16 (2000) 5059 – 5063.
- 71 J.L. Figueiredo, M.F.R. Pereira, M.M.A. Freitas, J.J.M. Órfão, Modification of the surface chemistry of activated carbons, *Carbon* 37 (1999) 1379 – 1389.
- 72 W. Shen, Z. Li, Y. Liu, Surface chemical functional groups modification of porous carbon, *Recent Pat. Chem. Eng.* 1 (2008) 27 – 40.
- 73 Na, L.; Xiaoliang, M.; Qingfang, Z.; Kyungsoo, K.; Yongsheng, C.; Chunshan. S.; ‘Maximizing the number of oxygen-containing functional groups on activated carbon by using ammonium

---

persulfate and improving the temperature-programmed desorption characterization of carbon surface chemistry. 'Volume 49, issue 15, December 2011, 5002 - 5013.

74 K. Yang, Q. Sun, F. Xue, D. Lin, Adsorption of volatile organic compounds bimetal–organic frameworks MIL-101: Influence of molecular size and shape. *Journal of Hazardous Materials* 195 (2011) 124 – 131.

75 Vizhemehr, A. K., 'Predicting the Performance of Activated Carbon Filters at Low Concentrations Using Accelerated Tests Data,' PhD thesis published on 2014, 9-75.

76 Q. Qian, C. Gong, Z. Zhang, G. Yuan, Removal of VOCs by activated carbon microspheres derived from polymer: a comparative study, *Adsorption* 21 (2015) 333 – 341.

77 K.J. Oh, D.-W. Park, S.S. Kim, S.W. Park, Breakthrough data analysis of adsorption of volatile organic compounds on granular activated carbon, *Korean Journal of Chemical Engineering*. 27 (2010) 632 – 638.

78 F. Qu, L. Zhu, K. Yang, Adsorption behaviors of volatile organic compounds (VOCs) on porous clay heterostructures (PCH), *Journal of Hazardous Materials* 170 (2009) 7 – 12.

79 Y.-C. Chiang, P.-C. Chiang, C.-P. Huang, Effects of pore structure and temperature on VOC adsorption on activated carbon, *Carbon* 39 (2001) 523 – 534.

80 Huang, Z. H., Kang, F., Liang, K. M., & Hao, J. (2003). Breakthrough of methylethylketone and benzene vapors in activated carbon fiber beds. *Journal of Hazardous Materials*, 98 (1–3), 107–115.

- 
- 81 Lashaki, M. J., Fayaz, M., Wang, H., Hashisho, Z., Philips, J. H., Anderson, J. E., & Nichols, M. (2012). Effect of Adsorption and Regeneration Temperature on Irreversible Adsorption of Organic Vapors on Beaded Activated Carbon. American Chemical Society, 46, 4083 – 4090.
- 82 Chiang, Y. C., Chiang, P., & Chang, E. (2001). Effect of surface characteristics of activated carbon on VOC adsorption. Journal of Environmental Engineering, 54, 54 – 62.
- 83 M. Dubinin, Water vapor adsorption and the microporous structures of carbonaceous adsorbents, Carbon 18 (1980) 355 – 364.
- 84 M.M. Dubinin, V.V. Serpinsky, Isotherm equation for water vapor adsorption by microporous carbonaceous adsorbents, Carbon 19 (1981) 402 – 403.
- 85 Shaverdi, G., ‘Developing a Model for Mass Transfer in Adsorption Packed Bed Filters,’ MSc thesis published on 2012.
- 86 C. R. Girish, V. Ramachandra Murty., ‘Mass Transfer Studies on Adsorption of Phenol from Wastewater Using *Lantana camara*, Forest Waste.’ International Journal of Chemical Engineering, Volume 2016, Article ID 5809505, 11.
- 87 Patel. H., ‘Fixed-bed column adsorption study: a comprehensive review,’ Applied Water Science (2019) 9:45.
- 88 Tefera, T. D., Hashisho, Z., Philips, J. H., Anderson, J. E., Nichols, M., ‘Modeling Competitive Adsorption of Mixtures of Volatile Organic Compounds in a Fixed-Bed of Beaded Activated Carbon.’ American Chemical Society 2014, 48, 5108 – 5117.

- 
- 89 Wang, K., Do, D. D. 'Multicomponent adsorption, desorption and displacement kinetics of hydrocarbons on activated carbon — dual diffusion and finite kinetics model', *Separation and Purification Technology* 17 (1999) 131–146
- 90 Papirio, S., Frunzo, L., Ferraro, A., Race, M., 'Heavy metal removal from wastewater by biosorption: Mechanisms and modeling.' Chapter 2, June 2017; 2.
- 91 Stavropoulos G.G.; P. Samaras, P.; Sakellaropoulos, G.P; 'Effect of activated carbons modification on porosity, surface structure and phenol adsorption' *Journal of Hazardous Materials* 151 (2008) 414 – 421.
- 92 EPA air pollution control cost manual. Sixth edition, June 2002, EPA/452/B-02-001, 196-216.
- 93 Danielsson, M. A.; Hudon, V. VOC emission control using a fluidized-bed adsorption system. *Metal Finishing* 1994, 92, 89 - 91.
- 94 Juan, C.; Pirajan, M.; David, R.; Amaya, B.; Vargas, E.M.; Giraldo, L; 'Design and construction of equipment to make adsorption at pilot plant scale of heavy metals.' 63a, 453 – 461 (2008); received November 29, 2006.
- 95 Chowdhury, Z. Z., Hamid, S. B. A., and Zain, S. M. (2015). "Evaluating design parameters for breakthrough curve analysis and kinetics of fixed bed columns for Cu (II) cations using lignocellulosic wastes," *BioRes.*10 (1), 732 - 749.
- 96 D. Downarowicz.; 'Adsorption characteristics of propan-2-ol vapors on activated carbon Sorbonorit in electrothermal temperature swing adsorption process.' *Adsorption* (2015) 21:87–98.
- 97 XU, Z., CAI, J., PAN, B., 'Mathematically modeling fixed-bed adsorption in aqueous systems', *Univ-Sci A (Applied Physics & Engineering)* 2013 14 (3):155 - 176.

---

98 Windey, B.; Riet, R.V.; Boutillara, Y.; Lodewyckx, P.; 'The influence of the flow pattern of the contaminated air on the adsorption behavior of an activated carbon filter.' *Adsorption* (2019) 25:757 – 763.

99 Wood, G. O., & Moyer, E. (1989). A Review of the Wheeler Equation and Comparison of its Applications to Organic Vapor Respirator Cartridge Breakthrough Data. *American Industrial Hygiene Association Journal*; 50(8), 400-407.

100 Product catalogue, Kynol activated carbon fiber and textiles; Gun Ei Chemical Industry Ltd.

101 Data sheet, OVC 4×8', Calgon Corporation.

102 Data sheets, BPL 4×10', Calgon Corporation.

103 Supplier information. Evoqua, wastewater technologies. 'Westates coconut shell granular activated carbon; VOCARB 48C carbon (formerly CC - 601).

104 Supplier information. Evoqua, wastewater technologies. 'Westates coconut shell granular activated carbon; VOCARB S series carbons.

105 Specification, Nuchar WV-A 1100 (8×25), Ingevity corporation.

106 Specification, Nuchar WV-A 1500 (10×25), Ingevity corporation.

107 [https://en.wikipedia.org/wiki/Isopropyl\\_alcohol](https://en.wikipedia.org/wiki/Isopropyl_alcohol), Accessed on March 2019.

108 <https://en.wikipedia.org/wiki/Acetone>, Accessed on March 2019.

109 <https://en.wikipedia.org/wiki/Ethanol>, Accessed on March 2019.

110 <https://en.wikipedia.org/wiki/Isobutanol>, Accessed on March 2019.

---

111 <https://en.wikipedia.org/wiki/N-Butanol>, Accessed on March 2019.

112 <https://sites.google.com/site/miller00828/in/solvent-polarity-table>, Accessed on March 2019.

113 Laskar, I.I., ‘Two-Dimensional Modeling of the Effect of Relative Humidity on Volatile Organic Compounds Adsorption in a Fixed Bed Adsorber.’ MSc thesis published on 2017, 15-171.

114 Madani, H.; Silvestre-Albero, A.; Biggs, M. J.; Rodriguez-Reinoso, F.; Pendleton, P.; ‘Immersion Calorimetry: Molecular Packing Effects in Micropores.’ *Chem phys chem* · September 2015, 16(18), 3984-3991.

115 Navaneethan, M.; Ganesh, R. S.; Mani, G.K.; Tsuchiya K.; ‘Influence of Al doping on the structural, morphological, optical, and gas sensing properties of ZnO nanorods.’ *Journal of Alloys and Compounds* 698 (2017) 555 - 564.

116 XPS (Kratos Axis Ultra) General Experimental Parameters by nano FAB, University of Alberta Accessed on March 2019 from <https://admin.nanofab.ualberta.ca/facility-resources.php>.

117 Goertzen, S.L.; K. D.; Oickle A. M., Tarasuk, A. C; Andreas, H. A. ‘Standardization of the Boehm titration. Part I. CO<sub>2</sub> expulsion and endpoint determination’ *carbon* 48 (2010) 1252 –1261.

118 Ren, H.; Cunha, E.; Sun Q.; Li, Z.; Kinloch, I. A.; Young J. R.; and Fan, Z.; ‘Surface functionality analysis by Boehm titration of Graphene nanoplatelets functionalized via a solvent-free cycloaddition reaction.’ *The Royal Society of Chemistry* 2019, *Nanoscale Advances*. 1(4), 1432-1441.



---

119 Stavropoulos G.G.; P. Samaras, P.; Sakellaropoulos, G.P; 'Effect of activated carbons modification on porosity, surface structure and phenol adsorption' *Journal of Hazardous Materials* 151 (2008) 414 – 421.

120 'Standard Guide for Gas-Phase Adsorption Testing of Activated Carbon1,'by ASTM International, Designation: D 5160 – 95 (Reapproved 2008).

121 Tedi, H.; Velicia, R.; 'Activated Carbon Fixed-Bed Adsorber Design for Treating Chromium Hexavalent Wastewater' *Makara J. Technol.* 22/3 (2018), 135 - 141.

122 Sullivan, P.D., Rood, M.J., Grevillot, G., Wander, J.D., and Hay, K.J. 2004. Activated carbon fiber cloth electrothermal swing adsorption system. *Environmental Science & Technology*, 38 (18): 4865 - 4877.

123 Burke, G.M.; Wurster, D.E.; Berg, M. J.; Veng-pedersen, P; and Schottelius, D.D.; 'Surface characterization of activated charcoal by X-ray photoelectron spectroscopy (XPS): correlation with phenobarbital adsorption data.' *Pharmaceutical Research*, vol 9, No 1 ,1992.

124 Hayashi, J., Kazahaya, A., Muroyama, K., Watkinson, A. P. 'Preparation of activated carbon from lignin by chemical activation,' *Carbon*, Volume 38, Issue 13, 2000, 1873-1878.

125 Marsh, H., Rodriguez-Reinoso, F., 'Chapter 6 – Activation Process (chemical activation process 2006, 322-365.

126 D. Lennon, D. T. Lundie, S. D. Jackson, G. J. Kelly, and S. F. Parker. 'Characterization of Activated Carbon Using X-ray Photoelectron Spectroscopy and Inelastic Neutron Scattering Spectroscopy.' *Langmuir* 2002, 18, 4667 – 4673.

---

127 M. Polovina, B. Babi, B. Kaluderovi and A. Dekanski surface characterization of oxidized activated carbon cloth, *Carbon* Vol. 35, No. 8, pp. 1047-1052. 1997.

128 Guedidi, H.; Reinert, L.; Jean-Marc L.; Soneda, Y.; Bellakhal, N.; Duclaux L. 'The effects of the surface oxidation of activated carbon, the solution pH and the temperature on adsorption of ibuprofen.' *Carbon* 54 (2013) 432-443.

129 X-ray photoelectron spectroscopy reference pages. Accessed from <http://www.xpsfitting.com/2011/01/what-is-adventitious-carbon.html>, on March, 2019.

130 Lashaki, M., Jahandar, Fayaz, M., Niknaddaf, S., and Hashisho, Z. 2012a. Effect of the adsorbate kinetic diameter on the accuracy of the Dubinin–Radushkevich equation for modeling adsorption of organic vapors on activated carbon. *Journal of Hazardous Materials*, 241-242: 154 – 163.

131 Romero-Anaya, A.J., Lillo-Ródenas, M.A., Linares-Solano, A., Factors governing the adsorption of ethanol on spherical activated carbons, *Carbon* (2014).

132 Atkins, R. C., & Carey, F. A. (2004). *Organic chemistry: a brief course: Recording for the Blind & Dyslexic*.

133 K. L. Foster, R. G. Fuerman, J. Economy, S. M. Larson, and M. J. Rood. 'Adsorption Characteristics of Trace Volatile Organic Compounds in Gas Streams onto Activated Carbon Fibers.' *Chem. Mater.* 1992, 4, 1068-1073.

134 Jahandar Lashaki, M.; Atkinson, J.D; Hashisho, Z.; Phillips, J.H.; Anderson, J.E.; Nichols, M. The impact of activated carbon's pore size distribution on heel formation during adsorption of

---

organic vapors. In proceedings of American Institute of Chemical Engineers Annual Meeting, Salt Lake City, UT, 2015, 162-183

## *Appendices*

*Appendix A***Table 15.** Summary of results for adsorption of 10 ppmv Ethanol on different adsorbents (IB: Immediate Breakthrough)

Adsorbents	Amount of Adsorbent (g)	Before Adsorption (g)	After Adsorption (g)	Capacity		5 % BT time (min)	50 % BT time (min)	Saturation time (min)
				By mass balance	By BT profile			
BAC	2.086	326.798	326.805	0.3 %	0.5 %	30	47	120
	2.074	327.768	327.774	0.3 %	0.5 %	26	42	120
Spent BAC	4.117	328.308	328.349	1.0 %	0.0 %	IB	6	37
	4.247	328.487	328.481	-0.1 %	0.0 %	IB	4	40
ACFC 10	0.507	324.923	324.918	-1.0 %	1.1 %	5	24	105
	0.510	324.923	324.919	-0.8 %	1.3 %	9	31	105
ACFC 15	0.545	324.944	324.949	0.9 %	0.4 %	1	10	65
	0.537	324.732	324.730	-0.4 %	0.6 %	3	17	65
ACFC 20	0.517	324.706	324.707	0.2 %	0.4%	2	12	30
	0.580	324.773	324.774	0.2 %	0.5%	4	13	30
OVC	2.144	327.562	327.575	0.6 %	0.7 %	38	103	300
	2.011	326.629	326.636	0.4 %	1.0 %	33	90	300
VC48C	2.014	326.403	326.401	-0.1 %	0.9 %	30	64	240
	2.036	327.355	327.353	-0.1 %	0.8 %	31	66	240
BPL	2.066	326.838	326.840	0.1 %	0.4 %	15	55	140
	2.019	326.790	326.795	0.3 %	0.5 %	15	49	140
VCRSD	2.254	327.585	327.587	0.1 %	0.4 %	17	41	120
	2.009	327.350	327.353	0.2 %	0.5 %	13	38	120
WV-A 1100	2.008	207.501	207.530	1.4 %	2.1 %	61	209	350
	2.036	207.534	207.570	1.8 %	2.1 %	62	215	350
WV-A 1500	2.248	326.704	326.713	0.4 %	1.1 %	42	147	297
	2.073	327.202	327.212	0.5 %	1.4 %	48	156	300

*Appendix B*

**Table 16.** Summary of results for adsorption of 10 ppmv Acetone on different adsorbents (IB: Immediate Breakthrough)

Adsorbents	Amount of Adsorbent (g)	Before Adsorption (g)	After Adsorption (g)	Capacity		5 % BT time (min)	50 % BT time (min)	Saturation time (min)
				By mass balance	By BT profile			
BAC	2.015	188.089	188.115	1.3 %	2.2 %	117	152	267
	2.005	188.071	188.098	1.4 %	1.7 %	129	157	292
Spent BAC	4.026	192.731	192.731	0.0 %	0.1 %	1	5	30
	4.068	192.764	192.765	0.0 %	0.1 %	1	5	27
ACFC 10	0.509	324.091	324.108	3.3 %	4.4 %	12	55	174
	0.516	324.835	324.847	2.4 %	4.8 %	17	62	193
ACFC 15	0.518	324.836	324.851	2.9 %	2.8 %	23	47	130
	0.506	324.821	324.830	1.8 %	2.8 %	21	49	138
ACFC 20	0.505	324.817	324.822	1.0 %	2.4 %	16	44	82
	0.512	325.552	325.560	1.6 %	2.4 %	15	45	89
OVC	2.018	325.836	325.858	1.1 %	2.2 %	113	174	332
	2.059	327.419	327.442	1.1 %	2.5 %	111	196	327
VC48C	2.019	326.517	326.544	1.3 %	2.3 %	136	181	284
	2.030	326.532	326.562	1.5 %	2.6 %	131	189	291
BPL	2.063	326.843	326.869	1.3 %	1.5 %	70	117	254
	2.181	326.063	326.093	1.4 %	1.8 %	83	144	268
VCRSD	2.324	326.069	326.093	1.3 %	2.1 %	56	159	357
	2.112	326.153	326.177	1.1 %	2.6 %	50	143	357
WV-A 1100	2.186	326.770	326.798	1.3 %	2.2 %	110	178	350
	2.201	325.939	325.967	1.4 %	2.3 %	101	188	350
WV-A 1500	2.294	326.381	326.394	0.6 %	2.0 %	99	168	303
	2.255	326.114	326.128	0.6 %	2.0 %	86	174	299

## Appendix C

Table 17. Summary of results for adsorption of 10 ppmv 2-propanol on different adsorbents (IB: Immediate Breakthrough)

Adsorbents	Amount of Adsorbent (g)	Before Adsorption (g)	After Adsorption (g)	Capacity		5 % BT time (min)	50 % BT time (min)	Saturation time (min)
				By mass balance	By BT profile			
BAC	2.029	188.077	188.121	2.2 %	2.3 %	121	194	332
	2.028	190.379	190.427	2.4 %	2.7 %	124	196	342
Spent BAC	2.014	190.522	190.518	-0.2 %	0.0 %	IB	008	23
	4.074	192.585	192.583	-0.1 %	0.1 %	IB	005	21
ACFC 10	0.516	324.631	324.658	5.2 %	6.1 %	63	118	221
	0.511	324.604	324.634	5.9 %	6.6 %	68	124	226
ACFC 15	0.506	324.431	324.446	3.0 %	4.5 %	35	68	158
	0.502	324.414	324.435	4.2 %	4.7 %	33	70	165
ACFC 20	0.511	324.423	324.438	2.9 %	3.6 %	29	58	150
	0.506	324.412	324.431	3.8 %	3.2 %	26	60	144
OVC	2.011	326.641	326.728	4.3 %	4.6 %	166	277	483
	2.039	326.077	326.148	3.5 %	4.1 %	169	286	472
VC48C	2.033	326.030	326.074	2.2 %	3.7%	171	281	482
	2.031	327.655	327.714	2.9 %	4.3 %	190	299	470
BPL	2.028	326.444	326.482	1.9 %	2.3 %	87	150	287
	2.022	327.650	327.697	2.3 %	2.3%	84	165	301
VCRSD	2.081	326.192	326.237	2.2 %	2.7 %	69	182	367
	2.100	326.216	326.257	2.0 %	2.2 %	53	174	358
WV-A 1100	2.059	327.262	327.302	1.9 %	4.3 %	216	327	480
	2.033	327.411	327.461	2.5 %	4.3 %	193	328	484
	2.046	326.619	326.678	2.9 %	4.7 %	173	318	494
WV-A 1500	2.140	327.022	327.077	2.6 %	3.2 %	120	265	473
	2.065	326.991	327.037	2.2 %	3.8 %	118	298	478

## Appendix D

Table 18. Summary of results for adsorption of 10 ppmv iso-butanol on different adsorbents (IB: Immediate Breakthrough)

Adsorbents	Amount of Adsorbent (g)	Before Adsorption (g)	After Adsorption (g)	Capacity		5 % BT time (min)	50 % BT time (min)	Saturation time (min)
				By mass balance	By BT profile			
BAC	2.093	325.451	325.729	13.3 %	19.6 %	625	941	1200
	2.082	328.494	328.795	14.5 %	18.2 %	588	898	1200
Spent BAC	4.250	327.997	328.040	1.1 %	0.1 %	84	175	350
	4.003	328.303	328.352	1.2 %	0.2 %	77	161	350
ACFC 10	0.593	324.982	324.069	14.7 %	14.7 %	125	314	600
	0.557	324.861	324.945	15.1 %	15.1 %	141	319	600
ACFC 15	0.546	324.850	324.956	19.5 %	25.6 %	136	255	650
	0.501	324.774	324.873	19.7 %	24.4 %	146	272	650
ACFC 20	0.550	325.030	325.127	17.6 %	25.0 %	105	304	520
	0.519	324.764	324.856	17.7 %	27.0 %	139	340	520
OVC	2.028	326.805	327.069	13.2 %	18.5 %	657	903	1200
	2.029	327.566	327.842	13.6 %	17.9 %	703	929	1200
VC48C	2.031	327.184	327.482	14.7 %	15.9 %	650	889	1250
	2.063	327.315	327.610	14.3 %	16.4 %	677	926	1250
BPL	2.039	327.286	327.507	10.8 %	12.7 %	438	754	1200
	2.034	326.075	326.273	9.7 %	13.2 %	419	736	1200
VCRSD	2.013	327.626	327.822	9.7 %	12.7 %	375	673	1250
	2.008	327.891	328.75	9.2 %	11.9 %	331	606	1250
WV-A 1100	2.028	326.305	326.455	6.3 %	12.5 %	481	661	1020
	2.031	326.283	326.410	7.4 %	14.5 %	491	668	1020
WV-A 1500	2.007	326.901	326.071	8.5 %	12.8 %	437	715	1000
	2.030	325.891	326.056	8.1 %	13.9 %	486	737	1000



*Appendix E*

**Table 19.** Summary of results for adsorption of 10 ppmv n-butanol on different adsorbents (IB: Immediate Breakthrough)

Adsorbents	Amount of Adsorbent (g)	Before Adsorption (g)	After Adsorption (g)	Capacity		5 % BT time (min)	50 % BT time (min)	Saturation time (min)
				By mass balance	By BT profile			
BAC	2.032	326.285	326.639	17.4 %	26.0 %	805	1190	1420
	2.014	326.263	326.595	16.5 %	27.4 %	843	1120	1420
Spent BAC	4.051	192.744	192.781	0.9 %	0.9 %	30	90	185
	4.068	328.484	328.526	1.3 %	0.7 %	24	86	185
ACFC 10	0.510	325.277	325.365	17.9 %	21.1 %	154	373	630
	0.519	323.476	323.578	19.7 %	21.8 %	151	365	630
ACFC 15	0.550	325.305	325.467	29.5 %	28.6 %	294	536	850
	0.549	325.314	325.474	29.4 %	30.91 %	296	545	850
ACFC 20	0.502	325.263	325.403	27.4 %	31.7 %	159	477	950
	0.501	325.392	325.533	27.4 %	33.3 %	141	458	950
OVC	2.063	326.473	326.838	17.7 %	28.3 %	1027	1282	1520
	2.054	326.484	326.855	18.6 %	26.4 %	1013	1289	1520
VC48C	2.038	327.730	328.128	19.5 %	25.7 %	1070	1351	1710
	2.032	327.624	328.021	19.5 %	26.3 %	1077	1366	1710
BPL	2.049	327.034	327.318	13.9 %	17.8 %	765	1012	1500
	2.091	327.468	327.760	14.0 %	20.5 %	744	1045	1500
VCRSD	2.060	327.901	328.150	12.1 %	19.8 %	609	997	1400
	2.057	326.442	326.686	11.9 %	19.3 %	600	975	1400
WV-A 1100	2.003	326.440	326.647	10.3 %	19.2 %	606	845	1320
	2.010	326.074	326.284	10.5 %	20.3 %	630	860	1320
WV-A 1500	2.035	326.573	326.840	13.2 %	17.3 %	677	978	1450
	2.010	326.559	326.807	12.4 %	18.5 %	632	966	1450

Appendix F

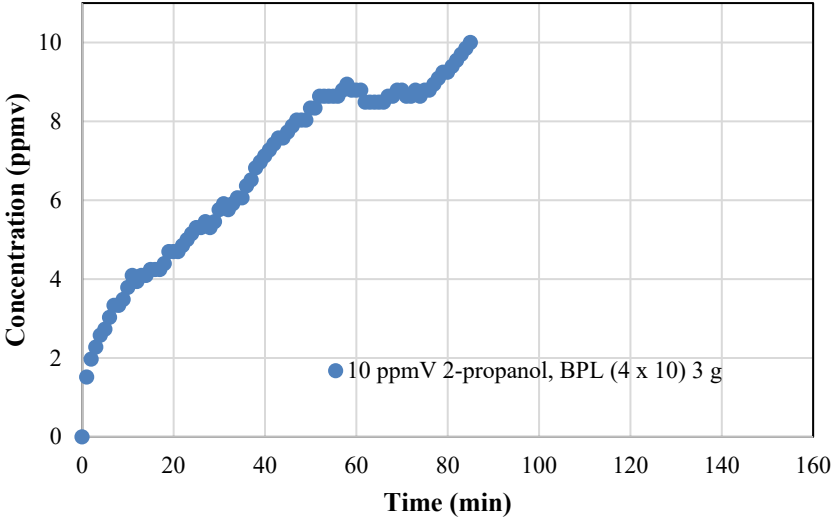


Figure 45. Adsorption Breakthrough profiles of 2-propanol on as received 3 g BPL (4×10) at 22 °C.

## Appendix G

**Table 20.** Results of 5 cycle Adsorption Desorption for WV-A 1100 With 2- propanol.

Cycles	B. Ad. <sup>1</sup> (g)	A. Ad. <sup>2</sup> (g)	Ads. <sup>3</sup> (g)	% Ads Cty by MB <sup>4</sup>	% Ads Cty, by BT <sup>5</sup>	5 % BT (min)	A. Reg. <sup>6</sup> (g)	Heel <sup>7</sup> (g)	Total Heel <sup>8</sup> (g)	TH % <sup>9</sup>
1	326.833	326.895	0.0620	3.02	3.67	158	326.835	0.0019	0.0019	0.093
2	326.835	326.895	0.0602	2.93	3.62	143	326.836	0.0009	0.0028	0.139
3	326.836	326.896	0.0599	2.92	3.51	133	326.837	0.0008	0.0038	0.185
4	326.837	326.896	0.0592	2.88	3.49	127	326.838	0.001	0.0048	0.234
5	326.838	326.897	0.0592	2.88	3.45	112	326.840	0.002	0.0067	0.325

Regeneration Temperature – 288 °C

<sup>1</sup>Weight of full reactor before adsorption

Desorption time – 180 min

<sup>2</sup>Weight of full reactor after adsorption

Initial Concentration -10 ppmv

<sup>3</sup>Weight of adsorbed adsorbate= After Adsorption - Before Adsorption

Weight of WV-A 1100 – 2.152 g

<sup>4</sup>Adsorption capacity = (Mass adsorbed/Mass of WV-A 1100) ×100

Adsorption flow: Air, 10 SLPM

<sup>5</sup>Adsorption capacity by BT profile

Regeneration flow: Nitrogen, 0.1 SLPM

<sup>6</sup>Weight of full reactor after regeneration

Adsorption Time – 440 min

<sup>7</sup>Weight of adsorbate remaining on the WV-A 1100 after regeneration= (After Regeneration- Before Adsorption)

<sup>8</sup>Weight of reactor after this regeneration test - weight of reactor before any adsorption

<sup>9</sup>Total heel (%) = (Total heel/mass of WV-A 1100) ×100

*Appendix H***Table 21.** Summary of results for adsorption isotherms of 2-propanol on WV-A 1100 at 22 °C.

Concentration ppmv	Adsorption capacity (Weight %)	
	1 <sup>st</sup> Run (initial=0.3672 g)	2 <sup>nd</sup> Run (initial=0.4105 g)
10	3.43	2.83
50	6.62	5.96
100	8.25	7.49
200	10.90	9.86
500	13.67	13.97
1000	16.46	19.38
5000	29.51	34.19
10000	39.57	46.95

## *Appendix I*

### **Details of Sacrificial Bed Design with 2-propanol adsorption on WV-A 1100**

#### **Length of Unused bed method**

5 % breakthrough time,  $t_{b5} = 205$  min

Bed saturation time,  $t_{b100} = 486$  min

Adsorbent capacity at 5 % BT,  $W_{b5} = 0.026$  kg/kg

Adsorbent capacity at 100 % bed saturation,  $W_{b100} = 0.045$  kg/kg

Total length of experimental bed,  $l = 0.041$  m

$$\% \text{ of Length of unused bed, LUB} = \left(1 - \frac{W_{b5}}{W_{sat}}\right) \times 100 \%$$

$$= \left(1 - \frac{0.026}{0.045}\right) \times 100 \%$$

$$= 42 \%$$

$\therefore$  Unused length of bed at 5% BT time LUB=  $(0.041 \times 0.42)$  m = 0.0178 m

So, 42 % of the bed is unused at 5 % breakthrough time. This unused bed length should be an additional amount with the full-scale LUB at 5 % BT.

#### **Reactor dimension used in lab-scale work**

Experimental bed length with AC,  $l = 0.041$  m

Outer Diameter – 14.9 mm, Thickness – 2 mm (approximately)

Here Inner Diameter =  $(14.9 - 4)$  mm = 10.9 mm = 0.011 m

$$\text{Inner radius} = \frac{0.011}{2} \text{ m}$$

$$= 5.46 \times 10^{-3} \text{ m}$$

$$\text{Cross sectional area} = 3.14 \times (0.008)^2 = 9.36 \times 10^{-5} \text{ m}^2$$

$$\text{Volume of the reactor bed} = (9.36 \times 10^{-5} \times 0.041) \text{ m}^3$$

$$= 3.83 \times 10^{-6} \text{ m}^3$$

$$\text{Mass of adsorbent taken, } m = 2\text{g} = 2.00 \times 10^{-3} \text{ kg}$$

$$\text{Bed bulk density, } \rho_b = \frac{\text{Mass of AC}}{\text{Volume of reactor bed}}$$

$$= \frac{2.00 \times 10^{-3}}{3.83 \times 10^{-6}} \text{ kgm}^{-3}$$

$$= 522.2 \text{ kgm}^{-3}$$

$$\text{Air flow rate during experiment} = 10 \text{ SLPM}$$

$$\text{Superficial velocity during experiment, } v = \frac{\text{Air flow rate}}{\text{Reactor area}}$$

$$= \frac{10 \text{ L} \times 1 \text{ m}^3 \times 1 \text{ min}}{1000 \text{ L} \times 60 \text{ sec} \times 9.36 \times 10^{-5} \text{ m}^2}$$

$$= 1.78 \text{ ms}^{-1}$$

$$= 106.84 \text{ mmin}^{-1}$$

$$\text{Actual air flow rate, } Q = 55000 \text{ ft}^3 \text{ min}^{-1} = 1557 \text{ m}^3 \text{ min}^{-1}$$

**The superficial velocity will be same in industrial bed to maintain the analogous mass transfer parameters.**

$$\text{Cross sectional area of the actual bed, } A = \frac{\text{Air feed rate (Q)}}{\text{Superficial velocity (v)}}$$

$$= \frac{1557}{106.84} \text{ m}^2$$

$$= 14.57 \text{ m}^2$$

$$\text{Diameter, } D = \sqrt{\frac{4A}{\pi}} = 4.31 \text{ m}$$

$$\text{Maximum Bed depth of Carbon} = \frac{\pi \times D}{12} = \frac{3.14 \times 4.31}{12} = 1.12 \text{ m}$$

Now, considering

Molecular weight of 2-propanol, MW = 60.1 gmol<sup>-1</sup>

Standard temperature, T = 0 °C = 273.15 K

Standard and practical pressure, P = 1 atm

Practical temperature = 22 °C = 295.15 K

$$1 \text{ ppmv} = \frac{1 \text{ volume of VOC}}{10^6 \text{ volume of air}}$$

From ideal gas law, PV = nRT

At standard temperature and pressure 1 mol of VOC occupies 22.4 L or 22.4 × 10<sup>-3</sup> m<sup>3</sup> volume.

$$1 \text{ ppmv} = \frac{1 \text{ m}^3 \text{ gas}}{10^6 \text{ m}^3 \text{ air}} \times \frac{1 \text{ mol gas}}{22.4 \times 10^{-3} \text{ m}^3 \text{ gas}} \times \frac{60.1 \text{ g}}{\text{mol}} = 2.68 \times 10^{-3} \text{ gm}^{-3} = 2.68 \times 10^{-6} \text{ kgm}^{-3}$$

$$\therefore \text{Inlet Concentration, } C_{\text{in}} = 10 \text{ ppmv} = 2.68 \times 10^{-5} \text{ kgm}^{-3}$$

$$\text{Actual federate of 2-propanol} = 2.68 \times 10^{-5} \text{ kgm}^{-3} \times 1557 \text{ m}^3 \text{min}^{-1}$$

$$= 0.042 \text{ kgmin}^{-1}$$

$$\text{Feed rate of 2-propanol per Area, } G_s = \frac{0.042}{14.57} \text{ kgm}^{-2}\text{min}^{-1}$$

$$= 2.88 \times 10^{-3} \text{ kgm}^{-2}\text{min}^{-1}$$

**$G_s$  is same for lab scale and full-scale system because it comes from superficial velocity.**

5 % BT time for large scale reactor,  $t_b = 1 \text{ day} = 1440 \text{ min}$

$$\text{Used bed length upto 5 \% BT, } \overset{\circ}{L} = \frac{G_s \times t_{b5}}{\rho_b \times W_{t100}}$$

$$= \frac{2.88 \times 10^{-3} \times 1440}{522.2 \times 0.045} \text{ m}$$

$$= 0.175 \text{ m}$$

Total Length of large-scale bed at 5 % BT,  $L = \overset{\circ}{L} + \text{LUB}$

$$= (0.175 + 0.0178) \text{ m}$$

$$= 0.192 \text{ m}$$

Empty bed contact time for full scale operation,  $\tau = \frac{\text{Area (A)} \times \text{Length (L)}}{\text{Air feed rate}}$

$$= \left( \frac{630}{1557} \times 60 \right) \text{ s} = 24 \text{ s}$$

**Carbon Consumption based on LUB at 5 % BT**

**Volume of used bed at 5 % BT =  $(14.42 \times 0.192) \text{ m}^3$**

$$= 2.77 \text{ m}^3$$



$$\begin{aligned}
 \text{Total Mass of Carbon required in sacrificial bed for 1 day} &= A \times L \times \rho \\
 &= (2.77 \times 522.2) \text{ kg} \\
 &\approx 1446 \text{ kg}
 \end{aligned}$$

### Results from Wheeler-Jonas model

According to this equation, Breakthrough Time,  $t_b = \frac{W_e \cdot W_{ads}}{Q \cdot C_{in}} - \frac{\rho_b W_e}{K_v C_{in}} \ln\left(\frac{C_{in}}{C_{out}}\right)$

$$\text{Rearranging for } K_v = \left[ \frac{\ln \frac{C_{in}}{C_{out}}}{\left( W_{ads} - \frac{t_b \times Q \times C_{in}}{W_e} \right)} \right] Q \times \rho_b \rightarrow (i)$$

$K_v$  is derived from equation (i) with the following experimental data, where -

Breakthrough time,  $t_b = 206 \text{ min}$

Adsorption capacity of carbon,  $W_e = 0.045 \text{ g VOC/g-carbon}$

Carbon bed weight,  $W_{ads} = 2.00 \text{ g}$

Challenge vapor concentration,  $C_{in} = 10 \text{ ppmv}$

$$= 2.68 \times 10^{-8} \text{ gcm}^{-3}$$

Breakthrough concentration (at 5% BT),  $C_{out} = 0.5 \text{ ppmv}$

$$= 1.34 \times 10^{-9} \text{ gcm}^{-3}$$

Airflow rate during experiment,  $Q = 10 \text{ SLPM}$

$$= 10,000 \text{ m}^3\text{min}^{-1}$$

Bed bulk density,  $\rho_b = 522.2 \text{ kgm}^{-3} = 0.522 \text{ gcm}^{-3}$

From equation (i), Adsorption **rate coefficient**  $K_v = 17892 \text{ min}^{-1}$

Now rearranging the basic formula, we can get the actual adsorbent requirement at 5 % breakthrough time in full-scale system,

$$W_{\text{ads}} = \left[ \frac{t_b \times C_{\text{in}} \times Q}{W_e} + \frac{P_b \times Q}{K_v} \ln \frac{C_{\text{in}}}{C_{\text{out}}} \right] \rightarrow \text{(ii)}$$

Actual air flow rate,  $Q = 55000 \text{ ft}^3 \text{ min}^{-1} = 1,557,426,585 \text{ cm}^3 \text{ min}^{-1}$

5 % BT time for large scale adsorber = 1 day = 1440 min

So, Amount of adsorbent required,  $W_{\text{ads}} = 1363 \text{ kg day}^{-1}$

### Results from Thomas model

According to Thomas model,

$$\text{Effluent concentration at 5 \% BT time, } C_{\text{out}} = \frac{C_{\text{in}}}{1 + \exp\left(\frac{K_{\text{th}} \times W_e \times W}{Q} - C_{\text{in}} \times K_{\text{th}} \times t_b\right)} \rightarrow \text{(iii)}$$

$K_{\text{th}}$  is derived from following bench scale data, where-

5 % Breakthrough time,  $t_b = 206 \text{ min} = 12360 \text{ s}$

Adsorption capacity of carbon,  $W_e = 0.045 \text{ kg VOC/kg-carbon}$

Carbon bed weight,  $W = 2.00 \text{ g} = 2 \times 10^{-3} \text{ kg}$

Inlet vapor concentration,  $C_{\text{in}} = 10 \text{ ppmv} = 2.68 \times 10^{-5} \text{ kgm}^{-3}$

Breakthrough concentration (at 5 % BT),  $C_{\text{out}} = 0.5 \text{ ppmv} = 1.34 \times 10^{-6} \text{ kgm}^{-3}$

Airflow rate during experiment,  $Q = 10 \text{ SLPM} = 1.66 \times 10^{-4} \text{ m}^3 \text{ s}^{-1}$

From equation (iii), **Thomas rate coefficient  $K_{th} = 147.22 \text{ kg}^{-1}\text{m}^3 \text{ s}^{-1}$**

For the full-scale operation,

Air flow rate,  $Q = 55000 \text{ ft}^3\text{min}^{-1} = 1,557 \text{ m}^3\text{min}^{-1} = 26 \text{ m}^3\text{s}^{-1}$

5 % BT time for large scale adsorber = 1 day = 1440 min = 86400 s

Again, from equation (iii), Amount of adsorbent required,  $W = 1348 \text{ kgday}^{-1}$

## Appendix J

From Ideal gas law we know,  $PV = nRT$

$$PV = \frac{m}{MW}RT$$

$$P = \frac{m}{V} \times \frac{RT}{MW}$$

$$P = \frac{\text{ppmv}}{10^6} \times \frac{RT}{MW}$$

$$= \frac{10}{10^6} \times \frac{8.314 \times 295.15}{60.1}$$

$$= 4.08 \times 10^{-4} \text{ Pa}$$

Where,

Molecular weight of 2-propanol,  $MW = 60.1 \text{ gmol}^{-1}$

Temperature,  $T = 22 \text{ }^\circ\text{C} = 295.15 \text{ K}$

Ideal Gas constant,  $R = 8.314 \text{ J mol}^{-1} \text{ K}^{-1}$

Concentration,  $\text{ppmv} = \frac{m}{V} \times 10^6$

Now Saturation vapor pressure of adsorbate at given temperature can be calculated using Antoine's equation –

$$P_s = 10^{A - \frac{B}{C+T}}$$

Where T is the temperature and A, B, C are the Antoine's dimensionless coefficient which depends on this temperature.

For temperature ranging from 10 °C to 90 °C, Antoine's Coefficients are –

$$A = 8.00308$$

$$B = 1505.52$$

$$C = 211.6$$

Now saturation vapor pressure of 2-Propanol at 22 °C –

$$\begin{aligned} P_s &= 10^{8.00308 - \frac{1505.52}{211.6 + 22}} \\ &= 36.1592 \text{ mm Hg} \\ &= \left( \frac{36.1592}{760} \times 101,325 \right) \text{ Pa} \\ &= 4820.84 \text{ pa} \end{aligned}$$

So, relative pressure for 2-Propanol at 22 °C,

$$\frac{p}{p_s} = \frac{4.08 \times 10^{-4} \text{ Ps}}{4820.84 \text{ pa}} = 8.46 \times 10^{-8}$$

Therefore, adsorption potential for 2-Propanol at 22 °C can be calculated as shown below –

$$\begin{aligned} \varepsilon &= RT \ln \frac{P_s}{p} \\ &= \left\{ 8.314 \times 295.15 \times \ln \left( \frac{1}{8.46 \times 10^{-8}} \right) \times \frac{1}{1000} \right\} \text{ KJ mol}^{-1} \\ &= 39.96 \text{ KJ mol}^{-1} \end{aligned}$$